



The University of
Nottingham

UNITED KINGDOM • CHINA • MALAYSIA

**An Examination of the Response
of Ethylene-vinyl Acetate Film to
Changes in Environmental
Conditions**

Amir Badiee

**Thesis submitted to the University of Nottingham
for the Degree of Doctor of Philosophy**

2016

I dedicate this to my father and mother for always being there for me.

Abstract

Photovoltaics are used for the direct conversion of sunlight into electricity. In order to provide useful power, the individual solar cells must be connected together. This electrically connected and environmentally protected unit is termed a photovoltaic (PV) module. The structure of a PV module consists of a number of layers of various materials with different properties. The encapsulation material is one of the critical components of a PV module. It mechanically protects the devices and electrically insulates them, ideally for at least the 20-25 year lifetime of the modules. The lifetime of a PV module is generally limited by the degradation of the constituent parts. The materials degrade and cause a decrease in the efficiency leading to eventual failure, with the encapsulant being particularly susceptible to degradation. The most common encapsulant material is Ethylene Vinyl Acetate (EVA) the degradation of which leads to a significant drop in a PV module's efficiency, durability and lifetime. EVA undergoes chemical degradation when it is exposed to environmental factors such as elevated temperature, humidity and Ultra Violet (UV) radiation. Although numerous works have been done in this field there is still a gap in knowledge to fully understand the degradation of EVA and develop a predictive tool. This work investigates the chemical degradation of an EVA encapsulant to understand the degradation mechanisms, develop a predictive model and correlate the degradation with changes in the structure and mechanical properties.

To determine the effect of environmental stresses on EVA environmental conditions were simulated in the laboratory in order to accelerate the test program. The ageing was classified into three main groups, namely thermal ageing, UV ageing and damp-heat ageing. In order to investigate the effect of elevated temperature on the mechanical and thermal properties and also to study the thermal degradation, EVA sheets were aged in a dark laboratory oven at 85°C for up to 80 days. To investigate the impact of UV exposure on

the properties and photodegradation of EVA the samples were exposed to UV radiation of 0.68 W/m^2 at 340 nm and 50°C . To study moisture diffusion and the impact of absorbed moisture on the mechanical properties and morphology, EVA sheets were aged in an environmental chamber at 85°C -85% RH and using a potassium chloride (KCl) salt solution in a sealed chamber to obtain 85% RH at room temperature ($22\pm 3^\circ\text{C}$).

Thermal analysis techniques including Differential Scanning Calorimetry (DSC), Thermo-gravimetric Analysis (TGA), Dynamic Mechanical Analysis (DMA) along with Attenuated Total Reflectance-Fourier Transform Infrared Spectroscopy (ATR-FTIR) and Gravimetrics were used to investigate the structure, degradation kinetics and viscoelastic mechanical properties of the EVA as a function of ageing.

The EVA was shown to have viscoelastic properties that were highly sensitive to the ambient temperature. Thermal ageing was shown to reduce the storage modulus due to the changes in the structure of the EVA and reduction in crystallinity. Over a longer time, chemical changes due to thermal activation also occurred, hence, these were insignificant compared with transient thermal effects. The activation energy of deacetylation was also shown not be affected by the ageing process.

Investigation of photodegradation showed notable chemical changes as a result of UV exposure, with FTIR absorbance peaks related to carboxylic acid, lactone and vinyl exhibiting a sharp increase after UV irradiation. Differences in the ATR-FTIR spectra of the UV irradiated and non-irradiated samples showed that the intensity is depth dependant. DMA results showed UV ageing had a significant influence on the mechanical properties of the EVA and reduces the storage modulus. The predictive photodegradation model showed a good agreement on the UV irradiated surface with the experimental data where it did not agree well with the results on the non-irradiated side which could be due to the presence of UV absorber.

The response of the EVA to damp heat was investigated at two conditions with same the RH level (85% RH) and different temperatures (room temperature and 85°C). The moisture diffusion coefficient was measured via gravimetry and Water Vapour Transmission Rate (WVTR) technique which were well-agreed. Results from DSC indicated that the crystallinity increased due to incorporation of moisture into the structure of the copolymer but decreased as ageing continued, showing the significant influence of elevated temperature and thermal degradation on the structure of EVA.

A comparative study of the impact of the ageing on the structure and mechanical properties indicated that UV has a stronger degrading influence comparing to other degradation factors. DSC results also suggested that property changes could be connected to structural modifications. The impact of different degradation factors can be summarised as $UV > T > DH$.

Acknowledgements

I would like to thank my supervisors Professor Ian Ashcroft and Professor Ricky Wildman for their guidance throughout the entire research.

I also like to thank the members of Additive Manufacturing and 3D Printing Research Group and Stability and Performance of Photovoltaic (STAPP) project for their valuable help and collaboration.

Finally and for most, I would like to thank my family, father, mother, Ali, Maryam and Manuela for everything.

Table of contents

Abstract	<i>i</i>
Acknowledgements	<i>iv</i>
Table of contents	<i>v</i>
List of Figures	<i>ix</i>
List of Tables	<i>xv</i>
Nomenclature	<i>xvii</i>
Abbreviations	<i>xvii</i>
Alphabetic	<i>xviii</i>
Greek symbols	<i>xx</i>
Chapter 1	<i>1</i>
Introduction	<i>1</i>
1.1 Background	<i>1</i>
1.2 Solar PV	<i>1</i>
1.3 Stability and Performance of Photovoltaics (STAPP) project	<i>5</i>
1.4 Aim	<i>6</i>
1.5 Objectives	<i>6</i>
1.6 Research novelty	<i>8</i>
1.7 Thesis structure	<i>8</i>
Chapter 2	<i>10</i>
Literature Review	<i>10</i>
2.1 Introduction	<i>10</i>
2.2 Photovoltaic (PV) system	<i>11</i>
2.2.1 Commonly observed PV module degradations in field	<i>15</i>
2.3 Ethylene-vinyl Acetate (EVA)	<i>16</i>

2.3.1 EVA storing condition and curing process	18
2.4 The effect of environmental stresses on the properties and structure of EVA	18
2.4.1 The effect of elevated temperature	19
2.4.2 The UV effect	22
2.4.3 The effect of damp-heat and moisture ingress	28
2.4.4 The effect of combined degradation factors	34
2.5 Gaps in the current durability and lifetime studies of PV modules academic research and industry	35
2.5.1 Research challenge 1	36
2.5.2 Research challenge 2	36
2.5.3 Research challenge 3	37
2.6 Conclusion	37
Chapter 3	38
Experimental Methods	38
3.1 Introduction	38
3.2 Material and storing condition	40
3.2.1 Material (sample preparation)	40
3.2.2 Storage of samples	47
3.3 Ageing conditions	47
3.3.1 Thermal ageing	48
3.3.2 UV ageing	49
3.3.3 Damp-heat ageing	49
3.4 Experimental techniques	51
3.4.1 Differential Scanning Calorimetry (DSC)	52
3.4.2 Dynamic Mechanical Analysis (DMA)	53
3.4.3 Thermogravimetric Analysis (TGA)	54
3.4.4 Attenuated Total Reflectance-Fourier Transform Infrared Spectroscopy (ATR-FTIR)	54
3.5 Moisture diffusion coefficient measurement methods	56
3.5.1 Gravimetric measurements	56
3.5.2 MOCON Water Vapour Transmission Rate technique to measure diffusion coefficient	57

3.5.3 Comparison of moisture diffusion coefficient measurement methods	58
3.6 Summary	59
Chapter 4	61
<i>Examination of the Response of Ethylene-vinyl Acetate Film to Thermal Ageing</i>	61
4.1 Introduction	61
4.2 Theory of kinetics of degradation	63
4.3 Results and discussion	66
4.3.1 Thermogravimetric Analysis (TGA)	66
4.3.2 Dynamic Mechanical Analysis (DMA)	71
4.3.3 Differential Scanning Calorimetry (DSC)	76
4.4 Conclusions	79
Chapter 5	80
<i>Examination of the Response of Ethylene-vinyl Acetate Film to UV Irradiation</i>	80
5.1 Introduction	80
5.2 Theory of photochemical reactions	81
5.3 Results and discussion	84
5.3.1 Fourier Transform Infrared Spectroscopy in Attenuated Total Reflectance (FTIR-ATR)	85
5.3.2 Analytical investigation of photodegradation	89
5.3.3 Differential Scanning Calorimetry (DSC)	94
5.3.4 Dynamic Mechanical Analysis (DMA)	98
5.4 Conclusions	103
Chapter 6	104
<i>Investigation of Moisture Diffusion and the Response of Ethylene-vinyl Acetate Film to Damp-Heat</i>	104
6.1 Introduction	104
6.2 Analytical Solution of the diffusion equation	105

6.2.1 Fickian Diffusion	105
6.3 Results and discussion	108
6.3.1 Measurement of moisture diffusion coefficient and predicting moisture concentration	108
6.3.2 Differential Scanning Calorimetry (DSC)	110
6.3.3 Dynamic Mechanical Analysis (DMA)	115
6.4 Conclusions	123
Chapter 7	125
<i>Comparative study of ageing impact on the structure and mechanical properties EVA under different ageing conditions</i>	125
7.1 Introduction	125
7.2 Comparative study of UV, thermal and damp heat ageing impact on the properties of EVA	126
7.3 Comparative study of influence of the UV thermal and damp-heat ageing factors on chemical changes in EVA	129
7.3 Conclusion	131
Chapter 8	132
<i>Conclusion and Recommendations for Future Work</i>	132
8.1 Conclusions	132
8.2 Recommendations for future work	134
References	135
Appendix A	153
Water Vapour Transmission Rate Results	153
Appendix B	155
Original DSC curves	155
Appendix C	158
Publications	158

List of Figures

Figure 1.1: Degradation in materials layers in roof installed PV modules in Scuola universitaria professionale della Svizzera italiana (SUPSI), Lugano, Switzerland. (a) Discolouration in EVA. (b) Corrosion in the back sheet.	4
Figure 1.2: Work packages of STAPP project.....	5
Figure 1.3: STAPP project program outline for the University of Nottingham. .	6
Figure 1.4: The work flow chart for the experimental programme.	7
Figure 2.1: An illustration of a solar array and its components.	11
Figure 2.2: Structure of a PV module showing different material layers (courtesy to Micro System Services (MSS)).	12
Figure 2.3: Chemical structure of EVA copolymer.....	17
Figure 2.4: Acetic acid formation (deacetylation).	19
Figure 2.5: Photodegradation mechanism in EVA (Morlat-Therias et al. 2007).	25
Figure 3.1: A general diagram showing the impact of the degradation factors.	39
Figure 3.2: A general diagram showing the experimental methodology used in this research.	40
Figure 3.3: Uncured EVA (courtesy to SINOVOLTAICS).	41
Figure 3.4: Schematic view of the mould used in the hot press.	42
Figure 3.5: Schematic view of the autoclave.....	44
Figure 3.6: Autoclave preparation for EVA curing.....	45
Figure 3.7: (a) Autoclave with samples, spacers and top plate, (b) Autoclave during EVA curing.	45
Figure 3.8: Thermal ageing conditions in the laboratory oven.	49

Figure 3.9: Damp heat ageing conditions in the environmental chamber.	50
Figure 3.10: Ageing conditions in the salt solution chamber.	50
Figure 3.11: Diagrammatic side view of WVTR test cell (Copyright 2012 MOCON® Inc).	58
Figure 4.1: Flowchart of investigation of EVA's response to thermal ageing. .	62
Figure 4.2: Flowchart of the investigation the weight loss of EVA regarding the thermal degradation only.	65
Figure 4.3: TGA thermograms of EVA at different heating rates (weight percentage versus temperature).	66
Figure 4.4: Rescaled TGA thermogram of EVA at different heating rates (weight percentage versus temperature).	67
Figure 4.5: Derivative of weight loss to temperature for unaged EVA at different heating rates.	67
Figure 4.6: Plot of $\ln(\beta/T_p^2)$ versus $1/(T_p)$ for unaged EVA based on Kissinger's method.	69
Figure 4.7: Experimental and calculated TGA curves.	69
Figure 4.8: Activation energy calculated for unaged and thermally aged EVA.	70
Figure 4.9: Weight loss of EVA versus time in the case of exposure to 85°C with standard deviation of 6.6521e-04.	71
Figure 4.10: Storage modulus vs temperature for aged and unaged EVA.	71
Figure 4.11: (a) $\tan(\delta)$ vs temperature for aged and unaged EVA, (b) Glass transition temperature versus ageing duration for EVA based on $\tan(\delta)$	72
Figure 4.12: Storage modulus measured at (a)-60°C, (b) 20°C (c), 40°C (d) 95°C as a function of ageing time at 85°C.	74
Figure 4.13: Average storage modulus versus ageing time for thermally aged EVA.	75

Figure 4.14: Typical DSC thermograms (heat flow versus temperature) of EVA under three steps, heating-cooling-heating-Exo Up.	76
Figure 4.15: DSC first heating thermograms (heat flow versus temperature) for the unaged and aged EVA (thermograms are reproduced with offsets added)-Exo Up.	77
Figure 4.16: Glass transition temperature versus ageing duration for EVA.....	77
Figure 4.17: Crystallinity versus ageing duration after first and second heating for aged and unaged EVA.	78
Figure 4.18: Storage modulus versus crystallinity for thermally aged EVA.	78
Figure 5.1: Flowchart of investigation of EVA's response to UV ageing.	81
Figure 5.2: Subtracted FTIR-ATR spectra ($A_t - A_0$) in the domain $1800-1650\text{ cm}^{-1}$	85
Figure 5.3: Variation of absorbance at 1740 cm^{-1} as a function of exposure time.	87
Figure 5.4: Variation of absorbance at 1720 cm^{-1} as function of exposure time.	88
Figure 5.5: Variation of absorbance at 1767 cm^{-1} as a function of exposure time.	88
Figure 5.6: Variation of absorbance at 910 cm^{-1} as a function of exposure time.	89
Figure 5.7: Flowchart of the investigation the lifetime of EVA regarding the photodegradation only.	90
Figure 5.8: Variation of absorbance at 1740 cm^{-1} (normalized) on the irradiated surface as a function of exposure time.	91
Figure 5.9: Variation of concentration of ester on the irradiated surface as a function of exposure time-validation of analytical and experimental results.	92
Figure 5.10: Variation of concentration of ester (photoreactant) on the irradiated surface as a function of time.	93

Figure 5.11: Variation of concentration of carboxylic acid versus concentration of ester.....	93
Figure 5.12: Variation of concentration of carboxylic acid (photoproduct) on the irradiated surface as a function of time.....	94
Figure 5.13: DSC first heating thermograms for the unaged and UV aged EVA-Exo Up.....	95
Figure 5.14: Crystallinity versus ageing time after first and second heating for unaged and UV aged EVA.	96
Figure 5.15: Variation of crystallinity versus changes in concentration of ester on the irradiated surface of UV aged EVA.....	97
Figure 5.16: Variation of crystallinity versus changes in concentration of carboxylic acid on the irradiated surface of UV aged EVA.	97
Figure 5.17: Glass transition temperature versus ageing for unaged and UV aged EVA.	98
Figure 5.18: Storage modulus versus temperature for unaged and UV aged EVA.....	98
Figure 5.19: (a) $\tan(\delta)$ vs temperature for unaged and UV aged EVA, (b) T_g versus ageing duration based on Figure (5.22: a).	99
Figure 5.20: Storage modulus measured at (a) -20°C , (b) 0°C (c), 20°C (d) 40°C as a function of ageing time.	100
Figure 5.21: Mean storage modulus versus ageing time for EVA.	101
Figure 5.22: Average storage modulus versus concentration of ester on the irradiated surface of UV aged EVA.	102
Figure 5.23: Average storage modulus versus concentration of carboxylic acid on the irradiated surface of UV aged EVA.....	102
Figure 6.1: Flowchart of investigation of EVA's response to damp heat ageing.	105

Figure 6.2: Moisture absorption curve for EVA film at 85°C-85% RH, (a) M_t/M_q vs time, (b) M_t/M_q vs $\sqrt{\text{time}/l}$	108
Figure 6.3: Simulated moisture concentration inside the EVA film at different depths (X1-X10) under the damp heat condition of 85°C-85% RH.	110
Figure 6.4: DSC first heating thermograms for the unaged and damp heat aged EVA at (a) 85°C-85% RH and (b) 22±3°C-85% RH-Exo Up.	111
Figure 6.5: Glass transition temperature versus ageing time for EVA at (a) 85°C-85% RH and (b) 22±3°C-85% RH.	112
Figure 6.6: Crystallinity versus ageing time after first and second heating for unaged and aged EVA at (a) 85°C-85% RH and (b) 22±3°C-85% RH.....	114
Figure 6.7: Crystallinity versus average concentration after first and second heating for unaged and aged EVA at 85°C-85% RH.....	114
Figure 6.8: Storage modulus vs temperature for unaged and aged EVA at (a) 85°C-85% RH and (b) 22±3°C-85% RH.	116
Figure 6.9: (a) $\tan(\delta)$ vs temperature for unaged and aged EVA at 85°C-85% RH, (b) T_g versus ageing duration based on Figure (6.9: a).	117
Figure 6.10: (a) $\tan(\delta)$ vs temperature for unaged and aged EVA at 22±3°C-85% RH, (b) T_g versus ageing duration based on Figure (6.10: a).	118
Figure 6.11: Storage modulus measured at (a) 0°C, (b) 20°C (c), 40°C (d) 60°C as a function of ageing time at 85°C-85% RH.	120
Figure 6.12: Storage modulus measured at (a) 0°C, (b) 20°C (c), 40°C (d) 60°C as a function of ageing time at 22±3°C-85% RH.	121
Figure 6.13: Average storage modulus versus ageing time for EVA aged at 85°C-85% RH and 22±3°C-85% RH.....	122
Figure 6.14: Average storage modulus versus average moisture concentration for EVA aged at 85°C-85% RH.	123
Figure 7.1: Crystallinity versus ageing duration for different ageing conditions.	127

Figure 7.2: Comparitive effect of degradation factors on the storage modulus of EVA at (a) 0°C, (s) 20°C, (c) 40°C versus ageing duration for control sample and aged EVA at different conditions..... 128

Figure App.1: Original DSC curves related to (a) Figure (4.15), (b) Figure (5.13), (c) Figure (6.4: a), (d) Figure (6.4: b)..... 156

List of Tables

Table 2.1: Kinetic parameters calculated by (Rimez, Rahier, Van Assche, Artoos & Van Mele 2008).....	21
Table 2.2: Activation energy calculated for EVA with 12% and 20% VAc (EVA-12 and EVA-20) by different methods (Marín et al. 1996).....	21
Table 2.3: Measured diffusion coefficient (<i>D</i>) in the literature.	31
Table 2.4: The characteristics of the ATR-FTIR absorption peaks.	33
Table 2.5: Some DSC results for EVA with 28% VAc (Shi 2008; X. Shi et al. 2009).....	34
Table 3.1: Release films and release agents used for sample preparation.....	43
Table 3.2: Overview of the curing techniques.....	48
Table 3.3: Water Vapour Transmission test condition provided by RDM TEST Equipment®.	58
Table 4.1: Temperature of peak degradation rate for aged and unaged EVA samples at different heating rates.	68
Table 4.2: The calculated kinetic parameters for unaged EVA.	69
Table 4.3: The fitting parameters for storage modulus at different fixed temperatures based on Figures (4.12: a-d).....	75
Table 4.4: The best fitting parameters of the average storage modulus versus ageing duration based on Figure (4.13), fitting function: $y=a_1x^2+a_2x+c$	75
Table 5.1: Attribution of infrared absorption bands of EVA film.	85
Table 5.2: Line of best fit parameters (Figure (5.5) UV aged top side).	88
Table 5.3: Best fit parameters (Figure (5.9)).	91
Table 5.4: The fitting parameters Figure (5.12).....	93

Table 5.5: The fitting parameters for storage modulus at different fixed temperatures based on Figures (5.23).	101
Table 6.1: Gravimetry test results.	109
Table 6.2: WVTR test results (the analyses were carried out on a MOCON® Permatran-W Water Vapour Permeability Instrument).....	109

Nomenclature

Abbreviations

BIPV	Building Integrated Photovoltaic
BP	British Petroleum
DMA	Dynamic Mechanical Analysis
DSC	Differential Scanning Calorimetry
DTA	Differential Thermal Analysis
EPFL	École Polytechnique Fédérale de Lausanne
EVA	Ethylene Vinyl Acetate
Fraunhofer ISE	Fraunhofer Institute for Solar Energy Systems
FTIR	Fourier Transform Infrared Spectroscopy
GC-MS	Gas Chromatography–Mass Spectrometry
HTGPC	High Temperature Gel Permeation Chromatography
IR spectroscopy	Infrared spectroscopy
NMR	Nuclear Magnetic Resonance
NREL	National Renewable Energy Laboratory
PV	Photovoltaic
RH	Relative Humidity
RMS	Root Mean Square

STAPP	Stability and Performance of Photovoltaics Scuola universitaria professionale della Svizzera italiana
SUPSI	University of Applied Sciences and Arts of Southern Switzerland
TGA	Thermogravimetric Analysis
UV	Ultra Violet
VAc	Vinyl acetate concent
WAXD	Wide Angle X-ray Diffraction
WVTR	Water Vapour Transmission Rate

Alphabetic

a	Pre-exponential factor
A	Absorbance
b	Path length
$c_{(x,t)}$	Moisture concentration
c_0	Initial moisture concentration
CI	Carbonyl Index
C_m	Concentration of medium
C_p	Concentration of product
C_r	Concentration of reactant
C_{sat}	Saturation moisture concentration

D	Moisture diffusion coefficient
E	Activation energy
E'	Storage modulus
E''	Loss modulus
F(C_r)	Rate function
F(ϕ)	Kinetic rate function
I	Intensity
k	Fractional decay rate
K(T)	Rate constant
l	Thickness
m₀	Initial sample mass
m_q	Final sample mass
m_t	Sample mass at time t
R	Universal gas constant
t	Time
T_g	Glass transition temperature
T_m	Melting Temperature
T_p	Temperature at maximum degradation rate
V	Volume
X_c	Crystallinity

z', t' Variables

Greek symbols

$\mu(z), \vartheta(t)$ Independent functions

α Molar extinction coefficient

β Heating rate

δ Phase Angle

λ Stoichiometric coefficient

ϕ Conversion degree

Chapter 1

Introduction

1.1 Background

Recent years have seen the UK government commit to cost effective renewable energy as part of a diverse, low-carbon and secure future energy mix. A key benefit of deploying renewable energy technologies is the potential reduction in carbon emissions when compared to fossil fuels (Harris & Annut 2013). The Kyoto Protocol commits governments, including the UK, to reduce the emission of greenhouse gases. The 2009 Renewable Energy Directive also set a target for the UK to achieve 15% of its energy consumption from renewable sources by 2020 (Department of Energy & Climate Change 2013). The UK has made progress towards this challenge and total solar PV capacity grew by 1.0 GW between July 2012 and June 2013 (Department of Energy & Climate Change 2013).

1.2 Solar PV

Solar energy reaches the surface of the Earth with a power density of 500 to 1000 W/m² which would ideally be used in an effective way and converted to usable form of energy for end use customers (Czanderna & Jorgensen 1997). Solar energy is one of the fastest-growing sources of electricity in the world. The total solar energy absorbed by Earth's atmosphere, oceans and land masses is approximately 3,850,000 exajoules (EJ) per year. In 2002, this was more energy in one hour than the world used in one year (Smil 2006). Solar radiation can be converted into electrical energy directly, without any intermediate process, by the use of solar photovoltaic (PV) cells. This form of

generation of electricity has considerable advantages to conventional forms which includes (J. C. McVeigh 1983; Ken 1990; Stone 1993):

- Little maintenance is required because there are no moving parts.
- It is pollution free and its source is renewable.
- There are no harmful waste products.
- Solar panels can be installed very quickly.

Although there has been progress towards meeting the 2020 renewable target, the scale of the increase over the next years represents a huge challenge and will require strong contributions from the three sectors of electricity, heat and transport. The mix of renewable energy generation needed to meet the 2020 target will require several technologies to make a significant contribution. Solar PV is one of the eight key technologies set out in the Renewable Energy Roadmap Update 2012 (Anon 2014) and plays an important role in the UK's energy generation owing to its reliability. Solar PV is not just important because of its energy generation potential, it can also contribute to UK economic growth (Anon 2013).

The extensive deployment of solar panels across the UK is among the most popular renewable energy technologies. Recently, solar received the highest public approval rating of all renewable energy technologies, at 85%. The major problem in using solar energy is not how to collect it but is how to collect it in a cost effective way in order to be competitive compared to conventional forms of energy (Claassen, R. S.; Butler 1980). The ability to deliver further reductions in the installed costs of solar PV will determine the level of sector growth and the ability for the levelised cost, the per-kilowatt hour cost of building and operating a power plant over an assumed financial life, of solar energy to become competitive with other energy sources.

PV modules are now accepted as a possible source of renewable energy for households. There are, however, problems with this technology, primarily that their lifetime is currently such that their cost makes benefits marginal. PV modules work under varying climatic conditions, exposed to environmental

stresses such as rain, snow, hail, temperature variation, etc. Since there are a number of different layers of various materials used in the structure of a PV module, the response to the environmental stresses will vary, which causes mismatches and results in defects in the PV module structure and affects the performance, reliability and durability of the PV module. To improve the lifetime and durability of photovoltaic modules we need a better understanding of the material degradation mechanisms to be able to predict the degradation under different climatic conditions.

The encapsulant is an essential part of a PV module for mechanical protection of the silicon solar cells and electrical insulation of the PV module. It also protects the metal contacts and interconnects against corrosion. The encapsulant packaging protects the solar cells from environmental damage and mechanical stresses. This protection must insure at least 20-25 years lifetime for the modules to be cost effective.

Recent developments in the PV industry have focused on the efficiency of the modules and the improvement of lifetime at the material level. Among the various material layers in a module's structure, the performance of encapsulant has become a subject of discussions in recent years. The subject arose from the observed degradation and discolouration of the encapsulants (Figure (1.1)) and degradation of generated electrical energy in PV modules especially those deployed in dry-hot or humid-hot climates (Czanderna & Pern 1996). Therefore, it is important to be able to predict the degradation of an encapsulant material and its lifetime under different environmental conditions in order to optimize the durability of PV modules. Figure (1.1) shows two types of PV module degradation in material level, the discolouration of EVA (a) and corrosion in the backsheets (b) in a roof installed PV module in Scuola universitaria professionale della Svizzera italiana (SUPSI), Lugano, Switzerland.

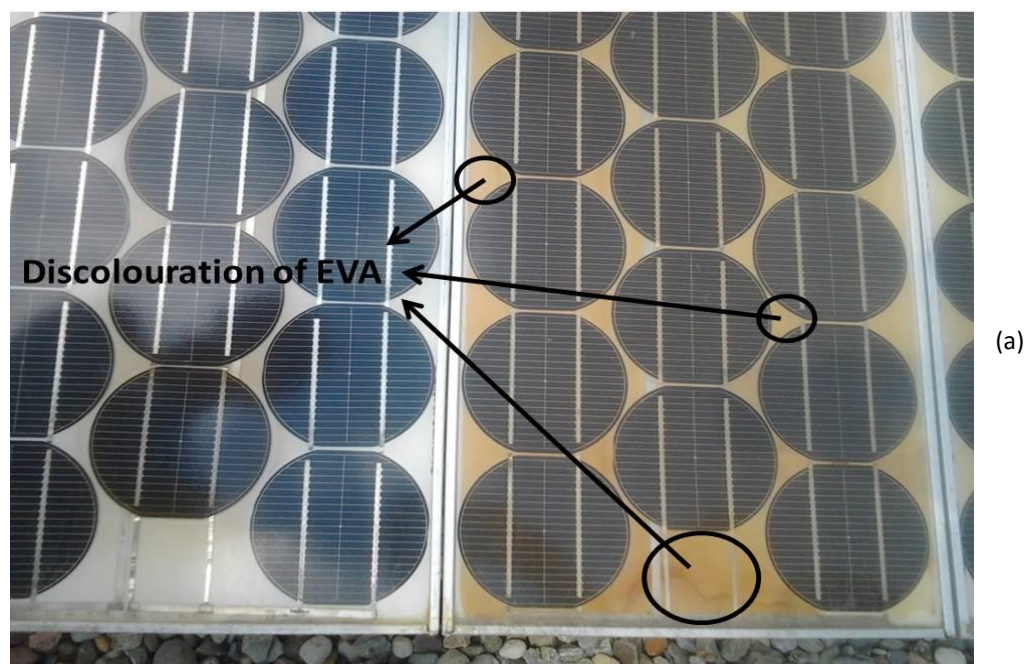


Figure 1.1: Degradation in materials layers in roof installed PV modules in Scuola universitaria professionale della Svizzera italiana (SUPSI), Lugano, Switzerland. (a) Discolouration in EVA. (b) Corrosion in the back sheet.

1.3 Stability and Performance of Photovoltaics (STAPP) project

The stability and Performance of Photovoltaics (STAPP) project was funded under the India-UK Collaborative Research Initiative in Solar Energy. It is a balanced consortium having four institutes from UK and four institutes from India. The emphasis of the project is on the stability and performance of photovoltaic modules and system. This project also involves many leading Photovoltaic companies, mainly from India and the UK. The project consists of 6 work packages (WP) as illustrated in Figure (1.2).

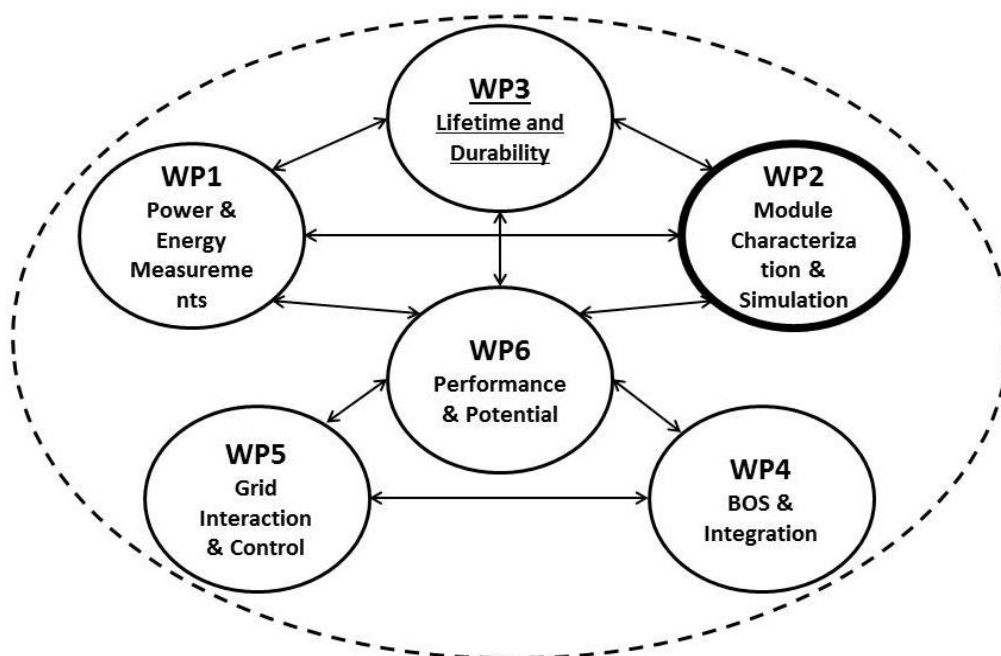


Figure 1.2: Work packages of STAPP project.

The University of Nottingham's contribution to STAPP focused on the chemical degradation, mechanical modelling and lifetime behaviour prediction of PV modules (WP2). This PhD thesis in particular investigates the chemical degradation of the encapsulant in order to understand the degradation mechanisms and predict ageing. Figure (1.3) shows the STAPP project program outline for the University of Nottingham.

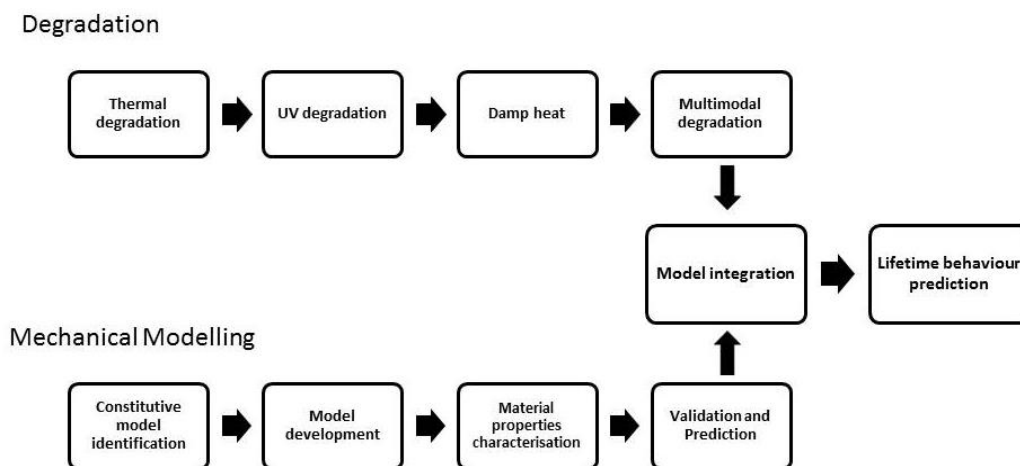


Figure 1.3: STAPP project program outline for the University of Nottingham.

1.4 Aim

This work aims to increase understanding and predict the degradation of the encapsulant material, EVA, under different environmental conditions and the associated changes in mechanical properties by examining the link between the chemistry, the structure and the intrinsic mechanical behaviour. This will enable module degradation to be understood and lead to better production of more durable PV modules.

1.5 Objectives

- 1) To understand the degradation mechanisms.
- 2) To identify the suitable characterisation techniques.
- 3) To develop reliable accelerated ageing methods.
- 4) To correlate chemical degradation and morphological changes with mechanical properties.
- 5) To investigate the kinetics of the thermal degradation of EVA and develop a predictive model to be able to predict weight loss of EVA when it is exposed to elevated temperature only.

- 6) To investigate the photodegradation of EVA in order to develop a predictive model to predict the degradation of EVA when it is exposed to UV only.

In order to meet the aim and the objectives of the project, a series of tests and experiments were designed to age the material under controlled conditions and perform thermal, optical and mechanical analysis on the aged material to study the effect of the ageing on the material properties, characterise the aged material and investigate the kinetic parameters in order to calculate the lifetime of the encapsulant and correlate it with mechanical properties. Figure (1.4) illustrates the work flow chart for the experimental programme. STAPP project emphasizes on the stability and performance of PV modules and system and as a part of STAPP this PhD thesis focuses on investigating the chemical degradation of encapsulant to understand the degradation mechanisms to be able to develop a predictive model for lifetime behaviour prediction.

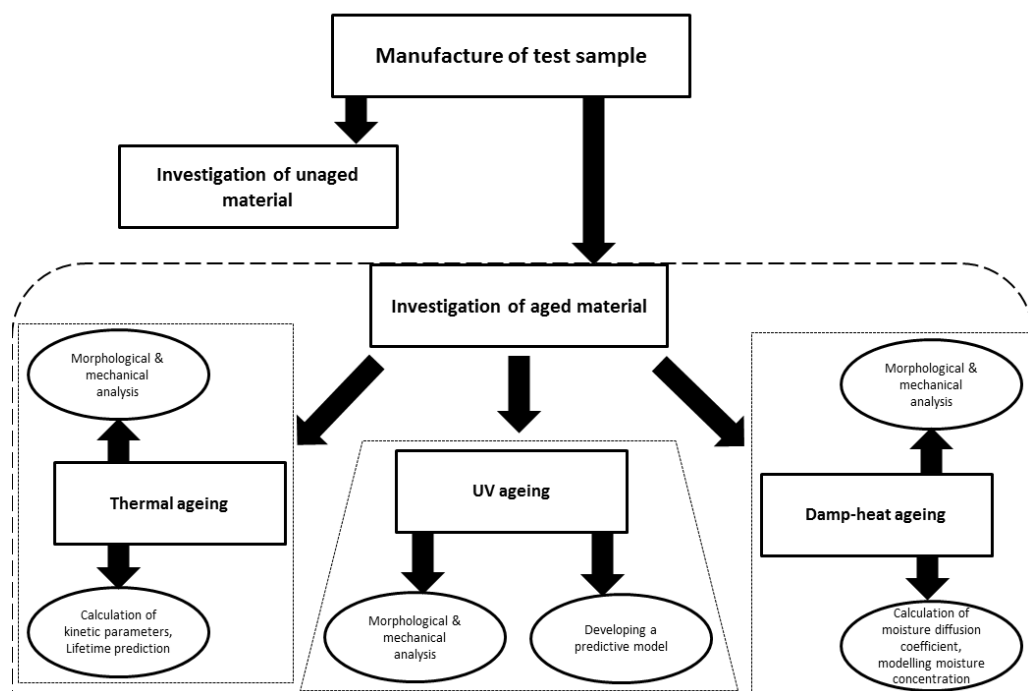


Figure 1.4: The work flow chart for the experimental programme.

1.6 Research novelty

There is number of previous works on the durability and reliability of PV modules; including an extensive description of the hydro-photo-thermal degradation mechanisms. There is, however, a missing link between the ageing and degradation process and their consequences within the context of morphological changes, mechanical behaviour and prediction of degradation at isolated UV and isolated thermal ageing conditions. Therefore, the novelty of this research can be summarised as

- Correlating of the material's degradation with its lifetime under in-service climatic conditions.
- Developing a predictive model in order to predict Photodegradation and thermal degradation of EVA.
- Investigation of link between moisture absorption and the changes in crystallinity and viscoelastic properties of EVA.
- Investigation of link between the chemical degradation, structure and mechanical behaviour of EVA.

1.7 Thesis structure

The thesis is structured as below:

Chapter 2 gives an introduction to photovoltaic (PV) systems and introduces Ethylene Vinyl Acetate (EVA) as a commonly used encapsulant. This chapter also reviews the effect of environmental stresses (elevated temperature, Ultraviolet (UV) and humidity) on the structure and behaviour of EVA and gaps in the knowledge are discussed.

Chapter 3 describes the methodology, equipment, techniques, material, sample preparation and artificial ageing process including elevated temperature, UV radiation and damp-heat used throughout the research project in order to conduct experiments.

Chapter 4 contains a detailed study on the effects of elevated temperature and thermal ageing on the structure, mechanical properties and chemical degradation of EVA. In particular, a correlation between chemical and mechanical degradation is presented. A general procedure for finding kinetic parameters is used in order to predict the material lifetime.

Chapter 5 discusses the impact of UV on the chemical degradation, structure and mechanical properties of EVA. Morphological changes, mechanical and chemical degradation are correlated and presented.

Chapter 6 describes the effect of the moisture/humidity ingress and damp-heat ageing on the structure and viscoelastic properties of EVA. It also discusses the measurement of moisture diffusion coefficient.

Chapter 7 Comparatively studies the ageing impact on the structure and mechanical properties EVA under different ageing conditions.

Chapter 8 presents conclusions from the thesis and recommendations for future work.

Chapter 2

Literature Review

2.1 Introduction

The global solar sector is going through a period of great change and it is important that its full potential is grasped, along with the wide economic and environmental benefits that it can bring. One of the challenges in this respect is to make PV modules cost effective in order to support the growing energy demand. Currently, however, PV module take-up and installation is dependent upon government subsidy, owing to the marginal economic benefit to the user as a consequence of the high capital cost and relatively low lifetime (Anon 2013).

The lifetime of a PV module is generally limited by the degradation of the constituent parts. The materials age and degrade and there is a continuous decrease in the efficiency leading to eventual failure. One part that is particularly susceptible to degradation is the encapsulant. The encapsulant packages the silicon cells into a weatherproof structure with a front sheet, usually of glass. This packaging is expected to protect the solar cells from environmental damage. The most common encapsulant material is Ethylene Vinyl Acetate (EVA) and degradation of this layer can lead to a significant drop in a PV module's efficiency, durability and lifetime.

Since EVA undergoes chemical degradation when it is exposed to heat, humidity and Ultra Violet (UV) radiation, there is the possibility of a complex interaction of several different ageing mechanisms. In order to be able to predict and control the behaviour of EVA under various environmental

conditions it is necessary to understand the degradation mechanisms and mechanical behaviour under different climatic conditions.

Determining the effect of environmental stresses and artificial ageing on polymeric materials is of concern in many engineering applications and has been the subject of significant research (Liu, Wildman, Ashcroft, et al. 2012a; Liu, Wildman & Ashcroft 2012; Elmahdy et al. 2010; Ashcroft et al. 2012; Ashcroft et al. 2001). In this chapter we look to explore the state of the art before discussing the gap in knowledge and the proposed programme of work.

2.2 Photovoltaic (PV) system

Photovoltaics is an approach to direct conversion of sunlight into electricity (Stone 1993). A solar cell is an electrical device that converts the sun's light energy into electricity. In order to provide useful power for any application, the individual solar cells must be connected together to give the appropriate current and voltage levels and they must also be protected from damage from the environment in which they operate. This electrically connected and environmentally protected unit is usually termed a photovoltaic (PV) module. A series of multiple photovoltaic modules form a photovoltaic array. Figure (2.1) illustrates the components of a solar array.

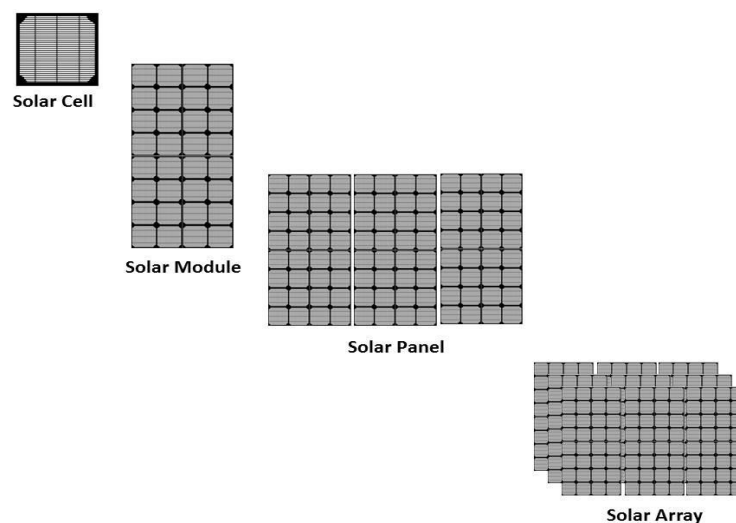


Figure 2.1: An illustration of a solar array and its components.

The structure of PV modules consists of various material layers. There is a top sheet, which is usually low iron glass, encapsulant surrounding the silicon wafers, a back sheet which can be glass or polymer and a junction box. The basic construction of a typical PV module is illustrated in Figure (2.2). This package is the PV module, or solar panel. In other words a PV module is a collection of individual solar cells integrated into a package which protects them from environmental factors including rain, snow, dust, thermal and mechanical stresses.

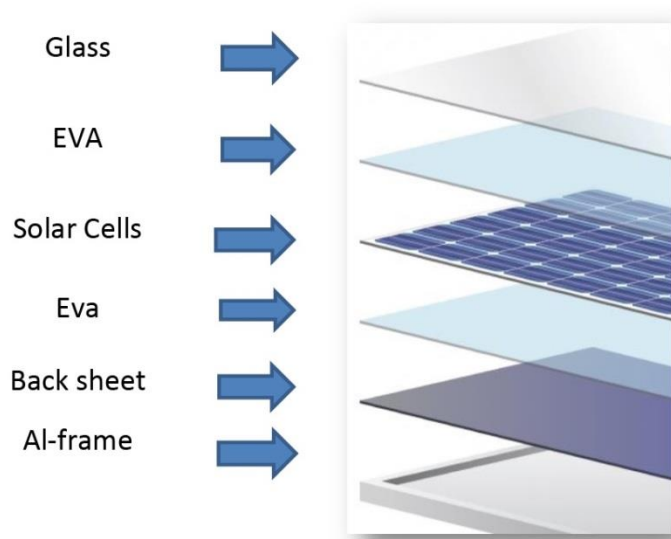


Figure 2.2: Structure of a PV module showing different material layers (courtesy to Micro System Services (MSS)).

A standard PV module has an area of 0.5 m^2 to 1 m^2 and thickness of 5-20 mm (Carlsson et al. 2006). The structure of the PV module is dictated by several requirements; including the electrical output, which determines the number of cells incorporated; the transfer of as much light as possible to the cells, the cell temperature, which should be kept as low as possible, and the protection of the cells from exposure to environmental stresses.

Environmental conditions play a crucial role in the durability, performance and lifetime of the PV systems. A PV module's performance deteriorates when it is exposed to outdoor environmental conditions, which affect the reliability

of the PV modules in the long term (Vázquez & Rey-Stolle 2008). PV modules are required to survive 20 to 25 years to achieve economic break even. The most important factor in PV electricity generation is to make it economically viable and assure maximum power output for the lifetime of PV modules (S.-H. Schulze, S. Dietrich, M. Ebert 2008).

Among the various materials in a PV module, the encapsulation material is one of the most critical components in terms of durability. The encapsulant serves a number of different purposes. It mechanically protects the devices and electrically insulates them (Jorgensen & McMahon 2008). It also packages the silicon cells into a weatherproof structure. Packaging cost is 50% of the total material cost in a PV module, which shows its economic importance (Osterwald & McMahon 2009).

The solar panel must be protected against these factors (Osterwald & McMahon 2009):

- Corrosion of metallic materials,
- Water vapour permeation/moisture ingress,
- Delamination of encapsulant,
- Damage from physical environmental factors such as wind, hail, etc.,
- Thermal expansion mismatch,
- UV exposure,
- Damage to external parts such as the junction box.

To avoid or limit moisture ingress, good sealing and adhesion are required. The adhesion quality is mainly dependant on factors such as (Lange et al. 2011):

- The cleanliness of the material sheets, e.g., the glass panel.
- The condition of encapsulant material prior to lamination i.e. storing.
- The lamination process, with process parameters including temperature, pressure, duration and homogeneity of the distribution of these factors.

- The homogeneity of the lamination temperature profile, which is important to achieve a high electrical yield and a long module lifetime.

Due to the importance of PV module durability there is increasing demand on the performance of the glass/encapsulant laminates (A.K. Plessing 2003). In numerous publications, delamination has been reported as one of the major failure mechanisms in PV modules, with the emphasis on the glass/encapsulant interface (Pern 1996; Pern & Glick 2003). However, delamination at the backsheet interface has also been reported to significantly contribute to failure initiation in PV encapsulation (Oreski & Wallner 2005).

Another crucial feature the encapsulant material must have is the ability to transmit light under long term UV exposure. Although the degradation may have a minor effect on light transmission it needs additional tests and research (Michael D Kempe 2008).

Since one of the PV encapsulant's roles is to serve as a mechanical support, it is essential to study the mechanical properties of the encapsulant. Kemp's investigation (M D Kempe 2005) showed that EVA experiences a phase transition over the temperature range of -40°C to 80°C where the elastic modulus decreases by a factor of 500. This transition can be attributed to EVA having a melting temperature $>65^{\circ}\text{C}$ and glass transition temperature (-15°C).

The mechanical stability of PV modules should ensure resistance against wind (up to 2.4 kPa) and snow (up to 5.4 kPa). To reach such mechanical stability, good support of the module glass and mounting of the module is required. However, reducing the support and mounting material is a key factor to lowering the cost of the module, which has led to the construction of modules without a frame being quite common. The complexity of the mechanical behaviour of PV modules requires us to consider various factors such as time, temperature and the age dependent properties of material. It is also reported that 68% of recorded module failures have occurred either at the free edge or the clamp, which can be correlated with stress concentration regions based

on Finite Element (FE) simulations (S. Dietrich, M. Sander, M. Ebert 2008; Sascha Dietrich, Matthias Pander 2009).

2.2.1 Commonly observed PV module degradations in field

The field degradation of PV modules can be classified into five categories:

- 1) Degradation of packaging materials such as glass breakage, discolouration of the encapsulant and back sheet cracking. In the case of thin film modules, 90% of the failures are related to the packaging materials (McMahon 2004).
- 2) Loss in adhesion strength or delamination. Field experience has shown delamination on the front side of the module is more common than the back side. This can also cause optical decoupling and prevent effective heat dissipation. Module reliability is inextricably related to the cohesion and adhesion of all material layers in the module (Jorgensen & McMahon 2008).
- 3) Degradation of cell/module interconnects.
- 4) Degradation caused by moisture ingress, which causes corrosion in metallic parts and increases current leakage. Moisture permeation also results in delamination (Dhere 2000; Dhere, Neelkanth G. and Pandit, Mandar 2001; Osterwald et al. 2003).
- 5) Degradation of the semiconductor devices.

These various degradations can lead to termination of the ability of the PV module to produce useful safe electricity and are dependent on various factors, some of which are difficult to simulate in the laboratory (Quintana et al. 2002). Data collection from field experiments started in the 1970s, but this has not been well coordinated. Different field data show different outcomes, which is due to different environmental and measurement conditions (Quintana et al. 2002). For instance a system tested for a period of ten years from the mid-eighties showed a power loss of 1% to 2% per year (A. L. Rosenthal, M. G. Thomas 1994). Field data collection from multi-crystalline modules for a period of eight years in Sandia, USA, showed 0.5% loss in

performance per year (King et al. 2000). A study performed by National Renewable Energy Laboratory (NREL) shows both single and multi-crystalline field modules to degrade at about 0.7% per year (Osterwald et al. 2002). These differences in the field data show the variability and dependency on environmental and measurement conditions.

In the next section, the properties and structure of the most common PV module encapsulant, Ethylene Vinyl Acetate (EVA), will be reviewed.

2.3 Ethylene-vinyl Acetate (EVA)

Copolymers were developed to expand industrial utilization of polymeric materials due to the limited use and restricted properties of homopolymers (Çopuroğlu & Şen 2004). EVA is a copolymer of ethylene and vinyl acetate with the structure shown in Figure (2.3). EVA is the most commonly used encapsulant in the PV industry due to its low cost, high adhesion strength and high transparency. EVA's flexibility has made it popular in many industries, including foot ware (Allen et al. 2005; Chiu & Wang 2007), the toy industry (Globus et al. 2004), agricultural (Abrusci et al. 2012) and in PV applications (Czanderna & Pern 1996).

EVA has been in commercial use in PV modules since 1981 (Wohlgemuth & Petersen 1991). The EVA used in the PV manufacturing industry is 28%-33% weight percentage vinyl acetate compounded with additives such as a curing agent, UV absorber, a photo antioxidant and a thermo antioxidant (Klemchuk et al. 1997). In the range of 400 nm-1100 nm, this EVA shows nearly the same optical transmission as glass. The properties of the EVA which make it a good encapsulation choice are high electrical resistivity, low polymerization temperature, low water absorption ratio and good optical transmission (Czanderna & Pern 1996; Schulze et al. 2009).

The vinyl acetate content (VAc) has a substantial effect in EVA's properties and structure. It is reported that the lower the amount of VAc the more the copolymer is akin to polyethylenes, with higher crystallisation, but increasing

VAc prevents adjacent polyethylene chains crystallizing and EVA's structure tends to be amorphous and rubbery (Rodríguez-Vázquez et al. 2006) this is mostly seen when the VAc exceeds beyond 43% by weight (Kamath & Wakefield 1965).

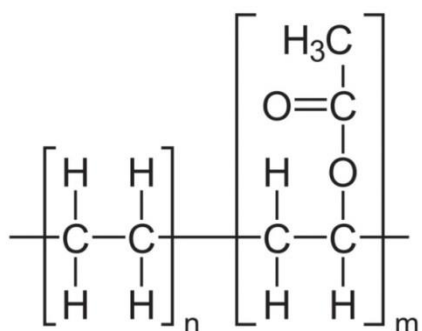


Figure 2.3: Chemical structure of EVA copolymer.

Recently the PV industry has focused on the improvement of lifetime at the material level, and the encapsulant has become the subject of research. EVA undergoes degradation when it is exposed to harsh environmental conditions. The main degradation product of the photo-thermo-chemical degradation of EVA is acetic acid, which causes corrosion in the metallic parts of PV modules and deteriorates the adhesion properties of the EVA. UV also causes discolouration in EVA, which affects the efficiency of PV systems. Moisture ingress causes problems such as delamination and corrosion. These problems show the important effect of environmental and climatic conditions on the durability of PV modules.

PV systems are used in many different continents and regions with very different environmental conditions. Therefore, it is important to be able to predict the potential failure modes of the system in different climates to achieve the desired reliability, durability and economical break even. Thus, there is a need to investigate and understand the degradation factors and mechanisms involved in this degradation.

2.3.1 EVA storing condition and curing process

Virgin (uncured) EVA is usually provided commercially in sheet form. As mentioned in section (2.2), the pre-lamination condition of EVA has a great influence on the quality of the lamination. The EVA manufacturers recommend an optimum temperature of 22°C (generally below 30°C) as a storage temperature and a relative humidity (RH) of 50% (Krauter et al. 2011). The virgin EVA should be kept out of direct sunlight and should not be stored for more than 6 months. The technical manual of Photocap® shows the adhesion strength of EVA reduces as the storage duration increases (Krauter et al. 2011).

In order to achieve suitable mechanical and optical properties EVA should be cured. The recommended curing level ranges between 70% and 90% which depends on the type of EVA and backsheet. A good combination of curing and lamination can slow down the ageing of solar cells and the delamination process. During curing cross-linking occurs and the EVA is converted from a thermoplastic into a thermosetting material, which provides the protection of the active PV elements in the module (Lange et al. 2011).

Previous research into the impact of the various EVA degradation factor is reviewed in the next section.

2.4 The effect of environmental stresses on the properties and structure of EVA

PV modules are exposed to various harsh environmental stresses such as UV radiation, heat, humidity, pollutants and thermal cycles. Additional physical climatic factors, e.g. rain, dust, wind and hail, can also have a deteriorating effect. All these factors deteriorate the durability, stability, reliability and performance of the PV modules (Czanderna & Pern 1996; Oreski & Wallner 2005). It is necessary, therefore, to understand the degradation mechanisms caused by the main environmental stresses in order to predict the lifetime and change to performance of a PV module in-service.

2.4.1 The effect of elevated temperature

EVA undergoes a two-step thermal degradation when it is exposed to elevated temperatures which is investigated by several researchers (Häußler, L. , Pompe, G., Albrecht, V., Voigt 1998). The first stage of the thermal decomposition of EVA is an acetate pyrolysis; evolving mainly acetic acid in a so-called deacetylation process, as shown in Figure (2.4). The second stage of the degradation is the degradation of any remaining partially unsaturated poly ethylene polymer and the production of a large number of straight-chain hydrocarbon products by breakdown of the hydrocarbon backbone (McGrattan 1994; Sultan & Sörvik 1991a; Sultan & Sörvik 1991b; Sultan & Sörvik 1991c; Camino et al. 2000; Zanetti et al. 2001; Riva et al. 2003; Kaczaj & Trickey 1969; Gilbert et al. 1962).

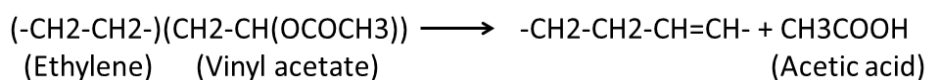


Figure 2.4: Acetic acid formation (deacetylation).

Allen et al. (2001) investigated the thermal degradation of EVA in the presence of oxygen (thermal oxidation) and reported that the main degradation of EVA is the loss of acetic acid (deacetylation), which is followed by oxidation and main chain breakdown. They also reported that the rate of degradation is greater in the presence of oxygen.

Numerous researchers (Trombetta et al. 2000; Gulmine et al. 2002; Bauer et al. 1999; Post et al. 1995; Price & Church 1997; McNeill et al. 1976) have used Fourier Transform Infrared Spectroscopy (FTIR) combined with other techniques to investigate pyrolysis of polymers. (Marcilla et al. 2005) studied the thermal pyrolysis of EVA; using combined thermogravimetry (TG)/FTIR to investigate evolved gas during the degradation. A TG analysis was used to decompose three commercial EVA copolymers in an inert atmosphere which was connected to a FTIR in order to study the evolved gas. Their experimental results clearly show a two-step decomposition. The FTIR spectra of the

evolved gas revealed that during the first stage of decomposition the evolved gas were mainly acetic acid and small quantities of CO, CO₂ and CH₄. The spectra from the second stage of the decomposition showed traces of alkene and alkane mixtures, plus small amounts of aromatic compounds.

Costache et al. (2005) used Gas Chromatography-Mass Spectroscopy (GC-MS) and TGA/FTIR to investigate the impact of nanoclay in the degradation of EVA. Their results also show a two-stage degradation. The TGA/FTIR results showed the evolution of acetic acid, CO₂ and water on the early stages of degradation. The presence of the nanoclay catalysed the loss of acetic acid in the first stage of the degradation. They reported that the thermal degradation process of EVA in the presence and absence of nanoclay are very similar, however, there are subtle changes, shown by differences in the quantity and quality of the products which are formed during the degradation. They finally concluded that nanoclay can promote one of the degradation pathways at the expense of another and thus lead to different volatilization rates and products.

Rimez et al. (2008) investigated the thermal degradation of EVA with 50% vinyl acetate (VAc) content through an experimental study. In order to investigate both the volatiles and the solid degradation products different techniques were used such as solid state Nuclear Magnetic Resonance (NMR), TG coupled with Mass Spectrometry (MS) and Differential Thermal Analysis (DTA). The results showed that the deacetylation occurs between 300°C and 400°C.

Rimez et al. (2008) studied the kinetics of the degradation of EVA with 33% of vinyl acetate according to a mechanistic approach in which isothermal, linear heating and High Resolution (Hi-Res) TGA were used. Their calculated values for activation energy (E) and pre-exponential (a) factor by the Kissinger method are shown in Table (2.1).

Table 2.1: Kinetic parameters calculated by (Rimez, Rahier, Van Assche, Artoos & Van Mele 2008).

Process	Parameter	Value
Deacetylation	log(a)	12.7 (s ⁻¹)
	E	177.5 (kJ/mol)

Marín et al. (1996) investigated the thermal degradation of EVA in granule form and focused on calculating the activation energy of the deacetylation process by establishing the polymer weight loss with temperature. Their TG results show that the deacetylation starts at about 286°C and finishes at 396°C. The maximum reaction rate occurred at around 317°C. They also reported that as the vinyl acetate concentration increases the degree of crystallinity decreases and the end-product shows behaviour similar to thermoplastic rubbers. The decomposition of EVA depends on the heating rate; the maximum deacetylation temperature increases with increasing heating rate. The calculated values of activation energy for EVA with different VAc (12% and 20%) by different methods are presented in Table (2.2).

X. E. Cai (1999) studied the two-step degradation of EVA with 43.8% VAc by TG/FTIR. They reported that heating rates from 5°C to 40°C gave good TG curves and used the Kissinger method to calculate 221 kJ/mol for activation energy.

Table 2.2: Activation energy calculated for EVA with 12% and 20% VAc (EVA-12 and EVA-20) by different methods (Marín et al. 1996).

Method	E _{EVA-12} (kJ/mol)	E _{EVA-20} (kJ/mol)
Van Krevelen	165±16	185±18
Horowitz-Metzger	168±17	188±19
Coats-Redfern	158±16	177±18

Palacios et al. (2012) have investigated the thermal degradation kinetics of EVA nanocomposites. They reported a two-step degradation with the first step (deacetylation) occurred in the range of 300°C-400°C. They calculated 179 kJ/mol for the deacetylation activation energy and 329 kJ/mol for the second stage (chain scission).

Despite all the previous research, there is still a missing link between the ageing process, lifetime and the consequences of that ageing within the context of morphological changes and mechanical behaviour.

2.4.2 The UV effect

EVA in a PV module exposed to outdoor conditions undergoes photothermal degradation, which may result in discolouration, developing from a light yellow to dark brown in about five years or more depending on the site, module configuration and operating temperature (Czanderna & Pern 1996). Data from Carrisa solar farm in California showed discolouration is also responsible for performance degradation at a rate of 10% per year (Pern 1993; Wenger et al. 1991).

Pern (1993) studied the optical characteristics and properties of EVA before and after weathering. His findings show that the uncured EVA develops yellowing even in the dark at room temperature after around one year while some cured EVA films have developed a lighter yellowing in two or three years. The degree of yellowing for uncured EVA is four times greater than that of cured EVA in five years. The front side of the EVA which was exposed to direct UV, degraded earlier, and to a greater extent and the results clearly show that the degradation of EVA starts from the top layer at the front side and extends to the grid side. Pern (1993) also reported that the discolouration of EVA is accompanied by acetic acid formation (deacetylation) and crosslinking.

Jin et al. (2010) focussed on the impact of UV on behaviour of EVA with different VAc. A Xenon lamp with an intensity of 0.53 W/m² at wavelength of 340 nm and constant temperature of 65°C was used to age samples up to 800 hours. The techniques used in their study include Attenuated Total

Reflectance-Fourier Transform Infrared Spectroscopy (ATR-FTIR), High Temperature Gel Permeation Chromatography (HTGPC), TGA, Differential Scanning Calorimetry (DSC) and mechanical tensile testing. In the case of EVA with 14 wt% VAc the ATR-FTIR results showed absorption shoulder at 1715 cm^{-1} and 1175 cm^{-1} associated with C=O stretching. This might indicate acetaldehyde evolution in the Norrish III photoreaction (Allen et al. 1994) or H_2O deprivation of hydroperoxide (Çopuroğlu & Şen 2005; Çopuroğlu & Şen 2004). In (Czanderna & Pern 1996; Morlat-Therias et al. 2007; Lacoste et al. 1991; Glikman et al. 1986) the major sequences of photothermal degradation including Norrish reactions are described and these are shown schematically in Figure (2.5). In the case of EVA with 18 wt% VAc the maximum carbonyl formation shifts to 1163 cm^{-1} , indicating the chain scission and greater damage to the EVA with the higher VAc (Çopuroğlu & Şen 2004; Allen et al. 2001). Growth was also seen in the 1735 cm^{-1} peak and the emergence of a new carbonyl band at 1780 cm^{-1} , which can be attributed to lactone formation (Allen et al. 2001). Variation was also seen at 1175 cm^{-1} , 1715 cm^{-1} and 1163 cm^{-1} due to formation of carboxylic acid, especially in the first 400 hours, with the higher VAc EVA showing greater variation comparing to the EVA with lower VAc. This is because vinyl acetate is vulnerable to UV and can easily form reactive radicals which can weaken the polymers resistance to UV irradiation. Degradation can extend from the surface to the entire polymer by the accumulation of radicals and penetration of oxygen. HTGPC results in this study showed that EVA with higher VAc had greater molecular weight reduction on ageing due to having shorter ethylene chain segments lengths. The DSC results showed that both EVA types exhibited multiple melting endotherms, starting at about 41.3°C which are stable during the ageing. The endotherms at the lower and medium temperatures can vary during the ageing and are due to secondary crystallizations while the major peak can be attributed to the primary crystallization (Chen et al. 2009b; X. Shi et al. 2009; Lee & Kim 2008; K.A. Moly et al. 2005; Brogly et al. 1997). Mobile vinyl acetate units can easily absorb photon energy and generate unstable radicals, where

photochemical degradations can then initiate (Jin et al. 2010a). TGA of the UV aged EVA showed a two-step weight loss where the first completed at about 403°C and the second one finished within 405°C and 510°C (Costache et al. 2005; Tambe et al. 2008). Mechanical testing showed a decreasing tendency in the tensile strength, elongation at break, and modulus at 100% elongation of EVA before and after ageing. However, EVA with lower VAc exhibited more rigid mechanical properties (tensile strength, elongation at break, and 100% stretching stress) which is due to the higher crystallinity (Jin et al. 2010a).

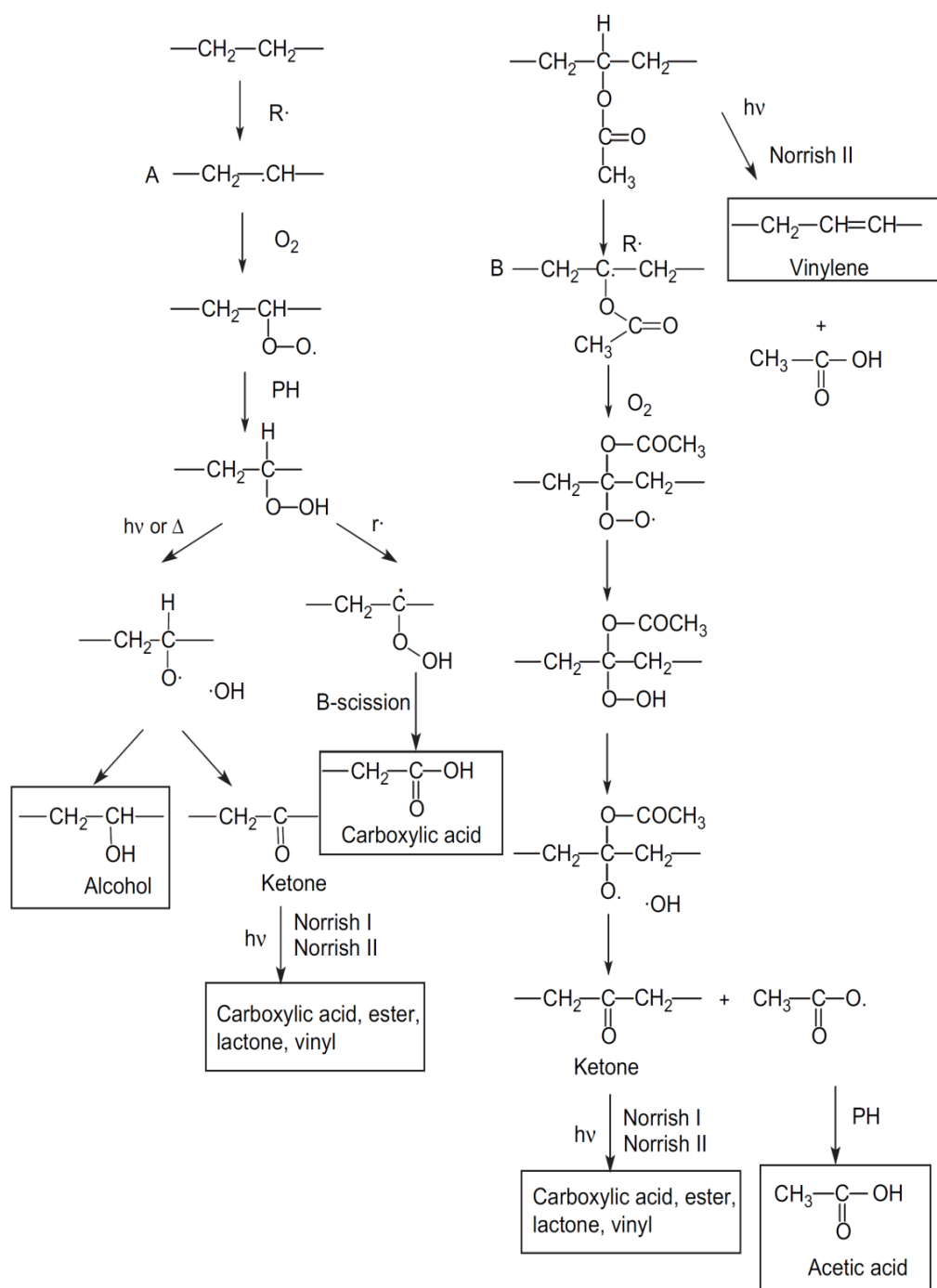


Figure 2.5: Photodegradation mechanism in EVA (Morlat-Therias et al. 2007).

Morlat-Therias et al. (2007) studied the influence of carbon nano-tubes on photodegradation of EVA and reported that the main acetate absorption band appears at 1740 cm^{-1} . There are two shoulders next to this main peak with maxima at 1718 cm^{-1} and 1780 cm^{-1} , which are attributed to the formation of carboxylic acid and lactone respectively. An unsaturated compound is a

chemical compound that contains carbon-carbon double bonds or triple bonds. In photodegradation, unsaturations are responsible for discolouration which corresponds to vinyl bonds at 909 cm^{-1} and 990 cm^{-1} . There is also a growing peak at 3520 cm^{-1} attributed to alcohols associated with the acetate group. It is also reported that the rates of photooxidation of EVA in different samples can be compared by measuring the increase of absorbance at 1718 cm^{-1} with the ageing time. Esterification is also important in EVA degradation since it results in acid formation which causes corrosion in the PV modules and affects the mechanical properties of EVA. Badiie et al. (2014) investigated the effect of UV ageing on the chemical degradation of EVA and found that UV makes significant chemical changes compared to other degradation factors, including the formation of carboxylic acid and lactone.

A typical way that PV modules fail is to lose optical transmission due to discolouration and yellowing, which is, however, less of a problem since the 1990s, due to improvements in UV absorbers and antioxidants (Pern & Glick 1997; Kempe et al. 2011; W.H. Holley, S.C. Agro & Yorgensen 1996). Although modern PV modules pass various UV exposure tests it should be noted that there might still be a reduction in optical transmission considering in-service as the standard test is around 6 months in an environmental chamber using highly UV transmissive glass, is much less than the desired PV lifetime (20-25 years) (Michael D Kempe 2008). Myer Ezrin et al. (1995) investigated the discolouration of EVA and reported that this is due to the developing long chain on conjugated double bonds as a result of loss of acetic acid from vinyl acetate units.

Klemchuk et al. (1997) investigated the degradation of EVA in field aged PV modules. They reported that UV-B transmission (285 nm-330 nm) is mostly responsible for EVA degradation and discolouration, with the spectrum of terrestrial sunlight ending at about 290 nm. Their findings showed that the discolouration started with a very thin layer at the interface under the front glass. Berman et al. (1995) and Berman & Faiman (1997) studied the effect of discolouration on module efficiency in field. They observed that the mean

maximum power value of 43.7 W for a set of discoloured modules was 5% below the manufacturer's guaranteed value. Kojima & Yanagisawa (2004) similarly made a comparative investigation on the degradation of EVA in the range of 280-380 nm. They observed slight yellowing in the EVA film after around 500 hours. Isarankura et al. (2008) investigated the photodegradation behaviour of EVA and the impact of antioxidants on the photostability of the material. They reported that EVA predominately degraded under UV irradiation via a chain scission process and the type and amount of antioxidants had a significant effect on the photostability of the EVA. They also found that some antioxidants caused the tensile strength of EVA to decrease after UV irradiation.

Numerous studies have been carried out at National Renewable Energy Laboratory (NREL), USA (Pern 1996; Pern & Glick 1997; Pern et al. 1996; Pern et al. 2000). These studies showed that the module service life can be greatly improved and extended if $UV \leq 350$ nm is removed, as this was seemed to reduce the UV-induced discolouration. They summarised the main discolouration factors as:

- The UV light intensity.
- UV filtering effect of glass.
- Lamination quality/delamination and Curing treatment and process.
- Film thickness.
- The photodecomposition of Cyasorb (UV absorber).
- The loss rate of UV absorber.
- EVA formulation and additives used.

Despite all the previous studies, there is still a missing link between the ageing process, prediction of the EVA's photodegradation and the consequences of that photodegradation within the context of mechanical behaviour and structural changes.

2.4.3 The effect of damp-heat and moisture ingress

The exposure of PV modules and especially the polymeric materials to permanently changing climatic conditions is one of the critical degradation factors. The components of the gaseous atmosphere, such as water vapour, cause hydrolysis and other chemical reactions which affect and reduce the lifetime of a PV module.

Moisture ingress in PV modules is via absorption with water molecules diffusing through the polymeric materials. The process includes adsorption of water molecules at the surface of the polymer followed by diffusion along a concentration gradient through the material. This process continues until equilibrium with the ambient condition, and the diffusion parameters can be approximated with Fick's second law (Vieth 1991; Crank 1968).

Moisture ingress into a PV module can deteriorate the performance and durability significantly during the module's lifetime in various ways. Moisture causes corrosion in metallic parts, increase the current leakage by increasing the conductivity of the encapsulant (Quintana et al. 2002), delamination and bubble formation. The moisture ingress in PV modules in Miami, Florida, has been correlated with failure rate, especially in hot and humid (damp) conditions (King et al. 2000). This plus other reports show the importance of moisture induced failures (Visoly-Fisher et al. 2003; Malmström et al. 2003).

Investigations by Kempe (Kempe 2006; M.D. Kempe 2005) showed the rate of moisture ingress into PV modules and reported that the diffusivity of water has an Arrhenius dependence on temperature. The diffusion was found to be Fickian within the experimental uncertainty. He reported that in modules with a breathable back-sheet the moisture absorbed at night is desorbed during the day due to the higher temperature of the module and higher ambient water vapour pressure. However, the module can saturate in a rainy climate, especially when there is a drop in the temperature, which can be a substantial problem owing to droplet formation by trapped water. Impermeable

backsheets are better moisture barriers, however, water can still penetrate and reach the centre of the module in a few years via the encapsulant.

Hülsmann et al. (2010) measured water vapour permeation into PV modules by a permeation test device developed and built in the Fraunhofer Institute for Solar Energy Systems (ISE), which is described in (Hülsmann et al. 2009). They conditioned the EVA at 85°C-85% RH, which is a commonly used condition for qualification testing for PV applications. Numerous researchers Hülsmann and colleagues (Hülsmann et al. 2013; Kim & Han 2013; Hülsmann et al. 2010) similarly investigated the water vapour ingress into PV modules under different climatic conditions. They reported that the water concentration in the encapsulant between the glass and solar cells is highly dependent on the climatic conditions. Another important factor is the temperature dependency of the mass transfer and the combination of encapsulant and back sheet materials.

Kapur et al. (2009) investigated the rate of moisture ingress through EVA laminated between impermeable substrates in damp heat conditions (85% RH, 85°C) for 1000 hours. The measurement was determined by the FTIR method and it was reported that the moisture level in the encapsulant could be determined by integration of the Infrared (IR) bands at 1880 nm and 1990 nm. It was seen that the experimental data compared well with that predicted by a Fickian based diffusion model. Table (2.3) presents a summary measured moisture diffusion coefficient in the literature.

Iwamoto & Matsuda (2005) and Rashtchi et al. (2012) investigated the moisture ingress and water concentration in the encapsulant within a PV module. They found that there are notable changes in the FTIR spectrum of EVA between 3400 and 3700 cm^{-1} which is a good indicator of the presence of water.

IEC 61215 is a qualification test that PV modules should pass in order to participate in the solar energy market. Modules that have passed the

qualification test are much more likely to survive in the field. Numerous researchers (Markus Bregulla, Michael Köhl, Benjamin Lampe, Gernot Oreski, Daniel Philipp, Gernot Wallner 2007) investigated the degradation of EVA at 85°C, 85% RH, which is comparable to test 10.13 (damp-heat test) of IEC 61215 Ed. 2 for PV modules. The ATR_FTIR spectra of standard cured EVA showed a growth in the peak at around 3500 cm⁻¹, which is due to water diffusion.

E. U. Reisner et al. (2006) reported that the peak temperature of an insulated Building Integrated Photovoltaic (BIPV) module was 60°C to 80°C while the peak temperature of a free standing module was 40°C to 50°C, where the ambient temperature ranges between 30°C and 35°C in Belem, Brazil. In the first six hours of night the encapsulant absorbed water. After sunrise the module desorbed water due to increasing module temperature which is greater than the ambient temperature. It should be noticed that the influence of relative humidity is not considered in this study.

X. Shi et al. (2009) and Chen et al. (2009) reported the effect of damp heat ageing on the structure and properties of EVA with different vinyl acetate content (VAc). In this study EVA was aged at 40°C-93% RH and analysed with various techniques including ATR-FTIR, DSC and Wide Angle X-ray Diffraction (WAXD). Based on ATR-FTIR results the characteristics of the absorption peaks were identified as presented in Table (2.4). For the sake of quantitative comparison a Carbonyl Index ($CI = A_{1735}/A_{720}$) was introduced and during the eight-week ageing the CI decreased in the first week of the ageing but then increased to equal or more than that of the original values on further ageing. This variation is due to a pyrolysis including a two-step decomposition; acetate pyrolysis evolving acetic acid, followed by the breakdown of the hydrocarbon backbone. However, the presence of oxygen causes ketone formation via acetaldehyde formation and then formation and destruction of aldehydes to form carboxylic acids. It can be concluded that the degradation of all EVA samples, with different VAc, can be characterised by the loss and formation of O=C group which explains the decrease and increase of CI. The

WAXD results suggested there was no significant change observed in the crystalline phase during the ageing. Their DSC results showed the EVA with lower VAc has longer average ethylene sequence length and therefore forms bigger crystals which require a higher temperature to melt. Some DSC results for EVA with 28% VAc (EVA28) showing onset melting temperature (T_m^{on}), final melting temperature (T_m^f) and crystallinity (X_c) are presented in Table (2.5). Their hardness results showed that hardness goes up with decreasing VAc and can be correlated to crystallization. Tensile tests results surprisingly indicated that damp heat ageing had no effect on the tensile properties of the EVA copolymers used in this study.

Table 2.3: Measured diffusion coefficient (D) in the literature.

Material	Method/device	Conditions	D (m ² /s)	Other information	Reference
EVA	Illinoise 7001	50°C, 35°C, 20°C, @ 60% RH	3×10^{-10} 2×10^{-10} 1.5×10^{-10}	-	(Kim & Han 2013)
EVA	Permeation test device (developed by Fraunhofer ISE (Hülsmann et al. 2009))	80°C, 75°C, 55°C, 50°C, 40°C, 30°C, 20°C	7×10^{-9} 8×10^{-9} 9×10^{-9} 9.5×10^{-9} 1×10^{-10} 5×10^{-10} 7×10^{-10}	-	(Hülsmann et al. 2013)
EVA	Gravimetric	60°C, 40°C, 20°C @ 85% RH	3.2×10^{-10} 1.2×10^{-10} 0.8×10^{-10}	Thickness: 1 mm, Laminated with TPT backsheet	(Hülsmann et al. 2010)
EVA	Self-developed permeation test device in Fraunhofer ISE	38°C, 30°C, 22°C @ 90% RH	1×10^{-10} 6.7×10^{-11} 4.2×10^{-11}	-	(Hülsmann et al. 2009)
EVA	Mocon Permatran-W® 3/31	85°C, 60°C, 40°C, 25°C @ 100% RH	7.5×10^{-10} 4×10^{-10} 1×10^{-10} 7×10^{-11}	1000 hours, Thickness: 0.46-2.84 mm	(Kempe 2006)

Oreski & Gernot M. Wallner (2010) investigated the thermal and thermo mechanical behaviour of EVA before and after damp heat ageing by DMA and DSC under three conditions (85°C-85% RH, 65°C-85% RH, 85°C-30% RH). They reported that at certain temperatures the aged materials became softer, showing smaller storage modulus values. The DSC results in this study showed a broad melting area between -20°C and 80°C with a single peak at 45°C and a shoulder at 55°C. There was a secondary melting point observed in the first heating whereas in the second heating the peak at 45°C disappeared and a regular melting peak at 55°C was seen. The secondary melting was assigned to the secondary crystallization, which happens in the area between primary crystals during storage at ambient temperature or exposure to an elevated temperature. Some have attributed the secondary melting point of EVA to a less organised crystal phase (Brogly et al. 1997). Since the melting process of ethylene copolymers starts immediately above the glass transition temperature (T_g) it is suggested that structural changes and rearrangements are possible at room temperature (Loo et al. 2005; Androsch 1999). It was also observed that several changes in the first 250 hours of exposure which strongly depended on the temperature. Whereas the humidity level has only a slight impact on the material properties. The changes observed include recrystallization and increase in storage modulus, which can cause some problems during the module's service life associated with delamination, thermal expansion or external physical stresses such as wind, hail, etc. The stiffening of the EVA can also result in silicon solar cell cracking.

Table 2.4: The characteristics of the ATR-FTIR absorption peaks.

	Absorption peak	Wave number (cm⁻¹)
Ethylene segment	Symmetrical stretching vibration of methylene	2920
	Asymmetrical stretching vibration of methylene	2852
	Deformation vibration of methylene	1465
	Flexural vibration of methyl	1370
	Inner rocking vibration of methylene	721
Vinyl acetate groups	Stretching vibration of C=O	1735
	Asymmetrical stretching vibration of C-O	1237
	Symmetric stretching vibration of C-O-C	1020

Table 2.5: Some DSC results for EVA with 28% VAc (Shi 2008; X. Shi et al. 2009).

Sample	Ageing duration (week)	T_m^{on} (°C)	T_m^f (°C)	X_c (%)
EVA28	0	48.4	81.5	10.10
	1	47.8	81.5	11.66
	8	50.8	82	13.5

In spite of all the previous work, there is still a missing link between the consequences of damp heat ageing, moisture diffusion and moisture concentration gradient within the context of mechanical behaviour and changes in the crystallinity of EVA.

2.4.4 The effect of combined degradation factors

As mentioned in the previous sections, the reliability and performance of PV modules are highly influenced by the behaviour of the encapsulant. The degradation of encapsulant is dependent on the environmental conditions, mainly humidity, elevated temperature and UV (Pern et al. 1996; Pern 1997; Kempe 2010; W. Herrmann, N. Bogdanski 2010).

Peike et al. (2012) investigated the impact of permeation properties and backsheets-encapsulant on the reliability of PV modules. They conditioned the sample under climatic conditions including combined ageing (85°C-85% RH, 85°C-90% RH-190 kWh/m², 60 kWh/m²) up to 1000 hours. The encapsulants used in this study were EVA, Thermoplastic Silicon Elastomer (TPSE), ionomer and Polyvinyl Butyral (PVB). The backsheets materials included Tedlar-PET-Tedlar (TPT) foil, polyamide (PA) sheet and Polyethylene Terephthalate (PET) composite film. The results of the study showed that the average Water Vapour Transmission Rate (WVTR) and Oxygen Transmission Rate (OTR) were higher for the encapsulants in comparison to the backsheets. Hence, the backsheets can be atmospheric gas ingress resistors. They also reported that

after combined UV/DH ageing, yellowing was three to five times greater in the TSPE/TPT, the TPSE/PA and the PVB/PA laminates in comparison to other combination of backsheet/encapsulant.

Kojima (2004) also investigated the effect of combined ageing on the degradation of EVA film. They reported that UV absorbance of EVA is dependent on surface coarseness or the state of moisture absorption. An increase was also seen in the transmissivity of EVA in the region of 250-400 nm which could be attributed to a reduction in the UV absorber used for suppressing photodegradation.

These previous studies have illustrated the influences of moisture/water vapour ingress on the behaviour, properties and structure of EVA. However, there is still a gap in the current knowledge which is the relation between field conditions and the consequences of field ageing on the performance of EVA as the encapsulant. This will be explained in the next section.

2.5 Gaps in the current durability and lifetime studies of PV modules academic research and industry

The proceeding literature review has demonstrated the significant previous work on the durability and reliability of PV modules at a material level, and in the encapsulation material in particular; including an extensive description of the hydro-photo-thermal degradation mechanisms. In particular, it was seen that one of the main degradation products is acetic acid which causes numerous problems such as corrosion in metallic parts and delamination. There is, however, a missing link between the ageing process and the consequences of that ageing within the context of mechanical behaviour and prediction of the EVA photodegradation and thermal degradation. Previous research on EVA has considerably shown that it undergoes degradation following exposure to environmental factors (e.g. UV, humidity and elevated temperature). Despite the information available in the literature on the degradation mechanisms, no work has been reported that correlates the

material's degradation under severe in-service climatic conditions, which is crucial for evaluating the performance of PV modules in a specific environment. There is also very limited work published on the link between the chemical degradation and mechanical behaviour of EVA which needs further investigation. These identified gaps in the literature form the basis for the research challenges identified for this thesis.

2.5.1 Research challenge 1

During operation in the field the temperature of modules can reach up to 85°C. Continuous long term exposure of EVA to high temperature causes thermal degradation. Therefore, it is necessary to isolate this degradation factor in order to predict the lifetime of EVA when it is exposed to the working condition of PV modules.

This research seeks to address the need to understand changes in the EVA as a result of thermal exposure by examining the link between the evolving chemistry, structure, mechanical behaviour and predict the weight loss as a result of thermal degradation.

2.5.2 Research challenge 2

Sunlight is a necessity to produce electricity via PV modules. However the sunlight spectrum includes UV which causes EVA to photochemically degrade. The main product of the photochemical degradation is acetic acid and the reaction also causes discolouration, which affects the durability and performance of the PV modules. Despite the numerous studies on the mechanisms of photodegradation of EVA, there is limited published work on correlating the photodegradation of EVA to structural changes and mechanical property degradation seen when exposing a PV module to operating conditions.

This study aims to address the need to understand the changes that are the result of UV exposure and how they affect the durability and mechanical properties over time. It will examine the link between the chemistry of

photodegradation, the structure, the intrinsic mechanical behaviour and prediction of photodegradation throughout the duration of an accelerated UV ageing degradation test.

2.5.3 Research challenge 3

One of the degradation factors the installed PV modules are exposed to, especially in environments like the UK's, is humidity. While PV modules are on site moisture can penetrate into the modules. The moisture ingress causes various problems such as corrosion, current leakage and delamination. Although there are studies which have investigated the moisture diffusion coefficient and moisture induced degradation, these studies have been performed in idealistic environment which does not represent the in-service environment of the installed PV modules. Thus, it is necessary to investigate the moisture diffusion properties, structure and behaviour of EVA in damp heat.

The present study seeks to address the need to understand the changes in mechanical properties as result of damp heat exposure by examining the link between moisture concentration, structural changes and the mechanical behaviour throughout the duration of an accelerated damp heat ageing test.

2.6 Conclusion

EVA has a complex response to environmental ageing, with noticeable changes in mechanical behaviour, structure, thermal and optical properties. Numerous researchers have studied the effect of environmental factors on the chemical degradation of EVA. In order to predict EVA's thermal and photodegradation in isolation and investigate the moisture absorption behaviour of EVA and its consequence of the structure and mechanical properties of EVA, a comprehensive analysis of the response of EVA to changes in environmental conditions is still required.

In the next chapter the experimental methods adopted for the achievement of the objectives of this research project will be presented.

Chapter 3

Experimental Methods

3.1 Introduction

The aim of the chapter is to describe the material, experimental techniques and general research approaches which were used in this research in order to address the research questions proposed in section (1.5). In particular, it describes:

- the materials used and their storage conditions,
- environmental ageing conditions,
- experimental techniques for the evaluation of the viscoelastic properties of EVA,
- a characterisation procedure to investigate the changes on the crystallinity of EVA as a result of ageing;
- a procedure to investigate the rate of thermal degradation and lifetime of EVA under PV operating conditions;
- a procedure for the evaluation of the chemical changes in the structure of the EVA;
- a procedure to investigate the photodegradation and lifetime of EVA,
- an experimental procedure to investigate the moisture absorption and calculate the moisture absorption coefficient.

As mentioned in the previous chapters, EVA undergoes chemical degradation when it is exposed to the degradation factors of elevated temperature, UV and humidity, which influences the mechanical properties of the material and causes changes in the structure of EVA (Figure (3.1)). In this research the general approach to address the research questions and achieve the research

aim (section (1.4)) is firstly to fully characterise the unaged EVA, which had been isolated from environmental degradation factors. Once the characteristics of the material were understood, the EVA was aged using artificial ageing equipment including a laboratory oven, UV chamber and environmental chamber. In order to understand the degradation mechanisms, each of the degradation factors was isolated and its influence on EVA investigated. With the purpose of investigating the impact of ageing and environmental factors on the properties, characteristics and structure of EVA, the characterisation of EVA was separated into three parts. First, the mechanical properties and morphological changes (crystallinity) as a function of temperature and artificial ageing were determined. Secondly, the chemical degradation of the material was investigated and the degradation rate was determined as a function of temperature/time. Thirdly, the rate of moisture absorption was determined as a function of time and artificial ageing conditions. Then all three factors were combined to investigate how these parts are related and influence each other. Figure (3.2) shows the general experimental approach and the methodology used in the research.

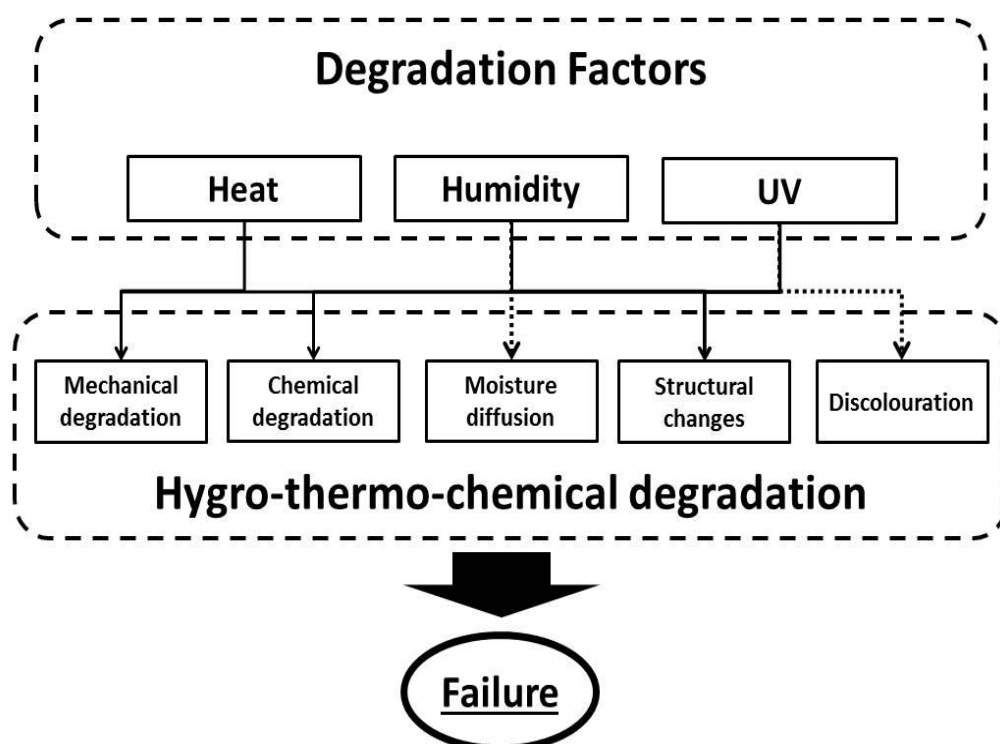


Figure 3.1: A general diagram showing the impact of the degradation factors.

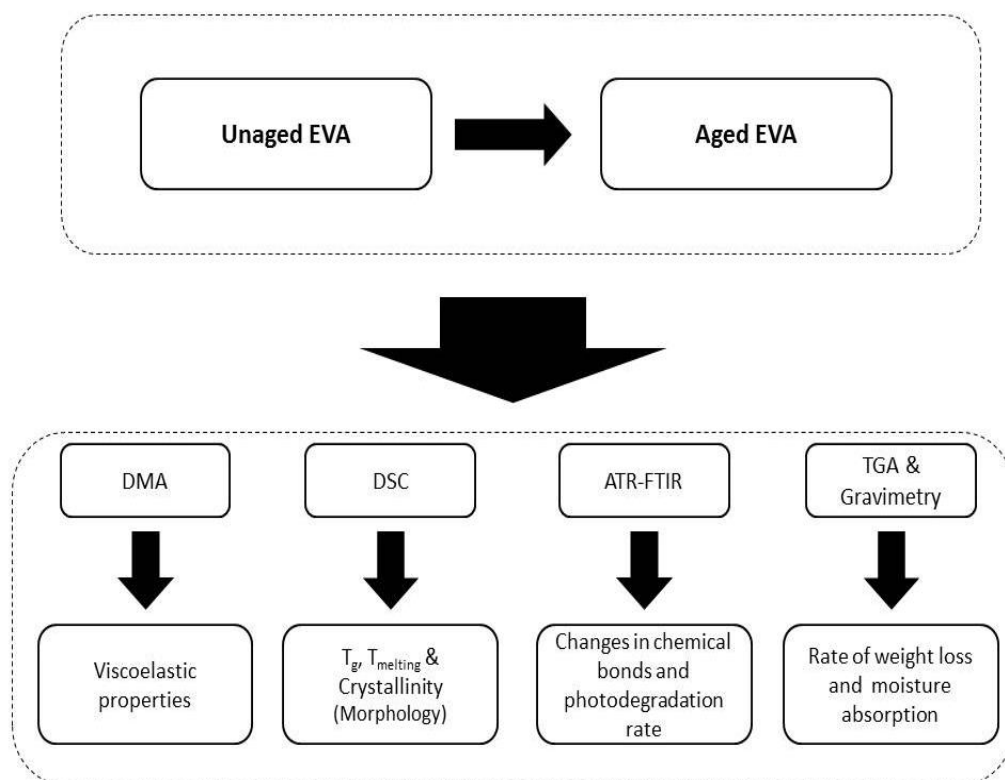


Figure 3.2: A general diagram showing the experimental methodology used in this research.

3.2 Material and storing condition

3.2.1 Material (sample preparation)

Uncured EVA is not suitable to be used as an encapsulant material in PV modules due to low transparency and poor mechanical properties. Figure (3.3) shows uncured EVA which has low transparency. The usual method in the PV industry for curing EVA is to use a laminator which provides a controlled vacuum atmosphere with suitable heating/cooling rates and pressure. Due to the unavailability of a laminator at the start of this research a number of techniques were investigated to prepare good quality samples, including a hot press and autoclave. A description of the various methods investigated for preparing samples is given below, followed by an evaluation of the quality samples manufactured.



Figure 3.3: Uncured EVA (courtesy to SINOVOLTAICS).

3.2.1.1 Hot press

The hot press was made up of two hot plates: the top one being fixed and the bottom one movable. In order to achieve the desired thickness a bespoke mould was designed, as illustrated schematically in Figure (3.4). The mould was of a rectangular shape with dimensions of 80 x 80 x 0.5 mm; consisting of a top plate for uniform distribution of the force, bottom plate and spacer. A release film was used to make sure the EVA samples did not stick to the mould and spacer. The spacer was used to control the thickness of the samples. Before using the mould, all the mould parts and the release film were cleaned with laboratory grade acetone. Uncured EVA (Figure (3.3)), was cut into small sheets with dimensions of 80 × 80 mm to fit in the mould. The samples were put in the mould as separate pieces to prevent air entrapment and bubble formation. The load was applied to the mould by a hydraulic system.

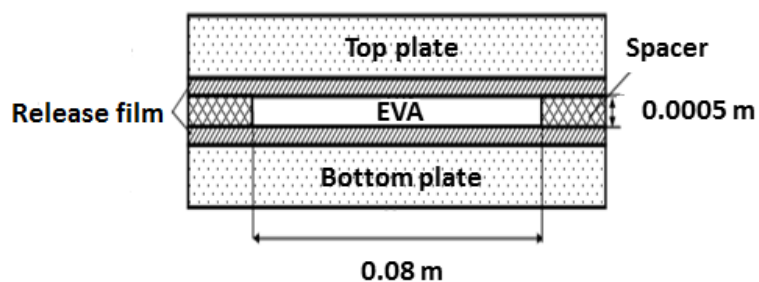


Figure 3.4: Schematic view of the mould used in the hot press.

A temperature of 150°C and duration of 20 minutes were suggested as optimum curing conditions by the EVA supplier. The influence of different pressures and release films on bubble formation, surface flatness and uniformity of thickness was then investigated. PET film was found to be the best release film, but it needed to be removed in hot water for best results. However, a uniform thickness was not achieved and the thickness fluctuates around 10%. Table (3.1) presents a comparative investigation of different release films.

Using a hot press was not an ideal technique due to the uncontrollable heating and cooling rate, inaccurate load control system (± 100 N) and most importantly the imperfect and non-parallel top and bottom plates which prevented the load to be applied to the mould uniformly, resulting in large thickness variation and poor quality cured samples. Therefore, further investigation was carried out to find a better method for EVA curing.

Table 3.1: Release films and release agents used for sample preparation.

Release Film	Problem	Solution	Picture of EVA samples	
Polytetrafluoroethylene (PTFE) film	Very sticky, Leaves residues on the sample			
Polyethylene terephthalate (PET) film	Very sticky	Peel off the film in hot water	First try	After applying solutions
	Forms bubbles	Increase the pressure		
Release mould spray – Long lasting PTFE mould	Very sticky			
Release liquid for epoxy-acrylique-polyester	Rough surface			

After further investigation to find a better curing technique due to unsuitability of the hot press technique, the autoclave was found to be a robust technique, as discussed in the next section.

3.2.1.2 Autoclave

Autoclaves are used for numerous applications, such as to cure coatings, grow crystals under high temperatures and pressures, manufacture carbon fibre composite, due to the capabilities below.

- Air removal (vacuum)
- Controllable heating rate
- Controllable pressure

An autoclave creates a vacuum atmosphere where the mould is and is separated from the pressure chamber with a vacuum bag. The autoclave enables the user to control various parameters including, the temperature of the hot plate, the heating rate and the pressure applied to the mould.

Figure (3.5) presents a schematic view of the autoclave used in this work. The mould is composed of a steel top plate and a steel spacer with a thickness of 0.5 mm. On each side of the spacer, there is a sheet of non-stick release film to prevent adherence of the EVA to the metallic parts of the mould. The mould is covered with a vacuum bag in order to create a vacuum atmosphere around the mould to prevent bubble formation in the sample. A second chamber over the vacuum bag was created by adding a cover plate to apply a uniform pressure to the top of the mould.

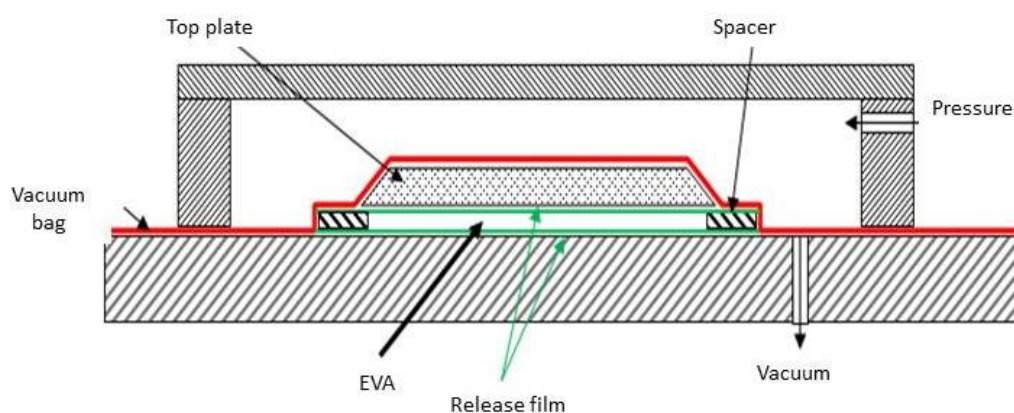


Figure 3.5: Schematic view of the autoclave.

The following procedure was used in curing the EVA in the autoclave.

- The mould was placed on the hot plate and covered with a breathable film and the vacuum bag film,
- A vacuum was applied between the vacuum bag and the hot plate,
- A uniform pressure of 0.21 MPa was applied to the top plate of the mould,
- The final temperature of 150°C was set at the heating rate of 4°C/min,
- After reaching the final temperature of 150°C, samples were kept at this temperature for curing,
- The mould was cooled down by natural convection while exposed to room temperature.

Figures (3.6)-(3.7) demonstrate the preparation of the autoclave and mould positions on the autoclave hot plate.

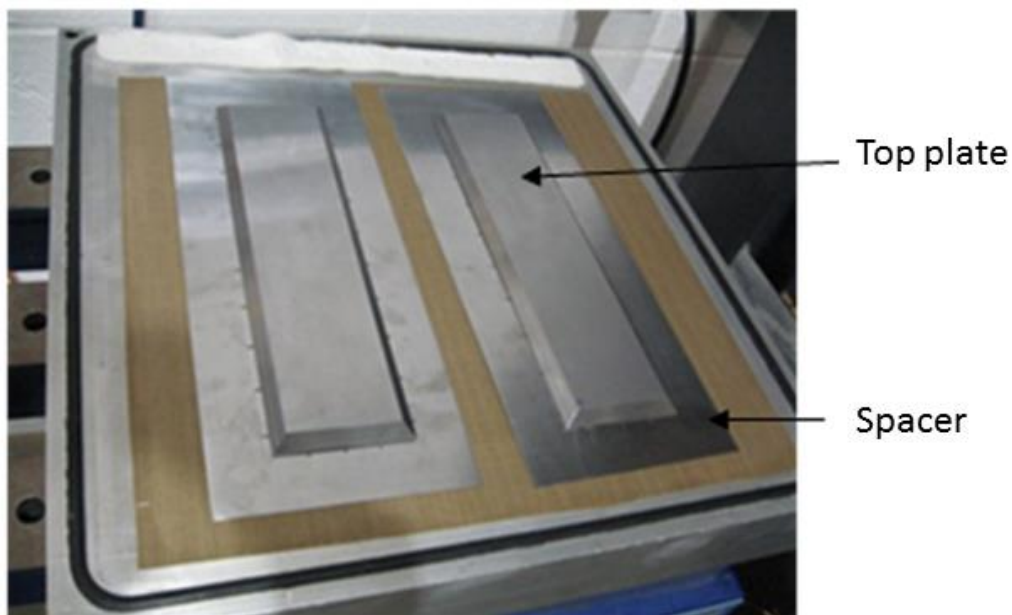


Figure 3.6: Autoclave preparation for EVA curing.

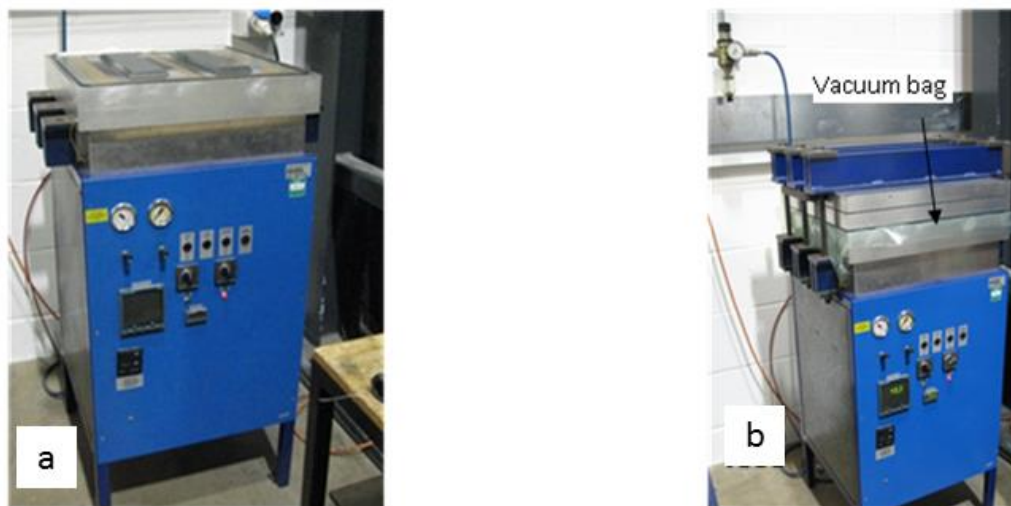


Figure 3.7: (a) Autoclave with samples, spacers and top plate, (b) Autoclave during EVA curing.

The autoclave cure process took approximately two hours and two samples with dimension of $300 \times 80 \times 0.5$ mm were cured at a time. The quality of the samples cured in autoclave was significantly better than that of the hot press cured EVA. The thickness was uniform, with a variation less than 2%, and the

samples were transparent. However due to the unavailability of the autoclave, uncontrollable cooling system and cooling the samples by natural convection this method was found not to be suitable and as consistent as laminator in curing the EVA samples. In the next section the laminator is described.

3.2.1.3 Laminator cured EVA

After trying different curing techniques it was found that hot press was not suitable to cure EVA due to its inability to create vacuum atmosphere, uncontrollable cooling rate and not parallel plates. Autoclave was also not an ideal method to cure the EVA due to uncontrollable cooling process. Finally, a laminator was used as the most reliable technique which is the common way to laminate PV modules in the PV industry. The base material used in this research was a laminator cured EVA copolymer with 33% vinyl acetate, which was supplied in 0.5 mm thick sheets (provided by Ecole Polytechnique Fédérale de Lausanne (EPFL)). The curing of EVA was performed in a controlled atmosphere in a 3S Swiss Solar Systems laminator S1815 manufactured by 3S Modultec, Switzerland. The curing process including the steps below was performed by (Heng-Yu Li, Laura-Emmanuelle Perret-Aebi, Ricardo Theron, Christophe Ballif, Yun Luo 2010; Li et al. 2013).

1. Preheating for approximately 300 seconds (plate temperature at 140°C),
2. A pressure of 0.1 MPa was applied to the laminates at the beginning of the curing time under vacuum at about 100 Pa,
3. Curing time was set to 1300 seconds,
4. The pressure was removed and the cooling process started.

In the next section the advantage and disadvantage of the curing methods are discussed.

3.2.1.4 Comparison of manufacturing methods

Various methods were used to cure the EVA. Table (3.2) presents the approach taken to select the most suitable curing method in this research.

The evaluation of manufacturing process indicated that a laminator is the most suitable method of manufacturing. Although hot press and autoclave manufactured samples were used in the early stage of this work all samples used to produce results in this study were manufactured using the laminator.

3.2.2 Storage of samples

In order to minimize stored samples from degradation factors (elevated temperature, UV and humidity) the EVA sheets were stored in a dark desiccator at room temperature ($22\pm 3^{\circ}\text{C}$) and humidity around 15% RH after manufacture. In order to include the influence of the storage conditions on the test results, control samples were tested along with the aged samples in the experiments. Control samples were kept in the desiccator during all ageing time and compared against the aged samples.

3.3 Ageing conditions

To determine the effect of environmental stresses on polymeric materials under controlled conditions the real environmental conditions experienced by PV modules were simulated in the laboratory. Artificial ageing was used since ageing in field conditions is prohibitively time consuming and difficult to control. Since the main degradation factors are elevated temperature, UV and humidity/moisture, to conduct a thorough investigation and cover all the environmental degradation factors the ageing has been classified in to three main groups as thermal ageing, UV ageing and damp-heat ageing, as described below.

Table 3.2: Overview of the curing techniques.

Technique	Disadvantage	Advantage	Problems	Selected
Hot press	No controllable heating/cooling rate, No precise pressure controlling, No parallel pressing plates, No vacuum atmosphere	–	Nonuniform thickness, bubble formation, low transparency	No
Autoclave	No controllable cooling rate, Limited sample curing size	Vacuum atmosphere, precise pressure controlling, controllable heating rate	Great amount of time and energy required, properties affected by improper cooling	No
Laminator	–	Controllable uniform pressure & heating/cooling rate, Vacuum atmosphere, large curing plate	–	<u>Yes</u>

3.3.1 Thermal ageing

In order to investigate the effect of heat on the mechanical and thermal properties of EVA and its thermal degradation the EVA sheets were aged in a dark laboratory oven at 85°C for up to 80 days. Figure (3.8) shows the thermal ageing condition. A batch of EVA samples was also aged at 65°C to be compared to the UV aged samples. The samples were kept in dark

atmosphere away from light and humidity in a desiccator to exclude the effects of UV and humidity and to isolate the effect of heat.

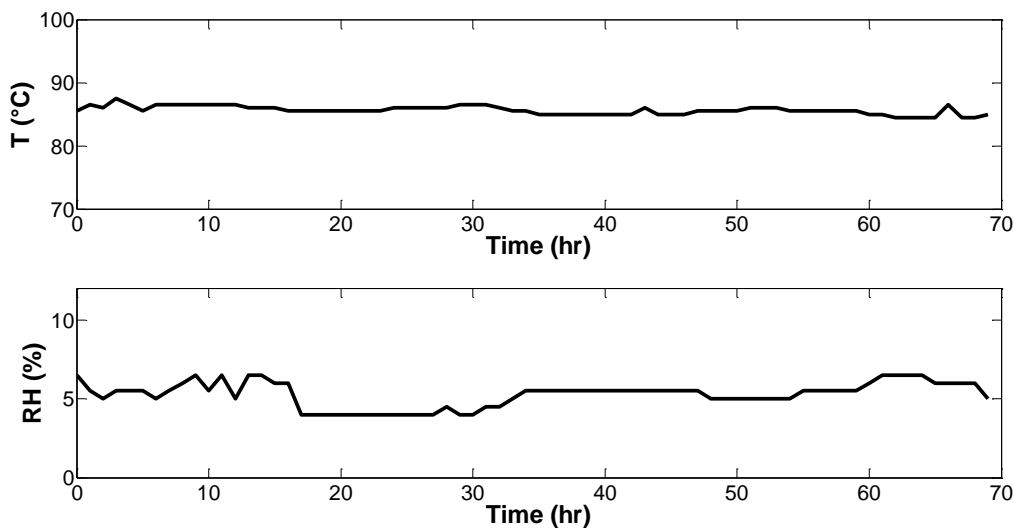


Figure 3.8: Thermal ageing conditions in the laboratory oven.

3.3.2 UV ageing

The effect of UV exposure on the properties and photodegradation of the EVA was investigated by ageing in a Q-Sun, 1-Xenon up to 800 hours using a daylight filter. The UV intensity was 0.68 W/m^2 at 340 nm and 50°C . This intensity is equal to July midday sunlight in Colorado, USA as mentioned in Q-Sun manual. For the sake of comparison, a batch of EVA samples were kept in a dark desiccator at room temperature as control samples and another batch was aged in a dark laboratory oven at 65°C as stated in section (3.3.1). The samples used for the analysis of UV effect included the UV irradiated side (top side) of the UV aged samples, the UV non-irradiated side (back side) of the UV aged samples, thermally aged sample (no UV) and control sample (no UV, no humidity, room temperature).

3.3.3 Damp-heat ageing

In order to study the presence of moisture diffusion in the EVA and the impact of absorbed moisture on its mechanical properties and morphology, samples were aged in an environmental chamber at 85°C -85% RH which is commonly used for material qualification testing of PV applications (Hülsmann et al.

2013) and by using a potassium chloride (KCl) salt solution in a sealed chamber to obtain conditions of $85\pm 3\%$ RH at room temperature ($22\pm 3^\circ\text{C}$). Figures (3.9) and (3.10) show the damp heat ageing conditions in the environmental chamber and the salt solution chamber respectively. DMA and DSC were conducted on samples aged up to 9 weeks. The amount of moisture absorbed as a function of time was measured by recording the samples' weight every 24 hours in the early ageing period and then every 48 hours. This was to enable the study of moisture diffusion kinetics and saturation equilibria.

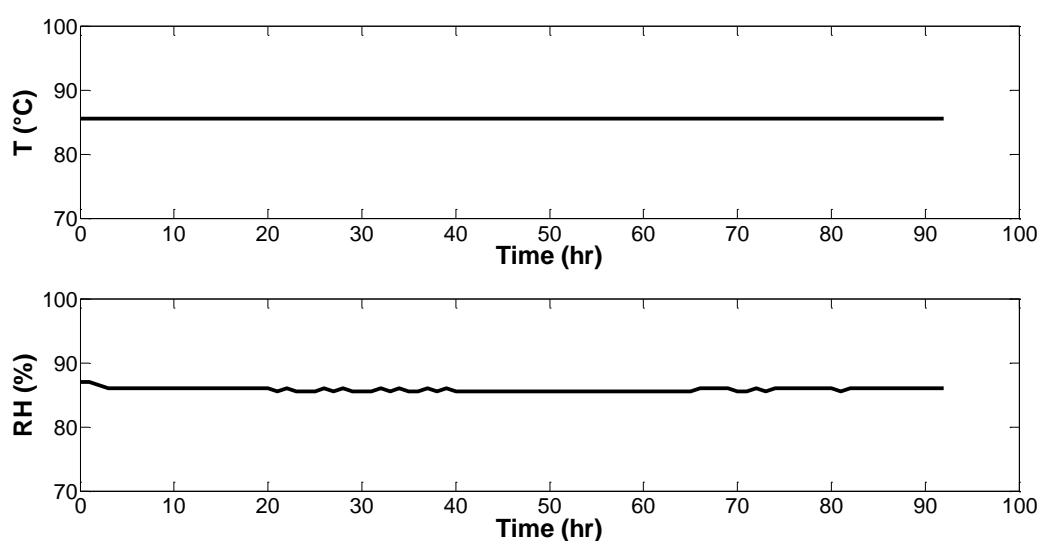


Figure 3.9: Damp heat ageing conditions in the environmental chamber.

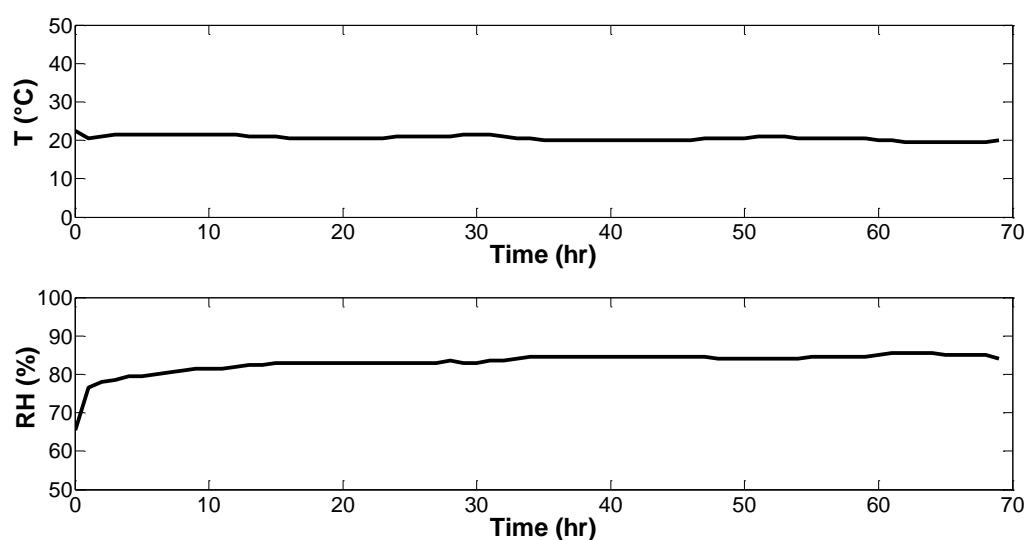


Figure 3.10: Ageing conditions in the salt solution chamber.

3.4 Experimental techniques

Krauter et al. (2011) reported that a single test cannot be used as the only measure to characterise durability, for instance there have been cases with perfectly cured EVA with poor mechanical properties. In order to carry out a comprehensive investigation of the material properties and the ageing impact on them the characterisation of EVA was separated into different parts. The general approach in order to address the research aims was to investigate various properties and characteristics of the EVA before and after ageing. Thus, degradation rate and the effect of ageing on the EVA properties were investigated as a function of ageing duration. These properties include:

- The rate of thermal degradation as a function of temperature and ageing duration.
- Viscoelastic mechanical properties as a function of temperature and artificial ageing.
- The thermal and morphological properties, such as glass transition temperature (T_g) and degree of crystallinity (X_c) as a function of ageing duration.
- The photodegradation rate as a function of exposure duration in the case of UV ageing.
- The rate of moisture absorption as a function of temperature.

A number of different experimental techniques were used to enable us to investigate the above mentioned properties as listed below.

- Differential Scanning Calorimetry (DSC); for investigation of the structure and state of the material as the temperature is changed
- Thermo-gravimetric Analysis (TGA) to investigate the evolution of degradation products from a sample exposed to changes in temperature and thus, the reaction rates
- Dynamic Mechanical Analysis (DMA) to study the viscoelastic mechanical properties of the material and their relation with the ageing conditions

- Attenuated Total Reflectance-Fourier Transform Infrared Spectroscopy (ATR-FTIR) to investigate the rate of the evolution of degradation products and chemical changes as the material aged.
- Gravimetric and Water Vapour Transmission Rate (WVTR) testing to calculate the moisture absorption rate when exposed to a damp heat environment.

The experimental techniques used in this work are explained in more detail below.

3.4.1 Differential Scanning Calorimetry (DSC)

DSC is a calorimetry method which measures heat flow as a function of temperature associated with thermally active transitions such as T_g and X_c . In this study DSC was used to investigate the impact of ageing on the thermal properties (T_g) and structural changes (X_c). The relative crystallinity, X_c , of the samples was calculated as a function of ageing duration through

$$X_c = \frac{\Delta H_f}{\Delta H_f^*} \times 100\% \quad (3.1)$$

where ΔH_f^* is the fusion enthalpy of a perfect polyethylene (277.1 J/g) crystal and ΔH_f is the enthalpy of fusion of the EVA samples, respectively (J. Brandrup 1999).

All DSC experiments were conducted in a nitrogen atmosphere with a flow rate of 50 ml/min using a TA-Q10 (TA Instruments, USA). In order to study the unaged and aged material and also the pure material after erasing the thermal history of the samples there was a need to program the DSC test steps. The DSC program used to evaluate the behaviour of the previously cured and aged EVA samples was a heat-cool-heat cycle based on ASTM-D 3418-08. In this study the first heating was at 10°C/min, from -75°C to 250°C.

The temperature was held at 250°C for 5 min, to make sure the sample is stabilized, and then cooled down at -10°C/min to -75°C and held at this temperature for 5 min. Finally the sample was heated again to 250°C at 10°C/min. It should be mentioned that the first heating was to investigate the impact of ageing on EVA and the second heating was to erase the thermal history regarding the curing, storing conditions and the ageing in order to investigate the properties of EVA independent from these effects. Samples were cut into circular disc shapes weighing around 7 mg. All DSC experiments were carried out in hermetic Aluminium pans and all the thermograms are Exo Up.

3.4.2 Dynamic Mechanical Analysis (DMA)

DMA is a technique where a small deformation is applied to a sample in a cyclic manner in order to investigate the properties of viscoelastic materials. This allows the material's response to stress, temperature and frequency to be studied. DMA works by applying a sinusoidal deformation to a sample of known geometry. The sample can be subjected to a controlled stress or strain. For a known stress, the sample will then deform a certain amount. How much it deforms is related to its stiffness. DMA measures stiffness and damping, these are characterised by modulus and $\tan(\delta)$. The storage modulus (E') and loss modulus (E'') are the measures of the sample's elastic and viscous behaviour respectively. The ratio of the loss modulus to the storage modulus is $\tan(\delta)$ which is a measure of the energy dissipation of a material.

Since EVA is a viscoelastic material it is important to apply a technique which is able to measure the viscous and elastic properties of EVA. In this research DMA was performed to investigate the temperature dependant viscoelastic properties of the EVA. Samples were loaded in tension at 1 Hz while the temperature was ramped from -70°C to 100°C at a heating rate of 5°C/min. DMA is tensile test used instead of shear test due to the capability of tensile test in temperatures below the glass transition temperature. DMA shear test is better test in temperature above the glass transition temperature.

3.4.3 Thermogravimetric Analysis (TGA)

TGA is a thermal analysis technique which measures the amount and rate of change in the weight of a material as a function of temperature or time in a controlled atmosphere. TGA measurements are used primarily to determine the composition of materials and to predict their thermal stability up to elevated temperatures.

Heat is one of the degradation factors which influences the performance of EVA as encapsulation material in PV modules, therefore, it is important to understand its thermal degradation and investigate the thermal stability. In this regards TGA was used as the technique in the present study. All experiments were performed in a nitrogen atmosphere with a flow rate of 100 ml/min. TGA analysis under dynamic conditions was carried out using a TA SDT-600 (TA Instruments, USA) at heating rates of 5, 10, 15 and 20°C/min, recording mass loss and the rate of mass loss as functions of temperature. Samples were cut into circular disc shapes weighing around 15 mg. All TGA experiments were carried out in platinum pans.

3.4.4 Attenuated Total Reflectance-Fourier Transform Infrared Spectroscopy (ATR-FTIR)

Fourier Transform Infrared (FTIR) spectroscopy is a technique that is often used to study the chemical changes that occur in a material as a function of temperature and/or time. FTIR spectroscopy is a reliable fingerprinting method. Many substances can be characterised, identified and also quantified. Traditionally IR spectrometers have been used to analyse solids, liquids and gases by means of transmitting infrared radiation directly through the sample. Attenuated Total Reflectance (ATR) has in recent years revolutionized solid sample analysis owing to its capability to resolve the challenging parts of infrared analysis, namely sample preparation and spectral reproducibility. ATR uses the property of total internal reflection resulting in an evanescent wave. A beam of infrared light is passed through the ATR crystal in such a way that it reflects at least once off the internal surface in

contact with the sample. This reflection forms the evanescent wave which extends into the sample. The penetration depth into the sample is typically between 0.5 and 2 micrometres.

Since the degradation factors cause structural changes in EVA it is needed to understand these changes and investigate the result of ageing in EVA. To fulfil this need, in this study ATR-FTIR was used to study the variation of different chemical bonds as a result of UV and thermal ageing. ATR is not a very useful technique to investigate chemical changes caused by moisture absorption because information is obtained only from a few microns of the surface (Morlat-Therias et al. 2007). ATR-FTIR spectra were obtained for the UV irradiated side and non-irradiated side during ageing at intervals of 48-72 hours in order to monitor molecular changes due to UV ageing. The scanning range was 500 cm^{-1} to 4000 cm^{-1} with a resolution of 8 cm^{-1} at 32 scans. In order to obtain quantitative comparison of specific functional group formation during ageing, the absorbance peak intensities were normalized with respect to the absorbance of the methylene sequence ($-\text{CH}_2-\text{CH}_2-\text{CH}_2-$) at 721 cm^{-1} (Eq. (3.2)). It is assumed that the amount of these sequences does not change with respect to changes in the other bands (Copuroglu & Sen 2005).

$$\text{Normalised absorbance} = \frac{A_{\text{specific peak}}}{A_{721}} \quad (3.2)$$

In order to eliminate the effect of the air present in the spectroscopy chamber, the spectra for air was subtracted from the final results.

3.5 Moisture diffusion coefficient measurement methods

3.5.1 Gravimetric measurements

Moisture diffusion in EVA films was investigated by the gravimetric method in which weight changes in samples were measured as a function of time using an OHAUS PA214 Pioneer Analytical Balance (Ohaus Corporation, USA) with a precision of 0.1 mg. Samples were taken out of the environmental chamber every 24 (early stage of ageing) and 48 hours to be weighed. Care was taken to make sure that the balance was clean and accurately calibrated and zeroed prior to each set of weighing.

3.5.1.1 Material and sample preparation

The unaged material was cut into square samples of 70×70 mm with a thickness of 0.5 mm, in order to perform gravimetric tests. To calculate the error 5 samples (free standing film) were prepared for each test.

3.5.1.2 Sorption measurements

The sorption experiment was carried out in a calibrated environmental chamber at the conditions described in section (3.3.3). During all damp-heat experiments the moisture contents were determined gravimetrically based on Eq. (3.3) (Abdelkader & White 2005).

$$M_t(\%) = \frac{m_t - m_{dry}}{m_{dry}} \times 100 \quad (3.3)$$

where M_t is the moisture content at time t , m_t is the specimen's weight at time t and m_{dry} is the weight of the dry specimen. The assumption, therefore, is that all mass change in the sample can be attributed to change in the amount of absorbed moisture only.

3.5.2 MOCON Water Vapour Transmission Rate technique to measure diffusion coefficient

An alternative technique that has been used to obtain the diffusion coefficient of EVA is by using MOCON® water vapour devices. MOCON® measures the Water Vapour Transmission Rate (WVTR). Assuming Fickian diffusivity WVTR can be described by Eq. (3.4).

$$WVTR_{(t)} = \frac{Dc_s}{l} \left[1 + 2 \sum_{n=1}^{\infty} (-1)^n e^{(-Dn^2\pi^2t/l^2)} \right] \quad (3.4)$$

where D is the moisture diffusion coefficient determined by the time required to reach steady state, c_s is saturation concentration which is determined by the steady state WVTR, l is sample thickness, and t is time.

As Figure (3.11) illustrate the MOCON® water vapour test instrument consists of one or more test cells. The test sample divides the cell into two chambers, one with water vapour at a constant relative humidity (RH) and the other with a nitrogen carrier gas to produce a dry environment. As soon as the water vapour molecules permeate through the film they are picked up by the nitrogen carrier stream and taken to the detector. The flow rate of the nitrogen stream keeps the carrier side of the film at virtually 0% RH, thus maintaining a constant flow gradient throughout the test. A pulse modulated infrared detector is used to measure the amount of water vapour in the nitrogen carrier stream. The WVTR is then calculated from the amount of moisture in the stream, the carrier gas flow rate and the area of film sample being tested. The water vapour permeability can then be calculated using the additional input of driving force and sample thickness.

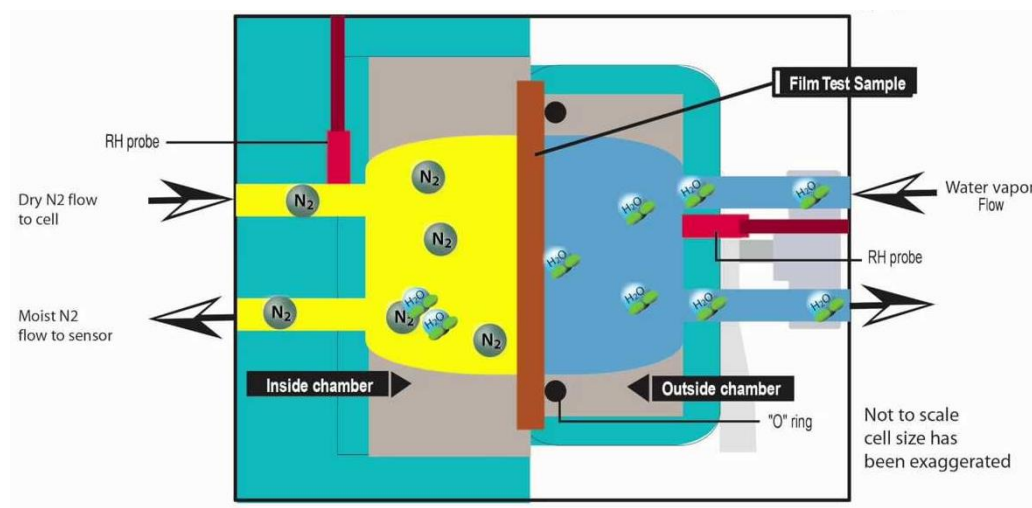


Figure 3.11: Diagrammatic side view of WVTR test cell (Copyright 2012 MOCON® Inc).

In order to obtain the diffusion coefficient of our EVA via the WVTR technique, samples were sent to RDM TEST EQUIPMENT® laboratory, the UK. All the samples were analysed on a Mocon Permatran-W Water Vapour Permeability Instrument (see appendix A). The test conditions are presented in Table (3.3).

Table 3.3: Water Vapour Transmission test condition provided by RDM TEST Equipment®.

Test Gas	Water Vapour	Test Temperature	40 (°C)
Test Gas Concentration	NA	Carrier Gas	Nitrogen
Test Gas Humidity	100% RH	Carries Gas Humidity	0% RH

3.5.3 Comparison of moisture diffusion coefficient measurement methods

Gravimetric measurement of moisture diffusion coefficient is a direct method where samples are exposed to humidity and the weight changes in samples were measured. Then moisture diffusion coefficient is determined via Fick's second law after reaching steady state where the diffusion is Fickian.

WVTR is an alternative method where the samples are placed in a MOCON[®] device at a controlled environment and exposed to humidity after being degassed. This method is performed in an environment where it is reassured there is no humidity in the samples prior to the test and the samples are isolated from external environmental factors such as UV and O₂. The device measures water vapour transmission rate and moisture diffusion coefficient comes from Eq. (3.4).

The MOCON[®] condition is ideal and the test time is much shorter where in gravimetric test the samples are exposed to elevated temperature and possibly to other degradation factors for a much longer time. It should also be mentioned that it is reported that using MOCON[®] devices are not suitable for barrier films with WVTR lower than 10^{-3} (g/m² d) (Hülsmann et al. 2009).

3.6 Summary

The following section summarises the previously described methodology adopted for the achievement of the objectives of this research project. In regard to the procedures mentioned in Sections (3.1)-(3.4), the following considerations could be made:

- Different curing techniques were investigated to prepare EVA samples for analysis and the lamination technique was found to be the most reliable. The EVA used in this work was provided by Ecole Polytechnique Fédérale de Lausanne (EPFL) in form of cured sheets with 33% of vinyl acetate and 80% of gel content.
- The EVA sheets were stored with minimal degradation factors, in a dark desiccator at room temperature and low humidity (around 15% RH) prior to testing or ageing.
- In order to investigate the influence of the environmental stresses (elevated temperature, UV, humidity), EVA was aged using artificial ageing under the conditions described in section (3.3).

- Various experimental techniques were used to characterise the effect of ageing on the EVA. These techniques enabled the investigation of structure and state of the material (DSC), the thermal stability and evolution of degradation products (TGA), the viscoelastic mechanical properties of the material (DMA), the rate of the evolution of degradation products and chemical changes as the material is aged (ATR-FTIR) and the moisture absorption rate (gravimetric and MOCON®).
- This chapter reported the methodologies and procedures which have been used for the achievement of the objectives (described in section (1.5)).
- Sections (3.2)-(3.4) outline the approaches that were used to achieve the results presented in Chapters 4 to 6.

Chapter 4

Examination of the Response of Ethylene-vinyl Acetate Film to Thermal Ageing

4.1 Introduction

The practical importance of EVA has meant that many studies have been carried out to investigate its chemical structure and thermal degradation, but very few studies have comprehensively investigated its performance under a PV module's working condition (Pern & Glick 1997; Agroui et al. 2007). The previous studies have illustrated the main mechanisms through which degradation of EVA occurs. However, the influence of thermal ageing on the mechanical properties and morphology of EVA used as PV encapsulation material, with high vinyl acetate content (>30% VAc), has not been investigated thoroughly and there is a missing link between the ageing process and consequences of that ageing within the context of its mechanical behaviour. This study is motivated by the need to investigate the thermal degradation and viscoelastic properties of unaged and aged EVA films and the generation of inputs to models that can then predict the lifetime of encapsulants in-service.

Thermal degradation in polymers is related to significant changes in molecular state as the thermal energy provides a driving force for chemical reactions. Elevated temperatures cause the components of the long chain backbone of the polymer to separate (molecular chain scission) and react with one another to change the properties of the polymer. Solid polymeric materials undergo both physical and chemical changes when heat is applied; this will usually

Examination of the Response of Ethylene-vinyl Acetate Film to Thermal Ageing

result in undesirable changes to the properties of the material (Pielichowski & Njuguna 2005).

This chapter seeks to address the need to understand the changes in mechanical properties on thermal ageing by examining the link between the chemistry, the structure and the mechanical behaviour throughout the duration of an accelerated thermal only ageing test. Figure (4.1) illustrates the approach taken and techniques used in this investigation.

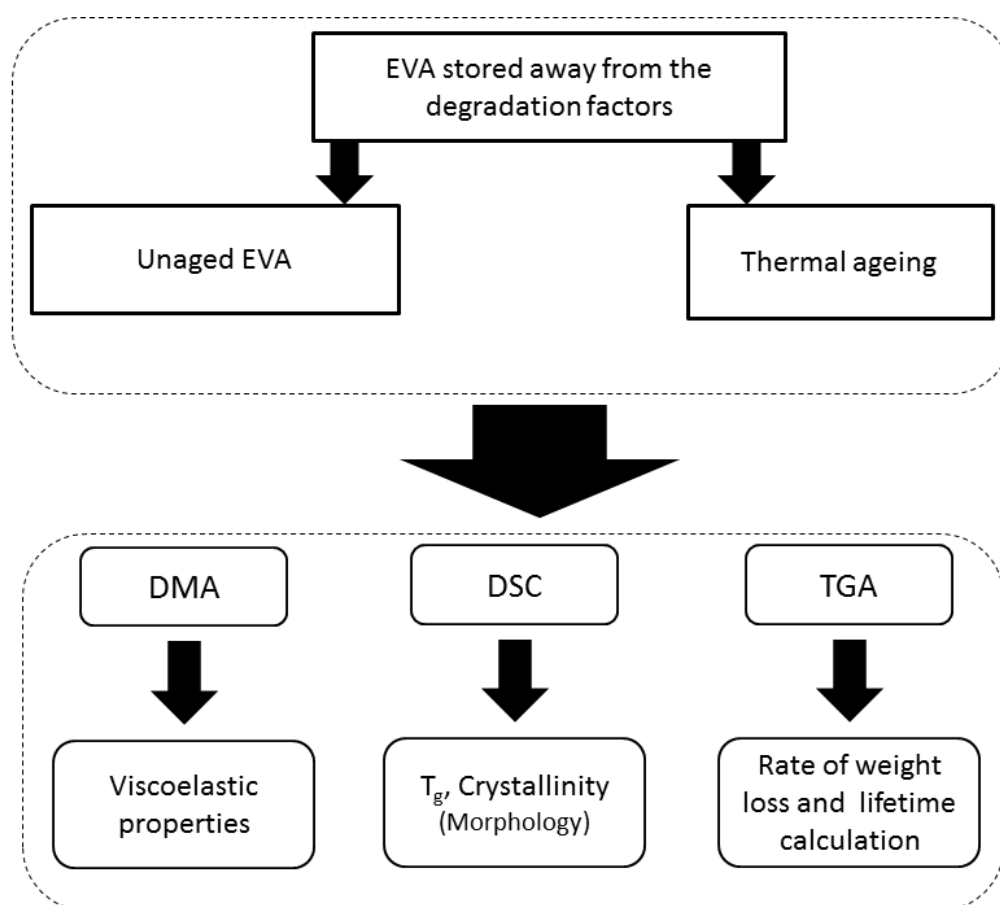


Figure 4.1: Flowchart of investigation of EVA's response to thermal ageing.

The approach taken in this study was to fully characterise the material behaviour and correlate this with measures of thermal degradation by measuring weight loss, determining the kinetics of reactions and investigating structural changes and changes in the mechanical properties, which can be

deduced from calorimetry techniques and dynamic mechanical analysis respectively.

4.2 Theory of kinetics of degradation

The modelling of thermally activated reactions is of concern in many engineering applications and has been the subject of significant research (Starink 2003; Vyazovkin 2006; Órfão & Martins 2002; Muralidhara & Sreenivasan 2010; Morshedien 2009; Wang et al. 2004; Gu et al. 2012; Salin & Seferis 1993; Hamed Gholami, Gholam Reza Razavi 2011). In order to investigate the kinetics of thermal degradation of EVA and calculate the kinetic parameters the Kissinger–Akahira–Sunose (KAS) method was used. This is also known as the generalised Kissinger method (Starink 2003).

The rate of material conversion ($d\phi/dt$) of a solid state process has the form presented by Eq. (4.1)

$$\frac{d\phi}{dt} = K(T)f(\phi) \quad (4.1)$$

where ϕ is the conversion degree, t is the reaction time, K is a reaction rate which depends on the temperature (T) and $f(\phi)$ is a kinetic model function which is a first order case for thermal degradation of EVA (Bianchi et al. 2011).

In this study the conversion degree is defined by Eq. (4.2)

$$\phi = \frac{m_0 - m_t}{m_0 - m_\infty} \quad (4.2)$$

where m_0 , m_t and m_∞ are initial sample mass, sample mass at time t and sample mass at the end of the reaction, respectively. As the reactions to be

considered here are related to thermal processes, $K(T)$ is assumed to be of an Arrhenius form, such that Eq. (4.1) becomes.

$$\frac{d\phi}{dt} = ae^{\left(\frac{-E}{RT}\right)}f(\phi) \quad (4.3)$$

where a is a pre-exponential (frequency) factor, E is the activation energy and R is the universal gas constant. For non-isothermal experiments carried out with a constant heating rate, $\beta = \frac{dT}{dt}$, it is possible to arrive at Eq. (4.4).

$$\frac{d\phi}{dT} = \frac{a}{\beta} e^{\left(\frac{-E}{RT}\right)}f(\phi) \quad (4.4)$$

E can then be obtained from non-isothermal data without choosing the reaction model. The generalised Kissinger's method is an established technique to calculate the activation energy based on the rate equation at the maximum reaction rate. At this point, $\left(\frac{d^2\phi}{dt^2}\right) = 0$ allows for the calculation of E at the maximum rate of degradation, when the heating rate is constant, and the time and temperature derivatives of weight loss are linearly related. Therefore, data can be plotted as a function of time or temperature and analysed using Eq. (4.5) which comes from Eq. (4.3) (Sánchez-Jiménez et al. 2008).

$$\ln \frac{\beta}{T_p^2} = \ln \left[\frac{a \cdot R}{E} \right] - \frac{E}{R \cdot T_p} \quad (4.5)$$

where T_p is temperature at the maximum degradation rate and β is the heating rate. It is possible, therefore, to plot $(\ln\beta/T_p^2)$ vs. $1/T_p$ and obtain the

activation energy and pre-exponential factor from the slope and intercept respectively. Figure (4.2) shows the flowchart of lifetime calculation. The advantage of this method is that it enables the activation energy to be obtained independently of the kinetic model (Starink 2003).

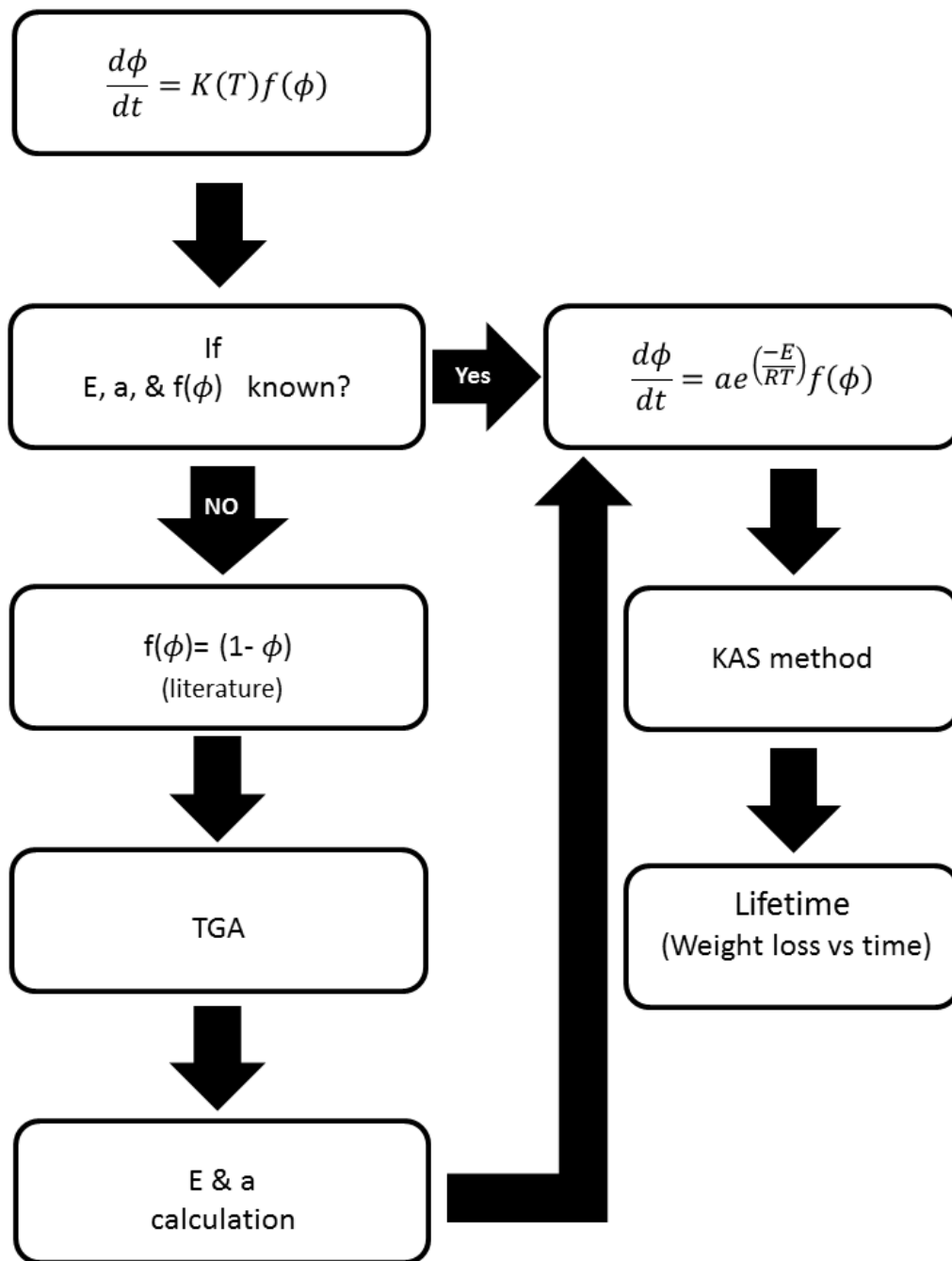


Figure 4.2: Flowchart of the investigation the weight loss of EVA regarding the thermal degradation only.

4.3 Results and discussion

The thermal ageing experiments were performed according to the ageing conditions and experimental techniques described in sections (3.3) and (3.4) respectively. The results of the TGA, DMA and DSC are presented below.

4.3.1 Thermogravimetric Analysis (TGA)

Figure (4.3) shows TGA curves corresponding to dynamic experiments carried out at a range of heating rates. The results show evidence of a two-step thermal degradation process. The first stage, completed at around 370°C (rescaled in Figure (4.4)), can be attributed to a deacetylation process in the vinyl acetate fraction, since it is reported that acetic acid is lost in the first thermal degradation step, leaving a polyunsaturated linear hydrocarbon (Dolores Fernández & Jesús Fernández 2007; Zanetti et al. 2001; McGrattan 1994). The (TG)/FTIR investigation of EVA's pyrolysis (Marcilla et al. 2005) showed that the evolved gas were mainly acetic acid and small quantities of CO, CO₂ and CH₄. The second stage has previously been identified as complete chain scission of the residual main chain (within temperature range of 380-480°C). As should be expected, the temperature at which the reaction is complete increases as the heating rate increases.

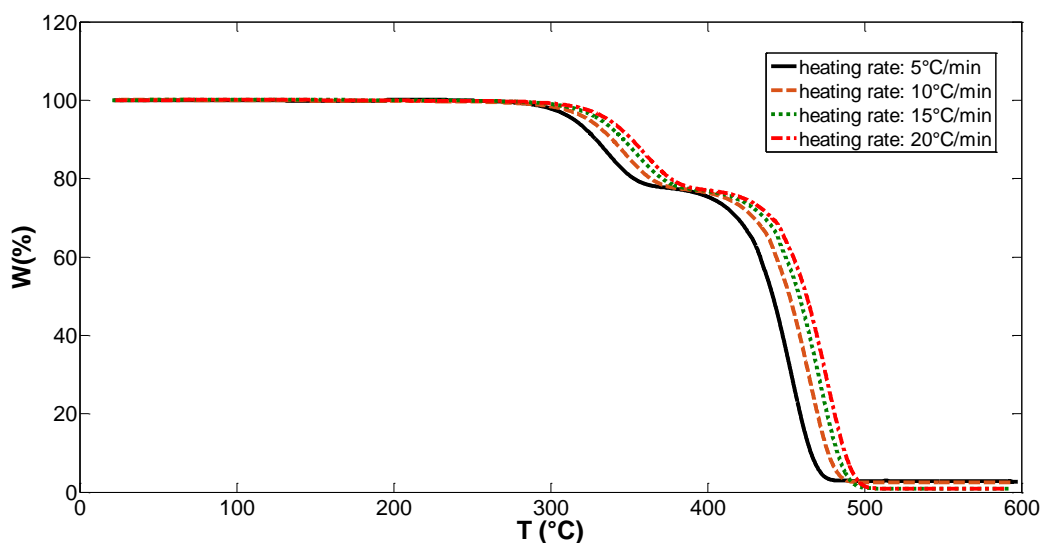


Figure 4.3: TGA thermograms of EVA at different heating rates (weight percentage versus temperature).

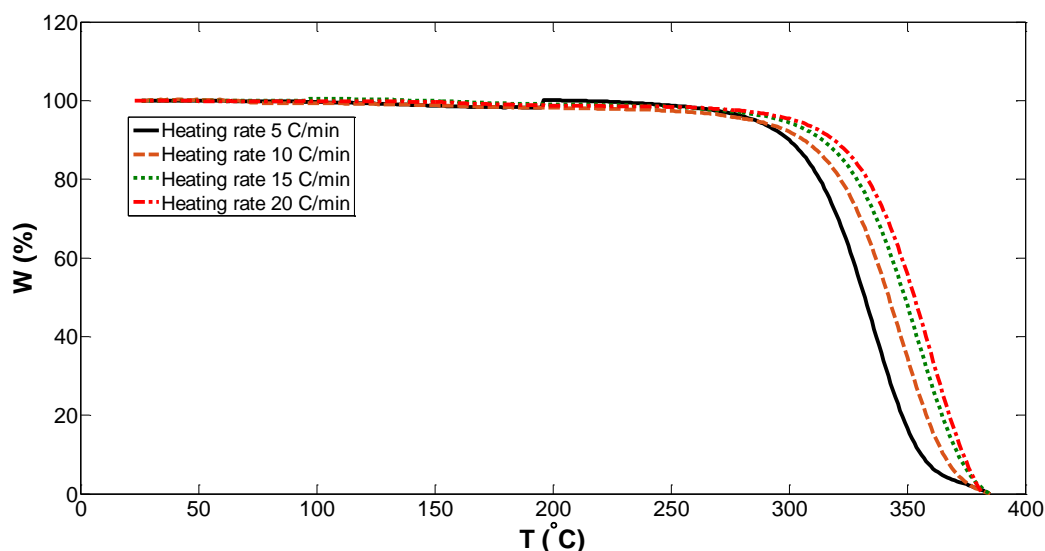


Figure 4.4: Rescaled TGA thermogram of EVA at different heating rates (weight percentage versus temperature).

Since the maximum temperature that photovoltaic systems operate is around 85°C, chain scission is not considered as significant in this work, therefore, the focus is on the deacetylation of EVA. Figure (4.5) shows the derivative of weight as a function of temperature, illustrating the temperature of the peak degradation rate, which is used to calculate the activation energy and pre-exponential factor based on the generalized Kissinger’s method, described earlier. Table (4.1) shows T_p for the first weight loss at different heating rates which were used in Kissinger method to calculate the activation energy.

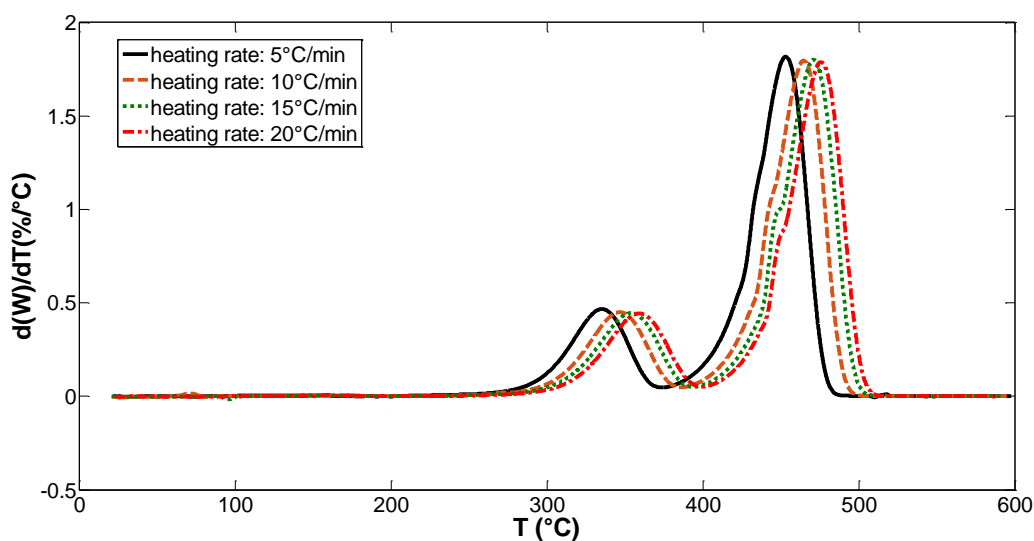


Figure 4.5: Derivative of weight loss to temperature for unaged EVA at different heating rates.

Table 4.1: Temperature of peak degradation rate for aged and unaged EVA samples at different heating rates.

Heating rate (°C/min)	Temperature of peak degradation rate T_p (°C)			
	Unaged	Aged for 40 days	Aged for 60 days	Aged for 80 days
5	335.24	336.53	336.61	336.58
10	346.61	348.80	348.60	348.72
15	354.19	355.36	365.05	356.31
20	359.17	361.83	362.28	362.03

Figure (4.6) show the relationship between $\ln \frac{\beta}{T_p^2}$ and $\frac{1}{T_p}$ for one heating rate. It can be seen that the activation energy and pre-exponential factor were obtained from the slope and intercept of line fitting to this plot using Eq. (4.5). The calculated values are listed in Table (4.2). Experimental data were fit to Eq. (4.4) in order to find the pre-exponential factor. Figure (4.7) shows this fit and the best agreement between the experimental and calculated curves around the peak degradation rate temperature, by definition, but beyond this point differences are observed, which could in part be attributable to other processes occurring, such as dehydration. The generalised Kissinger method was also applied to thermally aged EVA. Figure (4.8) shows the calculated activation energy for the aged EVA and indicates that there is no clear effect of ageing on the activation energy.

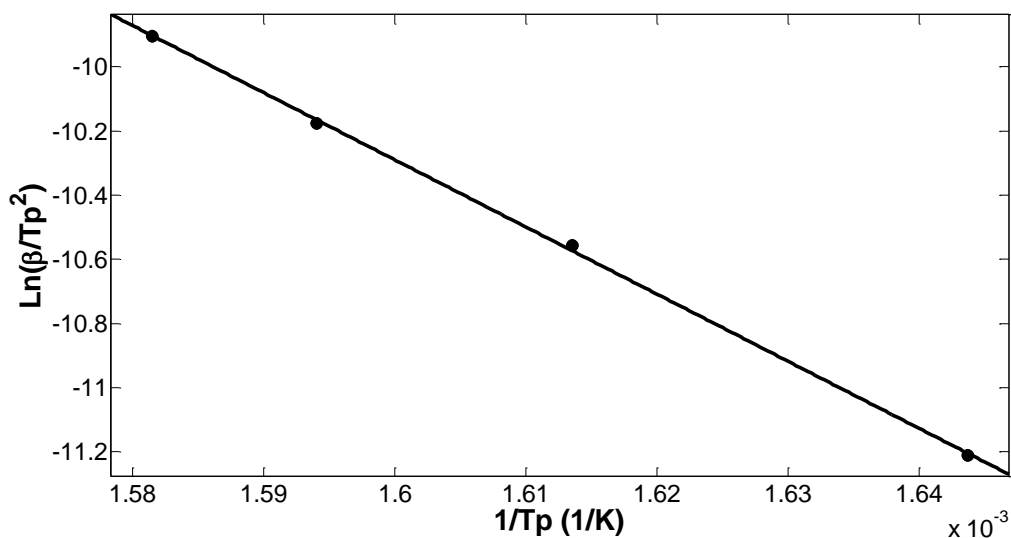


Figure 4.6: Plot of $\ln(\beta/T_p^2)$ versus $1/(T_p)$ for unaged EVA based on Kissinger's method.

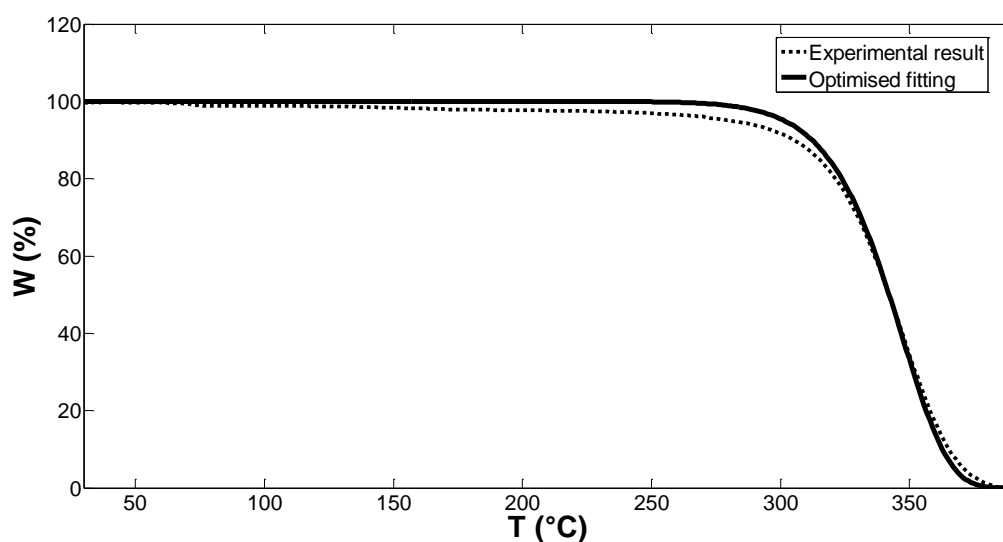


Figure 4.7: Experimental and calculated TGA curves.

Table 4.2: The calculated kinetic parameters for unaged EVA.

Sample	R ²	Slope of the line	E (kJ/mol)	a (min ⁻¹)
Unaged	0.9995	-20944	174.1284	2.4625×10 ¹⁴

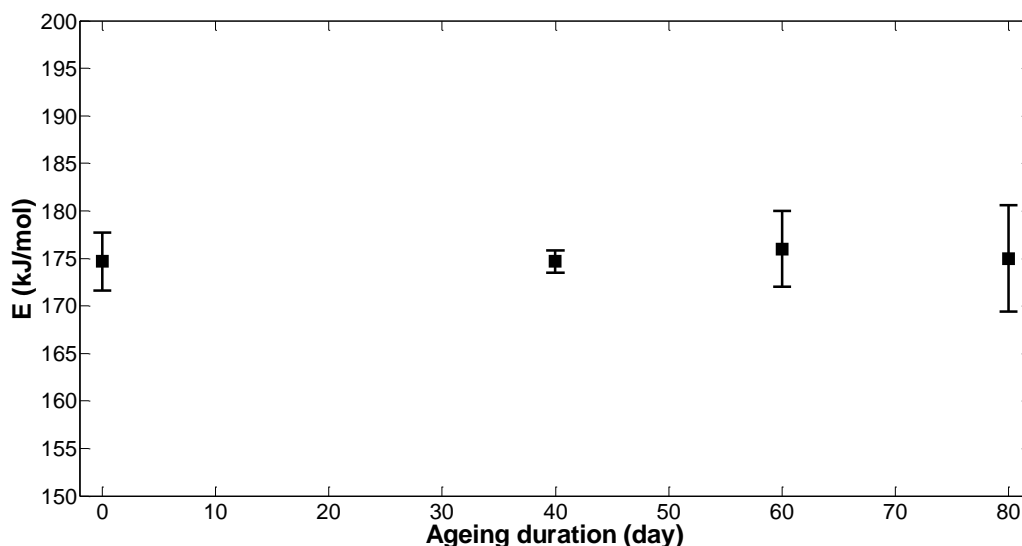


Figure 4.8: Activation energy calculated for unaged and thermally aged EVA.

The determination of the activation energy and the pre-exponential factor enables predictions to be made about the thermal degradation and associated weight loss over the lifetime of a module. Assuming that the material was at a module operating temperature of 85°C (which is the temperature of the material near to the cells as they generate heat during the conversion of photons to electronic potential), the determined activation energies and pre-exponential factors were used to determine the conversion of material as a function of time through the solution of Eq. (4.3). A failure criterion is suggested 5% weight loss from a Thermogravimetric Analysis (TGA) (Křižanovský & Mentlík 1978; Flynn 1995). In the case of the PV modules the typical lifetime of a module is usually considered to be around 30 years and Figure (4.9) shows that the weight loss in this period is predicted to be around 1%, which has little impact on the module performance. This also indicates that a more accurate method of determining the kinetics of degradation is unnecessary.

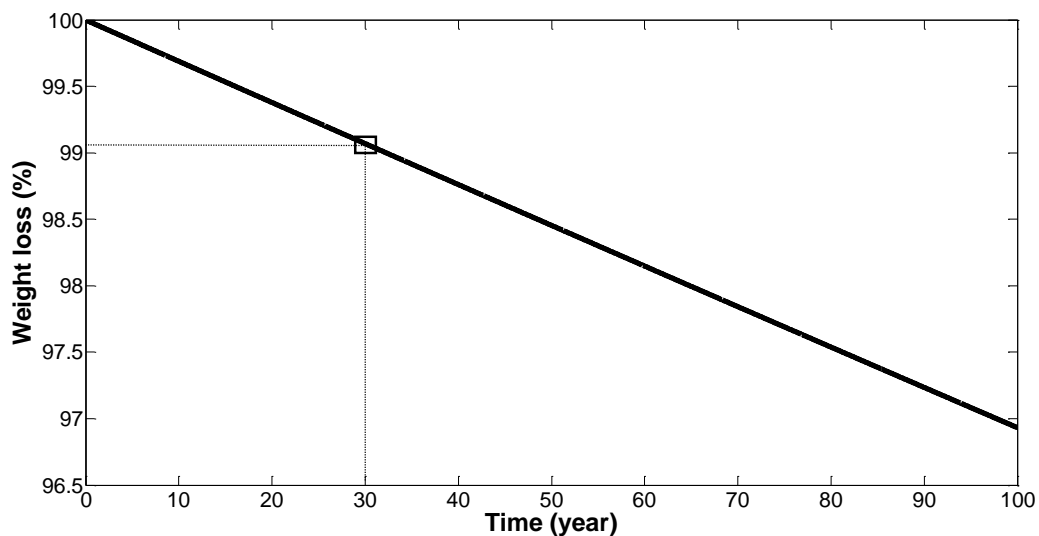


Figure 4.9: Weight loss of EVA versus time in the case of exposure to 85°C with standard deviation of 6.6521e-04.

4.3.2 Dynamic Mechanical Analysis (DMA)

Figure (4.10) shows the storage modulus (E') determined as a function of temperature at a frequency of 1 Hz. As the temperature increases the curves show the characteristic glassy, rubbery and viscous regions of a viscoelastic material (Stark & Jaunich 2011).

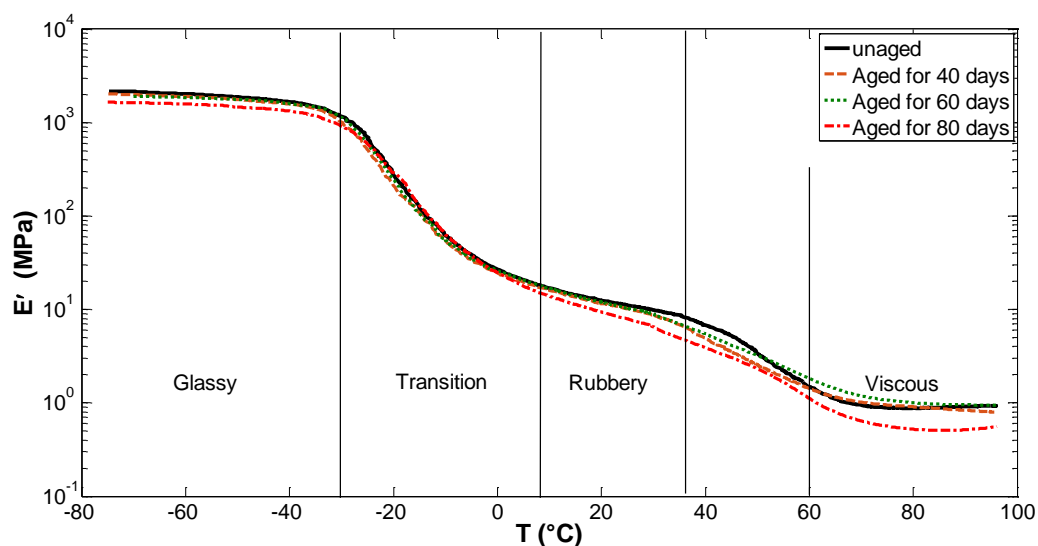


Figure 4.10: Storage modulus vs temperature for aged and unaged EVA.

Examination of the Response of Ethylene-vinyl Acetate Film to Thermal Ageing

Significant changes are seen in the storage modulus over the observed temperature range, with 3 decades difference between the moduli at -75°C and 95°C . There is a sharp decrease at around -30°C , which can be attributed to the glass transition and then another stepped decrease between 40°C and 65°C , indicating some crystal melting. Figure (4.11: a) shows $\tan(\delta)$ versus temperature, which can be used to emphasise the T_g of the samples as shown in Figure (4.11: b) (Varghese et al. 2002). It can be seen that T_g is approximately -20°C .

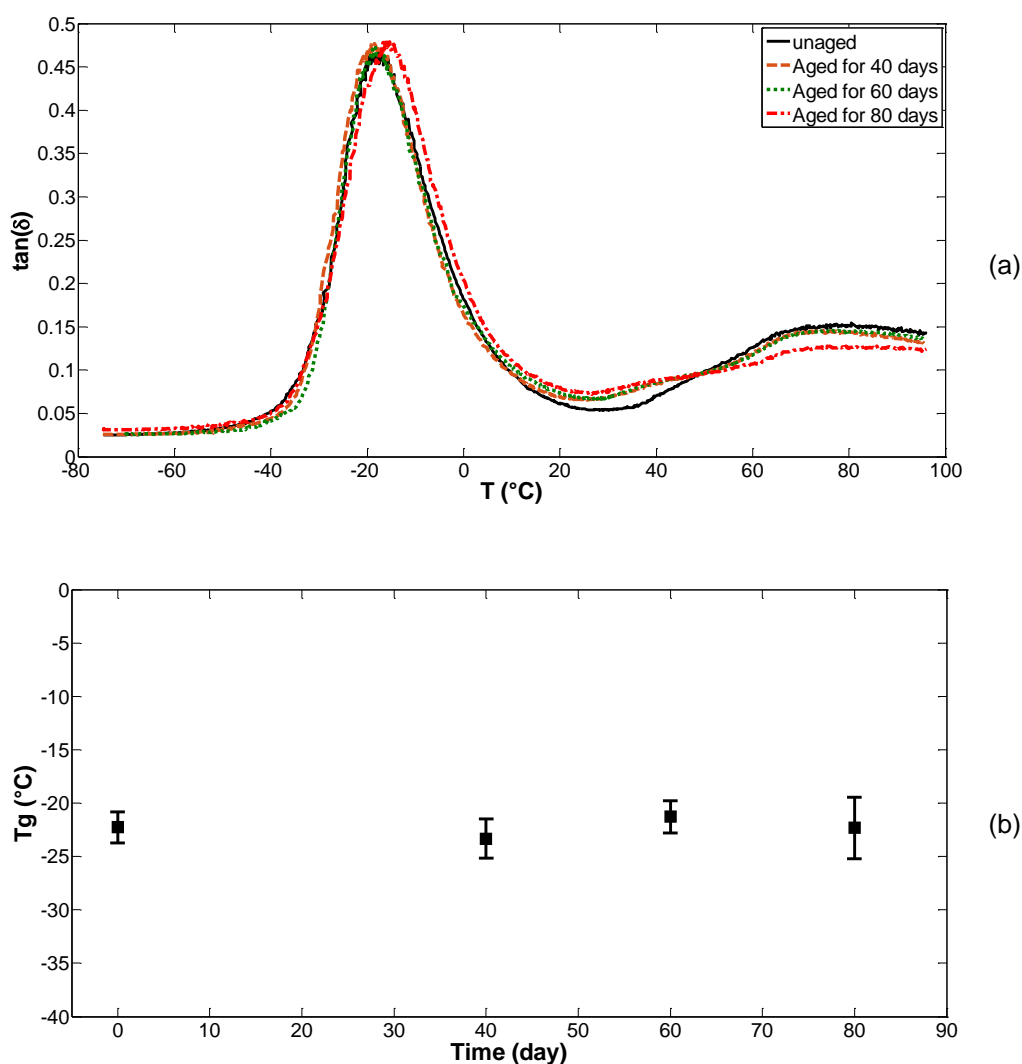


Figure 4.11: (a) $\tan(\delta)$ vs temperature for aged and unaged EVA, (b) Glass transition temperature versus ageing duration for EVA based on $\tan(\delta)$.

Examination of the Response of Ethylene-vinyl Acetate Film to Thermal Ageing

In order to further investigate the effect of ageing on the mechanical properties of the EVA, the storage modulus at a given temperature was plotted against the ageing time for the sample. Figure (4.12: a-d) shows this for four temperatures. One can see that E' reduces with increasing time of ageing, although the confidence in the fit and the calculated gradient decreases with increasing temperature as presented in Table (4.3). As a way of approximating the general trend, E' vs temperature for four temperature values was consolidated into one plot as a mean where the mean E' is the average of E' at the complete range of experimental temperature. This is shown in Figure (4.13), which shows a clear monotonically decreasing storage modulus as the material ages. Table (4.4) presents the parameters of best fit to changes of mean E' versus ageing duration. Further, the variation in modulus depends on temperature; as the measurement temperature increases, the dependence on the ageing duration weakens. That is to say, the storage modulus reduction rate, when measured at a given temperature, varies more slowly when measured at a higher temperature than a lower temperature. It is worth emphasising that this is for the same ageing condition of 85°C. It therefore appears that thermal ageing can result in significant changes in the mechanical properties, but considering the very small changes in weight loss, this is unlikely to be associated with chemical changes and any subsequent material volatilisation.

Examination of the Response of Ethylene-vinyl Acetate Film to Thermal Ageing

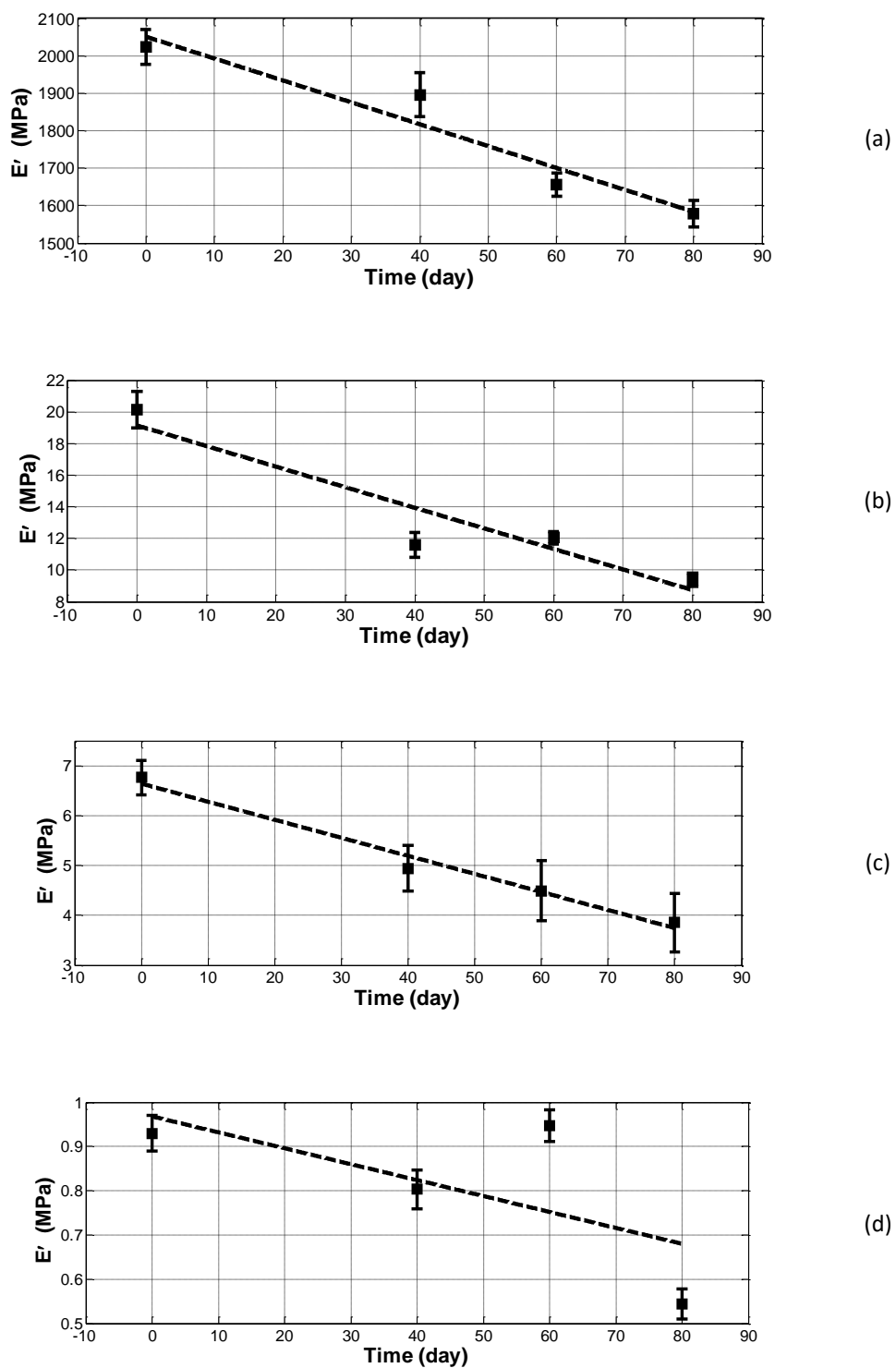


Figure 4.12: Storage modulus measured at (a) -60°C, (b) 20°C (c), 40°C (d) 95°C as a function of ageing time at 85°C.

Examination of the Response of Ethylene-vinyl Acetate Film to Thermal Ageing

Table 4.3: The fitting parameters for storage modulus at different fixed temperatures based on Figures (4.12: a-d).

T (°C)	Gradient	Intercept	R ²
-60	-5.8400	2051	0.93
20	-0.02667	5.521	0.93
40	-0.0155	2.652	0.85
95	-0.0036	0.968	0.44

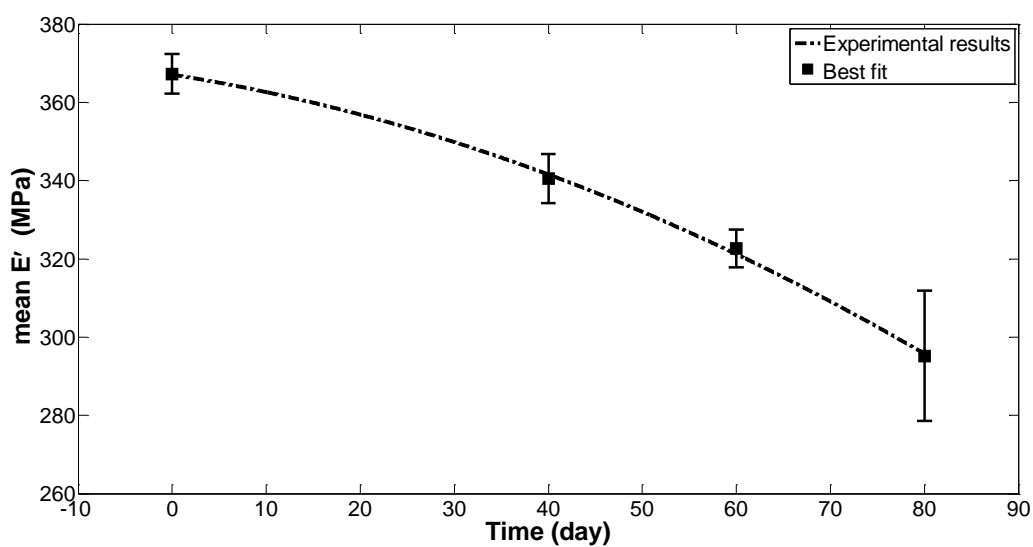


Figure 4.13: Average storage modulus versus ageing time for thermally aged EVA.

Table 4.4: The best fitting parameters of the average storage modulus versus ageing duration based on Figure (4.13), fitting function: $y = a_1x^2 + a_2x + c$.

a ₁	a ₂	Intercept	R ²
-0.006341	-0.3843	367.1	0.9987

4.3.3 Differential Scanning Calorimetry (DSC)

In order to understand the changes in morphological behaviour, DSC was performed, consisting of a heating, a cooling and final heating stage (described in section (3.4.1)). The results of these experiments can be seen in Figure (4.14), which shows typical DSC thermograms for samples that have been cycled. There are significant changes around 50°C and the peaks in this region can be associated with internal structural changes or crystallisation transition. This correlates with the step between 40°C and 60°C in the DMA results (Figure (4.10)) which were associated with crystal melting. In the second heating, it can be observed that the peaks have largely disappeared, suggesting that in the process of going through the previous cycle the structure has been eliminated and has not reformed during the cooling process. In Figure (4.15) the first heating thermograms of the unaged and aged EVA are reproduced with offsets added for the sake of comparison. The melting transition of the ethylene segment has been accepted as being associated with a peak with a shoulder which is observed between 40°C to 70°C (Li et al. 2013; Motta 1997). The glass transition, determined by a step change in the heat flow typically between -30°C and 20°C, can be seen at around -20°C for both aged and unaged samples, suggesting ageing has no significant effect on T_g which is shown in Figure (4.16).

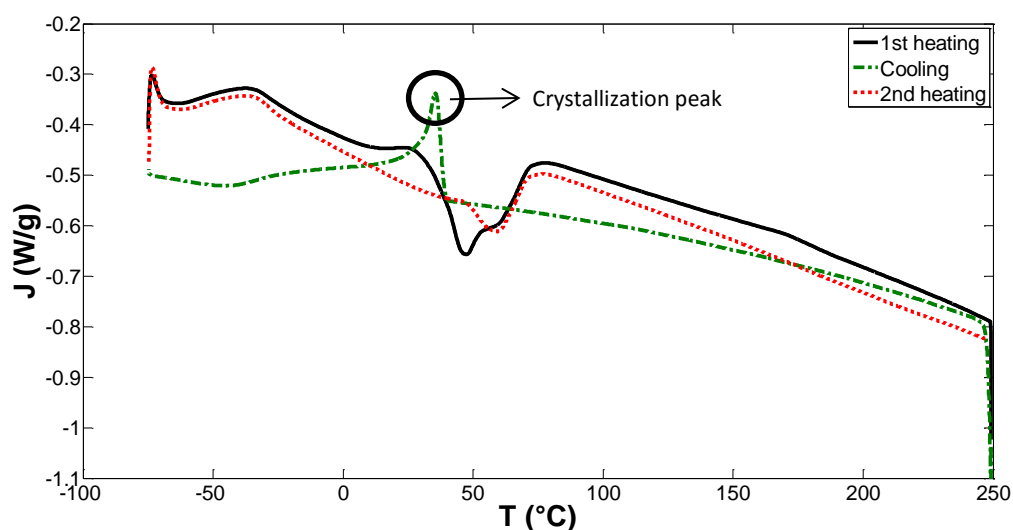


Figure 4.14: Typical DSC thermograms (heat flow versus temperature) of EVA under three steps, heating-cooling-heating-Exo Up.

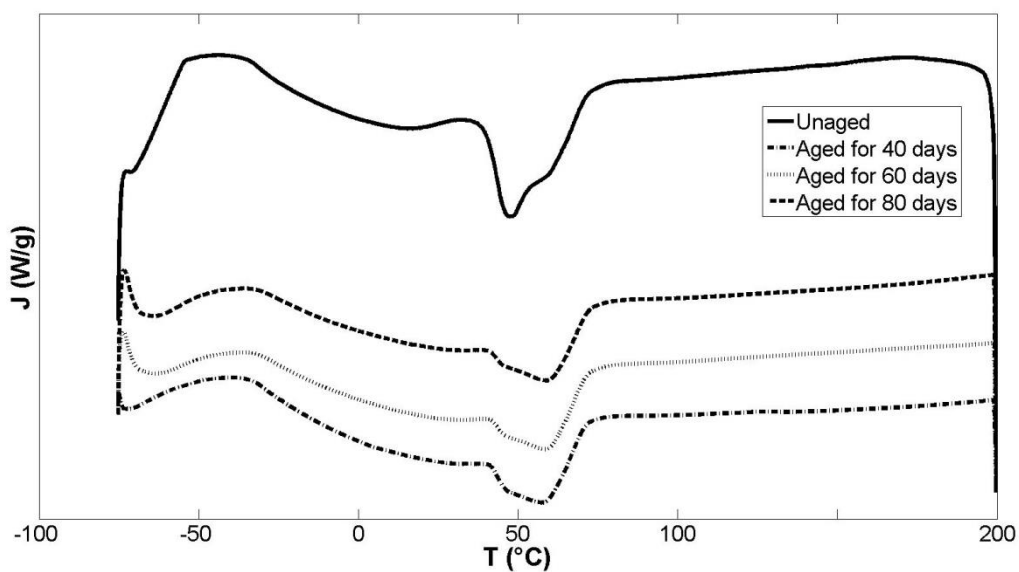


Figure 4.15: DSC first heating thermograms (heat flow versus temperature) for the unaged and aged EVA (thermograms are reproduced with offsets added)-Exo Up.

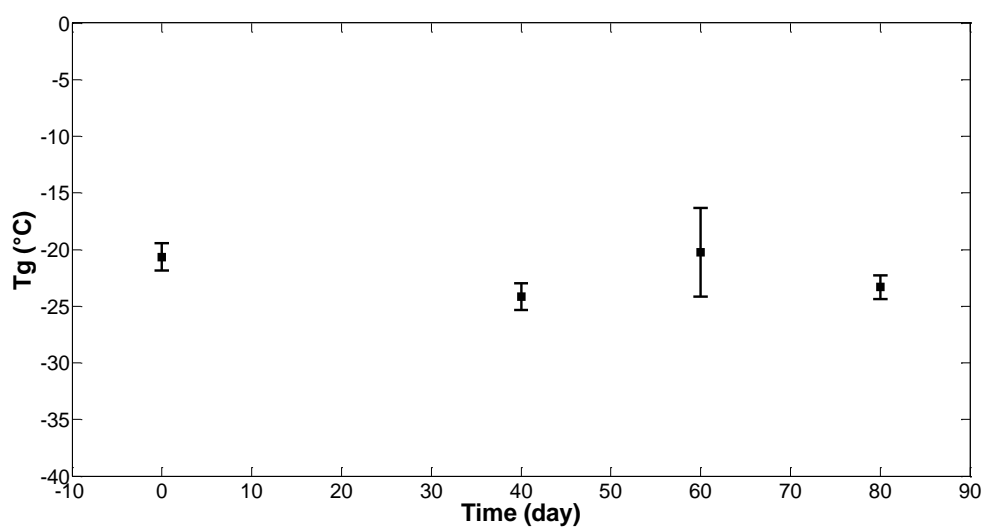


Figure 4.16: Glass transition temperature versus ageing duration for EVA.

Analysis of the first heating results shows that crystallinity decreases due to ageing as shown in Figure (4.17), which when correlated with the changes in mechanical behaviour, suggests that it is the changes in internal structure that drive the changes in the storage modulus, E' rather than the chemical changes discussed in section (4.3.1) as shown in Figure (4.18). It can also be seen in Figure (4.17) that there is no change in crystallisation in the second heating.

Examination of the Response of Ethylene-vinyl Acetate Film to Thermal Ageing

This reversion to a constant crystallisation content at the first heating cycle points towards a reduction in the structure at higher temperatures, with a consequent reduction in modulus and a weakening in the relationship between ageing driven modulus reduction at higher temperatures.

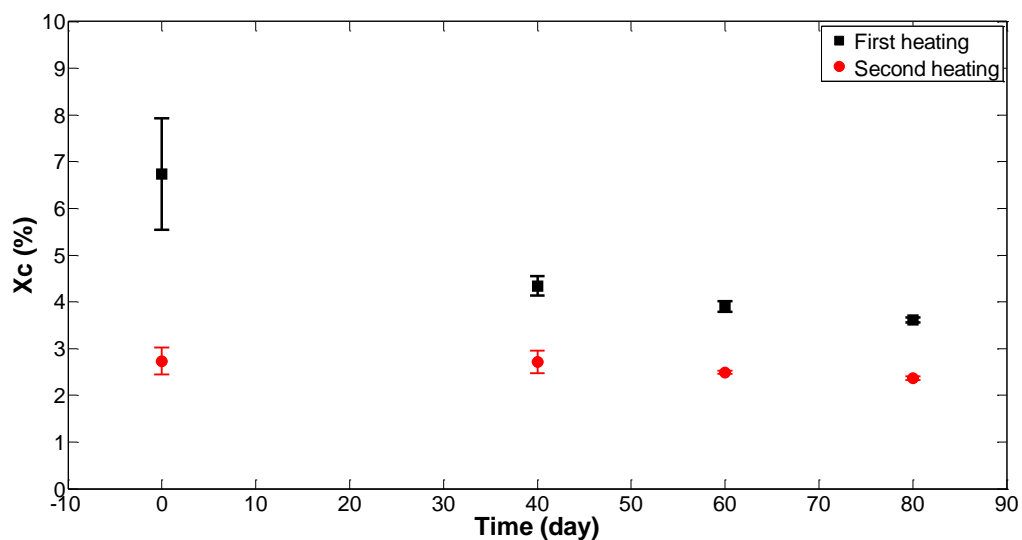


Figure 4.17: Crystallinity versus ageing duration after first and second heating for aged and unaged EVA.

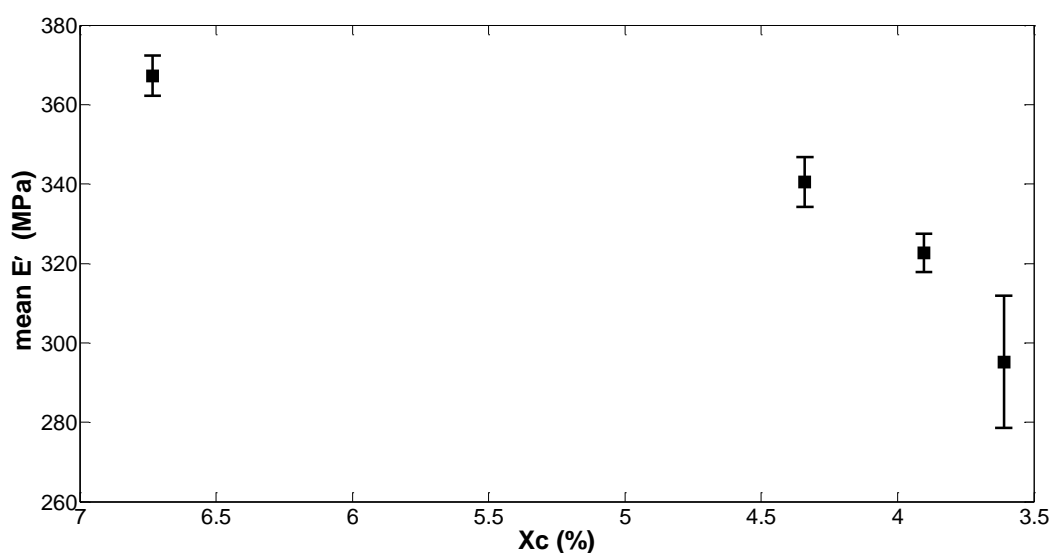


Figure 4.18: Storage modulus versus crystallinity for thermally aged EVA.

4.4 Conclusions

The thermal degradation of EVA has been studied using techniques that enabled the viscoelastic properties and thermal stability to be measured. Key findings were that the activation energy of the first stage of thermal degradation was unaffected by the ageing process whereas storage modulus at 1 Hz was significantly reduced with increases in temperature. Ageing was shown to reduce the storage modulus monotonically as a function of ageing degree, though this effect was weakened at elevated temperatures. TGA measurements showed that chemical changes due to thermal activation were insignificant, even over the typical lifetime of the module, but examination of DSC results suggested that property changes could be connected to structural modifications, specifically that thermally induced decreases in crystallinity resulted in a reduction in storage modulus. In the field, such modules will be subjected to light and humidity as well as elevated temperatures, and the interaction between these effects requires investigation. Hence, now that the influence of elevated temperature on the properties, structure and lifetime of EVA has been investigated, in the next chapter the impact of UV irradiance on the properties and photodegradation of EVA will be investigated.

Chapter 5

Examination of the Response of Ethylene-vinyl Acetate Film to UV Irradiation

5.1 Introduction

Photochemical reactions are of interest in diverse applications such as polymer degradation and solar energy capture. UV irradiation is one of the most important environmental factors affecting the deterioration of the mechanical strength of the encapsulant and the structural integrity of a PV module. EVA undergoes photochemical degradation when it is exposed to UV. UV irradiation causes discoloration and photodegradation which reduces the spectral transmission which causes a reduction in the conversion efficiency of the PV modules. Thus, there is a need to investigate the effect of photodegradation, on the EVA in a PV module.

It has been reported that the main photodegradation reactions in EVA are Norrish I and Norrish II (Czanderna & Pern 1996; Morlat-Therias et al. 2007; Lacoste et al. 1991; Glikman et al. 1986), this was shown in Figure (2.4). This comprehensive review of the photodegradation shows that the main products of the Norrish reactions are ester, carboxylic acid, lactone, vinyl and vinylene, which are fully investigated in this research.

This chapter investigates the photochemical degradation of EVA, develops a model to predict degradation and also studies the influence of the photodegradation on the structure and mechanical properties of EVA. Figure (5.1) illustrates the approach taken and techniques used in this chapter.

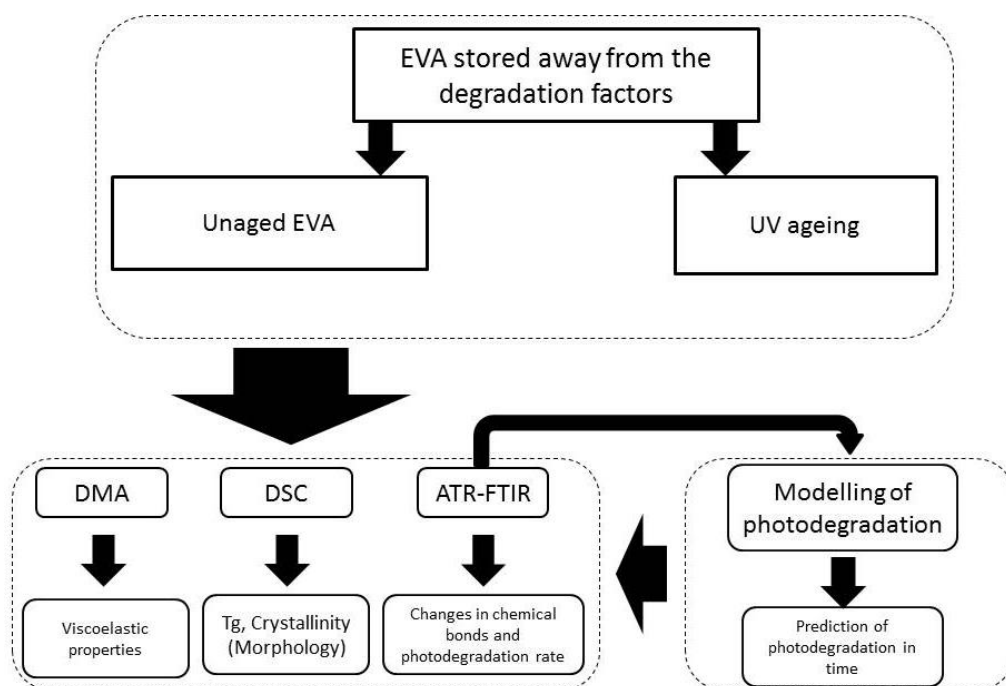


Figure 5.1: Flowchart of investigation of EVA's response to UV ageing.

The approach taken in this research was to make a comprehensive investigation of photodegradation chemically by spectroscopic methods (FTIR-ATR). Once the degradation mechanisms were fully understood a predictive model was developed to predict the photochemical degradation in time. The influence of photodegradation on the material behaviour and properties were also investigated.

5.2 Theory of photochemical reactions

Sheats & Diamond (1988) introduced a pair of coupled partial differential equations (PDE) the chemical transformation in photochemical reactions. Since EVA is highly UV absorbing as reported in the literature (Pern 1996; Skowronski et al. 1984; Czanderna & Pern 1996; McIntosh et al. 2009; Kempe et al. 2011; Jin et al. 2009), the introduces PDEs can be applied in this case.

$$-\frac{\partial C_r(z,t)}{\partial t} = k \cdot I \cdot F_{(C_r)} \quad 5.1$$

$$-\frac{\partial I_{(z,t)}}{\partial z} = (\alpha_r C_r + \alpha_p C_p + \alpha_m C_m)I \quad 5.2$$

where C_r , C_p and C_m are concentration of reactant, products and medium respectively. k is the fractional decay rate per unit intensity (Dill et al. 1975), α is the respective molar extinction coefficients, z and t refer to position and time respectively. The molar extinction coefficient, α , used in this study is related to the decadic molar extinction coefficient, ϵ , via Eq. (5.3) (Sheats & Diamond 1988). $I_{(z,t)}$ is the light intensity at depth z at time t and $F_{(Cr)}$ represents a rate function.

$$\alpha = \epsilon \ln 10 \quad 5.3$$

In general, the quantities C_r , C_p and I depend on position and time, resulting in the coupling of the differential equations. Therefore, the equations can be articulated as

$$-\frac{\partial C_{r(z,t)}}{\partial t} = kI_{(z,t)}F[C_{r(z,t)}] \quad 5.4$$

$$-\frac{\partial}{\partial z} \ln \frac{I_{(z,t)}}{I_{(z_0,t)}} = \alpha_r C_{r(z,t)} + \alpha_p C_{p(z,t)} + \alpha_m C_{m(z,t)} \quad 5.5$$

which are subjected to the boundary conditions

$$C_{r(z,t_0)} = C_r^0(z) \quad 5.6$$

$$I_{(z_0,t)} = I_0(t) \quad 5.7$$

where $I_0(t)$ is the light intensity in the medium inside the surface z_0 at time t . Equations (5.4)-(5.5) and the associated boundary conditions are taken as the

basic coupled PDEs, which describe the photoreaction in the absence of change in surface reflectivity, scattering or diffraction.

Considering the first order case, reaction rate is first order in both Eq. (5.4)-(5.5) and only the reactant absorbs light. Therefore, Eq. (5.4)-(5.5) become

$$-\frac{\partial C_{r(z,t)}}{\partial t} = k C_{r(z,t)} I_{(z,t)} \quad 5.8$$

$$-\frac{\partial I_{(z,t)}}{\partial z} = \alpha_r C_{r(z,t)} I_{(z,t)} \quad 5.9$$

The solutions for Eq. (5.8)-(5.9) have been reported by (Herrick 1966). The general solutions are

$$C_{r(z,t)} = C_r^0(z) \frac{e^{\mu(z)}}{e^{\mu(z)} + e^{\vartheta(t)} - 1} \quad 5.10$$

$$I_{(z,t)} = I_0(t) \frac{e^{\vartheta(t)}}{e^{\mu(z)} + e^{\vartheta(t)} - 1} \quad 5.11$$

where $\mu(z)$ and $\vartheta(t)$ are determined by the initial conditions

$$\mu(z) = \alpha_r \int_{z_0}^z C_r(z') dz' \quad 5.12$$

$$\vartheta(t) = k \int_{t_0}^t I_0(t') dz' \quad 5.13$$

The general solutions subject to boundary conditions, Eq. (5.6)-(5.7).

In order to find k the changes of the concentration on the surface is considered which is independent of z , therefore Eq. (5.8) becomes

$$\frac{dC_r(t)}{dt} = k C_r(t) I \quad 5.14$$

The solution for Eq. (5.14) is

$$C_r(t) = C_r(0)e^{-kt} \quad 5.15$$

where k can be found by fitting Eq. (5.15) to the experimental data.

The time dependent concentration of photoproduct is related to the concentration of photoreactant via stoichiometric coefficient, λ , and equation (Sheats & Diamond 1988)

$$C_p(z, t) = C_p^0(z) + \lambda (C_r^0(z) - C_{r(z,t)}) \quad 5.16$$

where λ is the ratio of the stoichiometric coefficient in the reaction.

The initial concentration can be determined by Beer-Lambert law, Eq. (5.17) using FTIR-ATR results,

$$A = \epsilon bC \quad 5.17$$

where A , ϵ , b and C are absorbance, molar extinction coefficient, path length of the sample and concentration respectively. The path length is 0.65 μm based ATR catalogue (Bruker Optics 2011), the absorbance comes from the FTIR-ATR measurements and ϵ is known from (Morlat-Therias et al. 2007).

5.3 Results and discussion

The results are based on the ageing conditions and experimental techniques described in sections (3.3)-(3.4).

5.3.1 Fourier Transform Infrared Spectroscopy in Attenuated Total Reflectance (FTIR-ATR)

FTIR-ATR was used to study the variation of different chemical bonds as a result of UV aging. FTIR-ATR spectra were obtained for the UV aged samples at 50°C, including the UV irradiated side, the non-irradiated side, a thermally aged sample at 65°C and a control sample (see section (3.2.2)).

In order to perform a thorough investigation the impact of ageing on the individual peaks these peaks should be identified. To identify the exact wave numbers for the specific peaks the spectra of unaged EVA (A_0) was subtracted from the spectra of the aged EVA (A_t) as shown in Figure (5.2). The identified peaks are presented in Table (5.1).

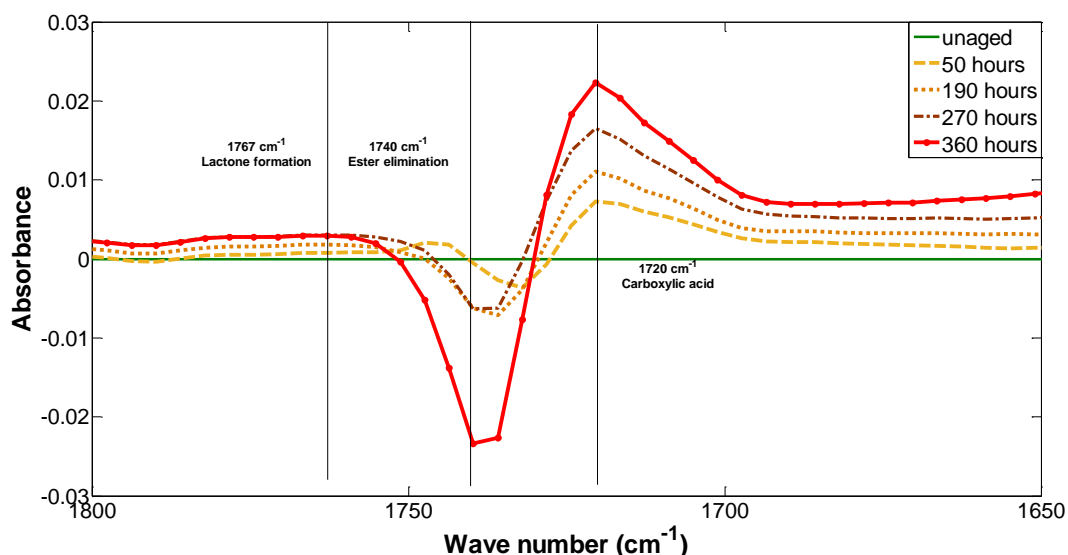


Figure 5.2: Subtracted FTIR-ATR spectra ($A_t - A_0$) in the domain 1800-1650 cm^{-1} .

Table 5.1: Attribution of infrared absorption bands of EVA film.

Chemical component	Wave number (cm^{-1})	Phenomena
Vinyl	910	Norrish I & II
Carboxylic acid	1720	Norrish I & II
Ester carbonyl stretching	1740	Norrish I & II
Lactone	1767	Norrish I & II

To have an accurate and more detailed view of how the absorbance changes with ageing time as a result of UV exposure plots of absorbance versus ageing duration were produced. Figure (5.3) shows the changes in IR spectra of unaged and UV aged EVA at 1740 cm^{-1} (ester carbonyl stretching), normalized as A_{1740}/A_{721} (described as Eq. (3.2)) versus exposure time. Ester is important in this case since one of the main products of the photodegradation of EVA is acetic acid which come via ester elimination (Copuroglu & Sen 2005). The absorbance for the top side of the UV aged EVA shows a sharp decrease up to around 300 hours which is due to ester elimination. This levels off after 300 hours due to the predominant aldehyde development (Copuroglu & Sen 2005). Aldehyde and ester have the same absorbance peak identification and aldehyde formation overlaps the ester elimination, meaning that although, no changes are observed after 300 hours it does not mean the ester elimination has stopped. The FTIR technique is not able to separate these two phenomena and other techniques should be used for further investigation. A slow decrease in absorbance is also seen in the thermally aged sample but no noticeable changes are observed on the back side of the UV aged EVA and the control sample, despite the fluctuation in data. The results for the back side of the UV aged sample show that the UV has not been able to penetrate and affect it which can be due to the presence of UV absorber. Therefore, the only difference between the back side of the UV aged sample and the thermally aged is the ageing temperature. The thermally aged EVA has been exposed to a higher temperature (65°C) which is the reason for the decrease in the absorbance for thermally aged EVA. Thus, UV has the dominant ageing effect while the effect of temperature is minor.

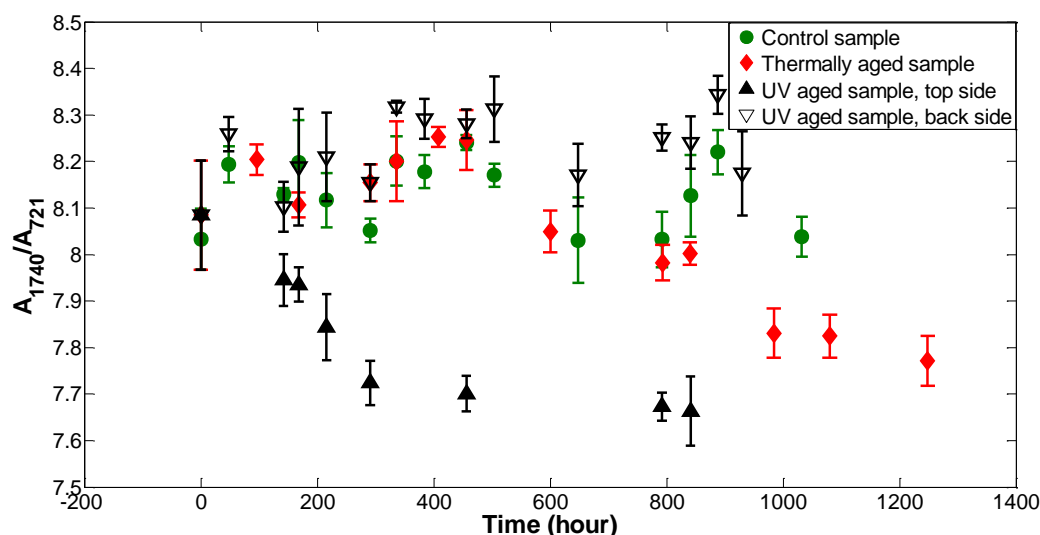


Figure 5.3: Variation of absorbance at 1740 cm^{-1} as a function of exposure time.

Figure (5.4) shows the absorbance changes at 1720 cm^{-1} (carboxylic acid) as A_{1720}/A_{721} for all samples. As expected, no significant changes are observed in the case of the control sample and the non-irradiated side of the UV aged sample. Nevertheless, there are notable changes seen in the UV and thermally aged samples in which the rate of changes for the UV aged sample is more significant and shows the dominant ageing effect of UV. It was expected that the thermally aged and back side of the UV aged samples show similar behaviour but due to elevated ageing temperatures in thermal ageing the rate of changes for the thermally aged sample is higher. The rate of photodegradation comes from the changes at 1720 cm^{-1} versus ageing time (Morlat-Therias et al. 2007). Table (5.2) presents the best fit parameters for the changes in A_{1720} for the top side of the UV aged sample.

Examination of the Response of Ethylene-vinyl Acetate Film to UV Irradiation

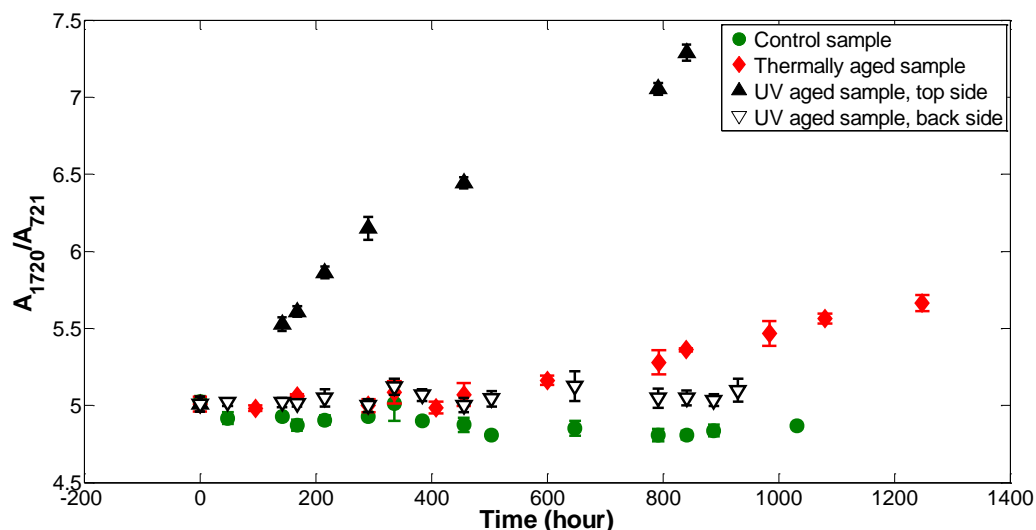


Figure 5.4: Variation of absorbance at 1720 cm^{-1} as function of exposure time.

Table 5.2: Line of best fit parameters (Figure (5.4) UV aged top side).

Sample	Wave number (cm^{-1})	R^2	Gradient
UV aged (top side)	1720	0.9699	0.00249

Figure (5.5) shows the variation of absorbance at 1767 cm^{-1} (lactone) by ageing time as A_{1767}/A_{721} . The absorbance for the top side of the UV aged EVA has increased dramatically while there are no changes observed in the control sample, thermally aged sample and the back side of the UV aged sample.

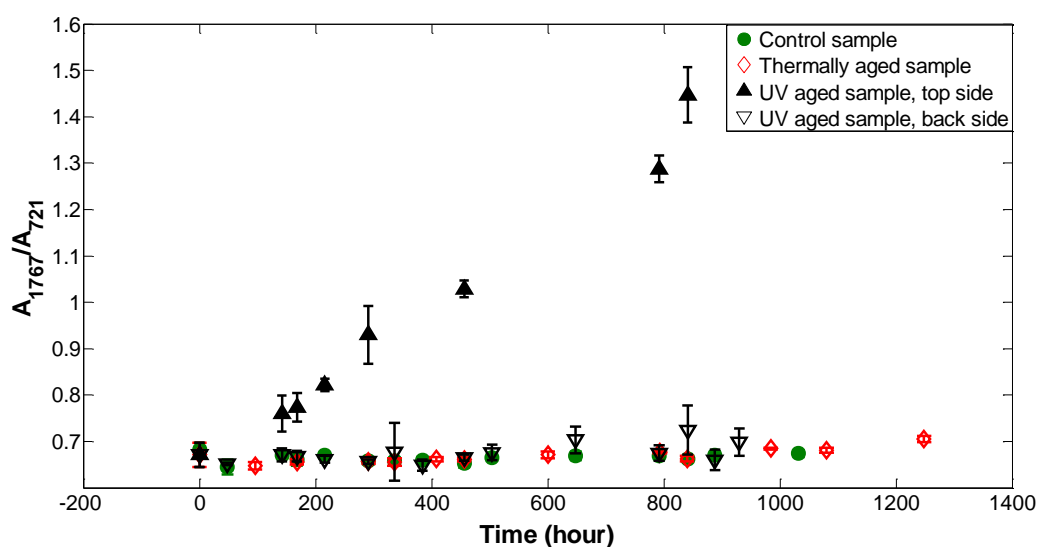


Figure 5.5: Variation of absorbance at 1767 cm^{-1} as a function of exposure time.

Figure (5.7) shows the absorbance change at 910 cm^{-1} (A_{910}/A_{721}) versus exposure time. A_{910} is the attributed wave number for vinyl group which is an unsaturated group and responsible for discolouration of EVA, Therefore the rate of vinyl formation can be a measure for EVA discolouration. The absorbance for the top side of the UV aged EVA has sharply increased while there is a very slight increase in the case of the thermally aged EVA is observed. As expected no changes are observed in the control sample and the back side of the UV aged EVA which, is due to being away from the degradation factors and not exposed to a high temperature respectively. Once again the results indicate the dominant ageing effect of the UV in chemical degradation of EVA and particularly in discolouration of EVA.

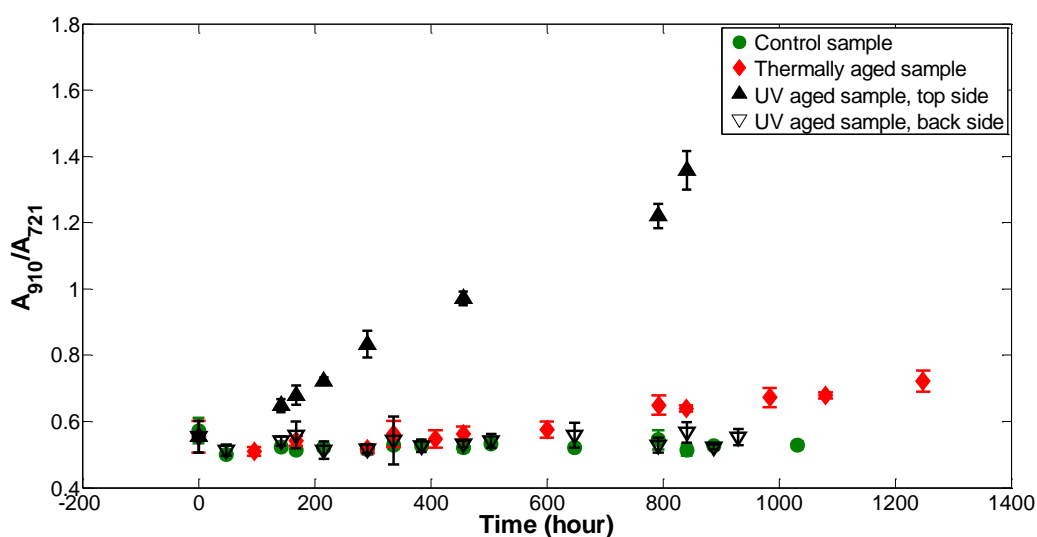


Figure 5.6: Variation of absorbance at 910 cm^{-1} as a function of exposure time.

5.3.2 Analytical investigation of photodegradation

Figure (5.7) shows the flowchart of the taken approach to predict EVA's photodegradation only. In order to calculate k (fractional decay rate), Eq. (5.15) was fitted to variation of experimental data in Figure (5.3). Figure (5.8) and Table (5.3) show the fitting and its parameters respectively.

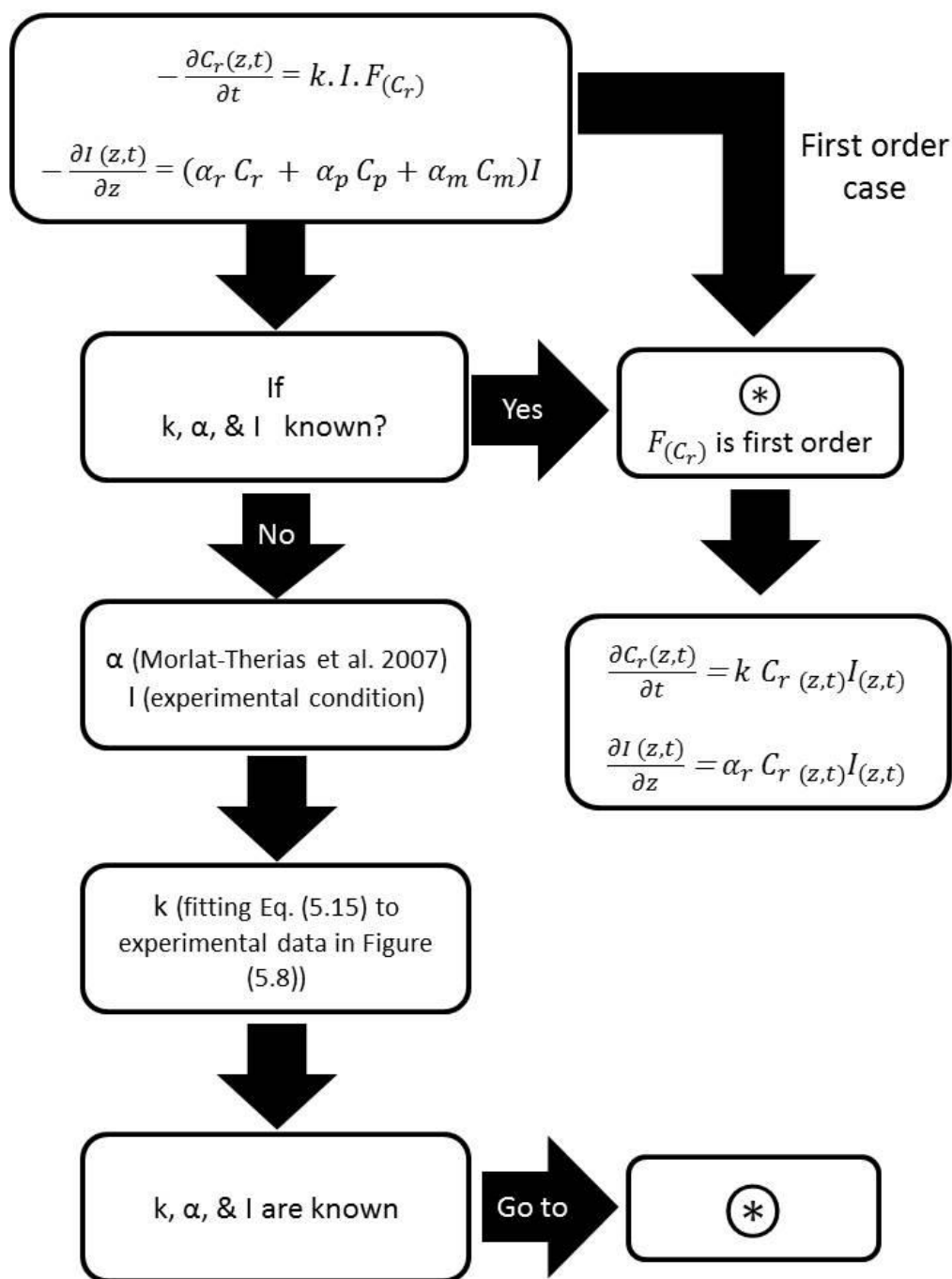


Figure 5.7: Flowchart of the investigation the lifetime of EVA regarding the photodegradation only.

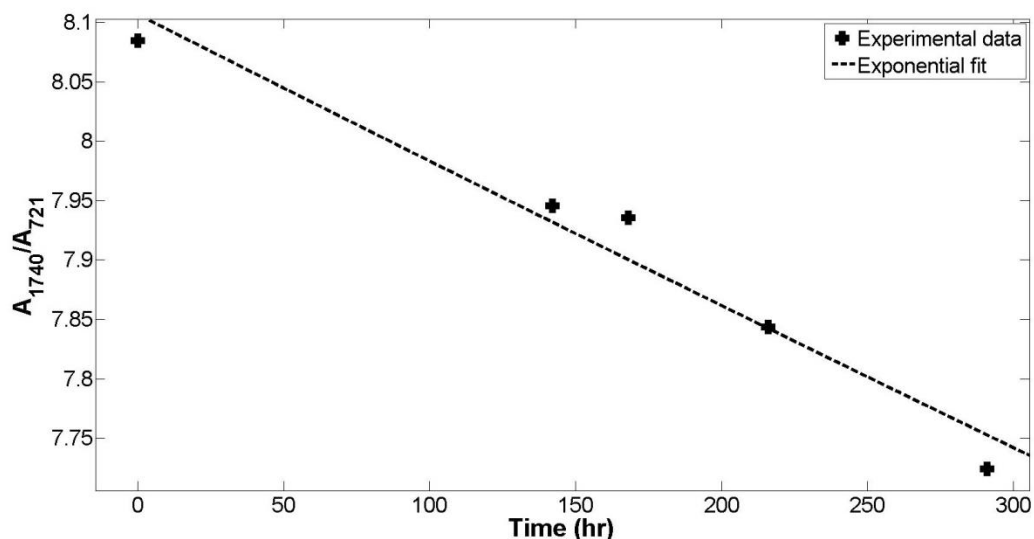


Figure 5.8: Variation of absorbance at 1740 cm^{-1} (normalized) on the irradiated surface as a function of exposure time.

Table 5.3: Best fit parameters (Figure (5.8)).

Sample	$k\text{ (m}^2/\text{J)}$	Intercept	R^2
Irradiated surface, UV aged EVA	29400	-0.0001533	0.949

Once k is found concentration of ester (photoreactant) can be modelled as function of time on the irradiated surface of EVA. Figure (5.9) shows concentration of ester as function of exposure time for the first 300 hours of the exposure time. The results show a good agreement between the experimental and analytical results with an error in the range 5%. The source of error may be variation of intensity in UV chamber, thermal ageing of EVA (described in chapter 4).

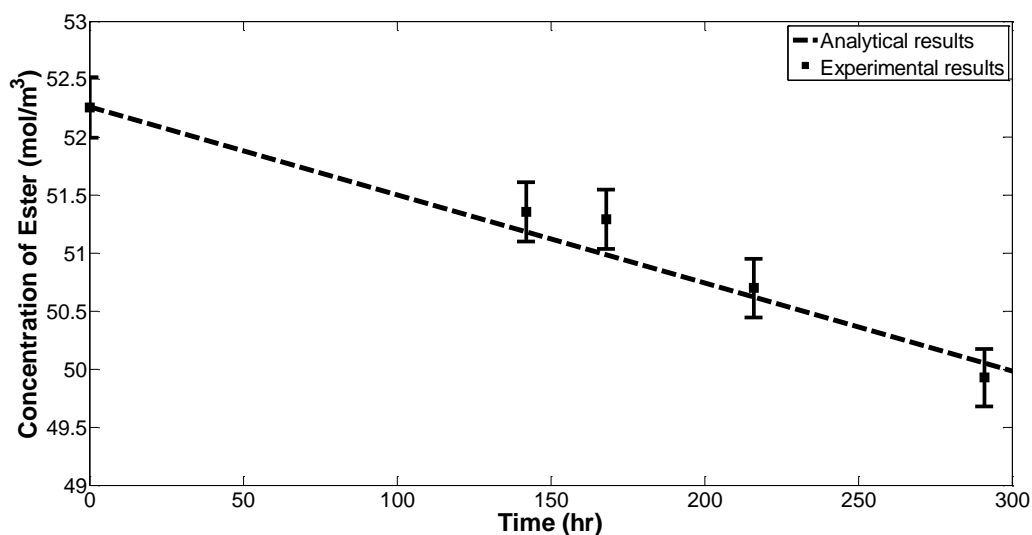


Figure 5.9: Variation of concentration of ester on the irradiated surface as a function of exposure time-validation of analytical and experimental results.

Now the concentration of photoreactant can be predicted on the surface of EVA in time. Figure (5.10) shows the variation of concentration of ester on the irradiated surface of EVA in 30 years. The results show that the photoreaction is completed on the surface after around 5 years of continuous UV exposure at the intensity of 0.68 W/m^2 however, in the field due to cycles of day and night and various weather conditions this time will be longer in the real field conditions. These results are in agreement with the field data presented in (Czanderna & Pern 1996).

In order to achieve the concentration of photoproduct (carboxylic acid), λ (stoichiometric coefficient) should be known. Figure (5.11) shows the variation of concentration of carboxylic acid versus concentration of ester where λ comes from the gradient of the fitted line. Table (5.4) shows the calculated λ and the fitting parameters.

Examination of the Response of Ethylene-vinyl Acetate Film to UV Irradiation

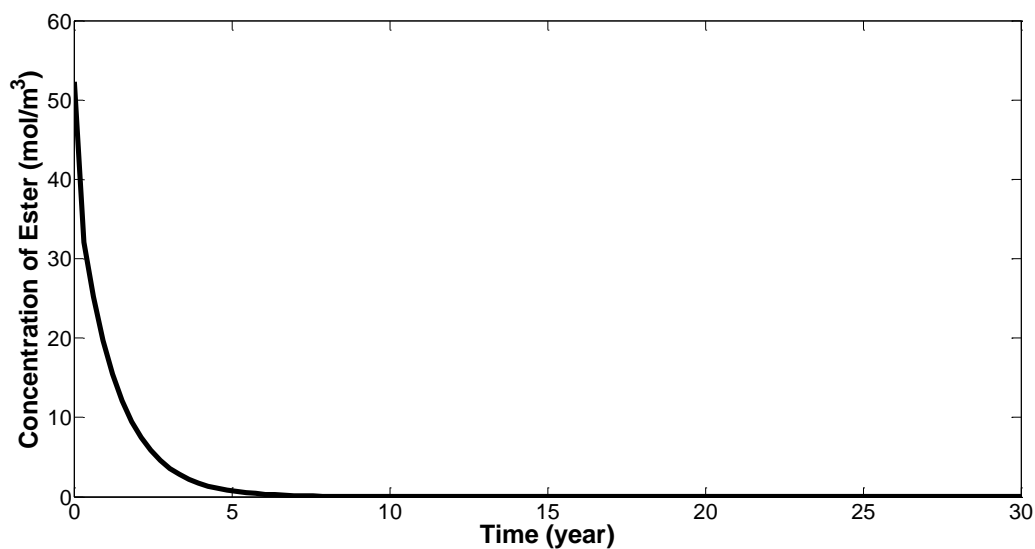


Figure 5.10: Variation of concentration of ester (photoreactant) on the irradiated surface as a function of time.

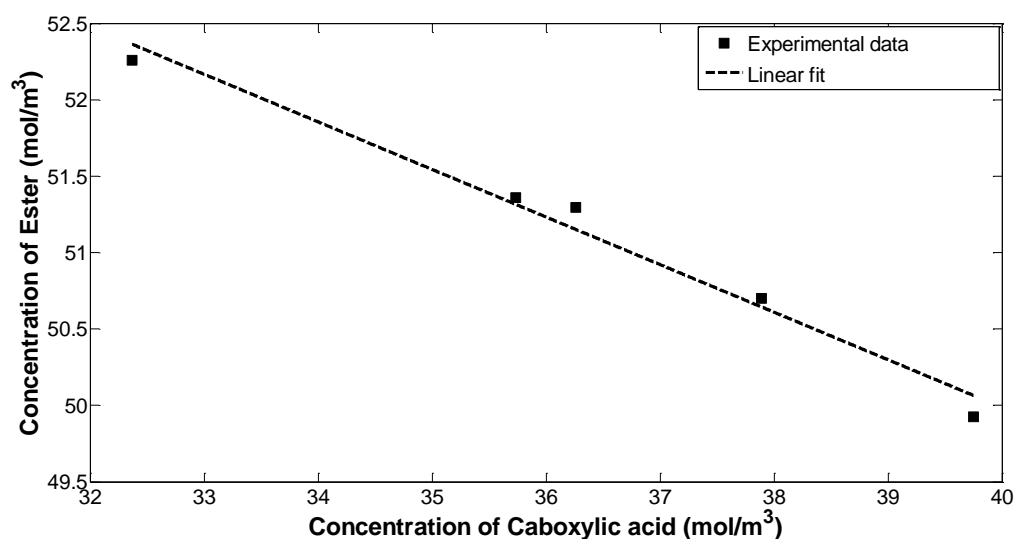


Figure 5.11: Variation of concentration of carboxylic acid versus concentration of ester.

Table 5.4: The fitting parameters Figure (5.11).

Gradient	Intercept	R ²
-0.3113	62.44	0.98

Now the concentration of photoproduct can be predicted on the surface of EVA. Figure (5.12) shows the variation of carboxylic acid concentration on the irradiated surface of EVA in 30 years. The results show a similar trend to the variation of ester which indicates that the photoreaction is completed on the surface after 5 year.

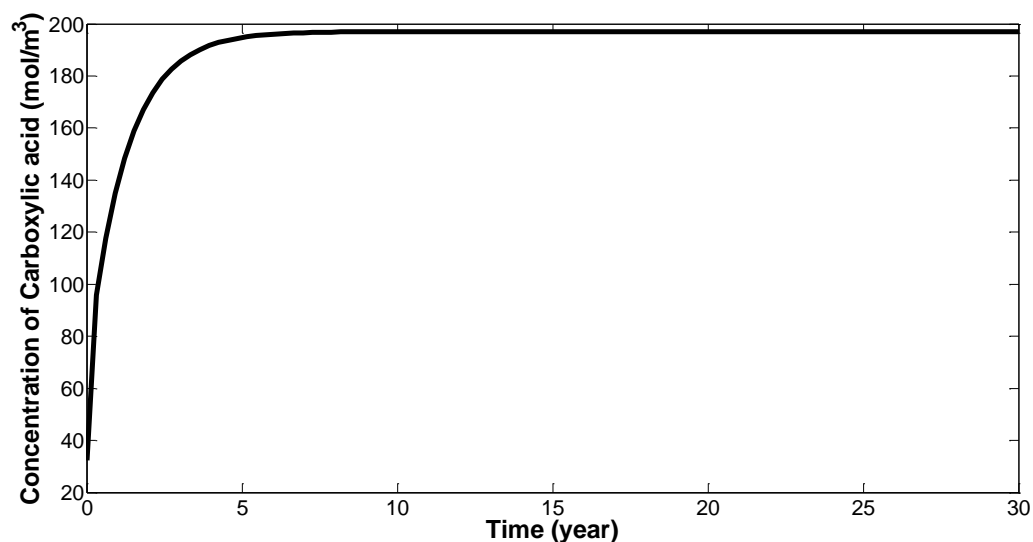


Figure 5.12: Variation of concentration of carboxylic acid (photoproduct) on the irradiated surface as a function of time.

Since the experimental data were only achieved on the surface of EVA, it is not possible to predict the photodegradation in depth and validate the model however, it should be mentioned that in the field the top side of EVA is more susceptible to photodegradation and the discolouration and delamination also start from interface of EVA-Glass. Therefore, it is concluded that the model is valid for the surface.

5.3.3 Differential Scanning Calorimetry (DSC)

As mentioned in section (5.3.1) UV makes significant changes in EVA's structure owing to photodegradation. In order to investigate these changes DSC technique was applied as described in section (3.4.1).

Figure (5.13) shows the DSC thermograms before and after ageing. Both unaged and aged EVAs show double melting peaks. In the case of unaged EVA the melting peak appears around 46°C with a shoulder around 57°C. After ageing, the peak and the shoulder separate and the peaks' temperatures increase as the ageing time increase. The separation of melting peaks is due to primary and secondary crystallisation (Chen et al. 2009b; X. Shi et al. 2009; Lee & Kim 2008; K. A. Moly et al. 2005; Li et al. 2004; Brogly et al. 1997b; Feng & Kamal 2005; Alizadeh et al. 1999). The entire ageing process includes physical variations in crystallization and photochemical degradation.

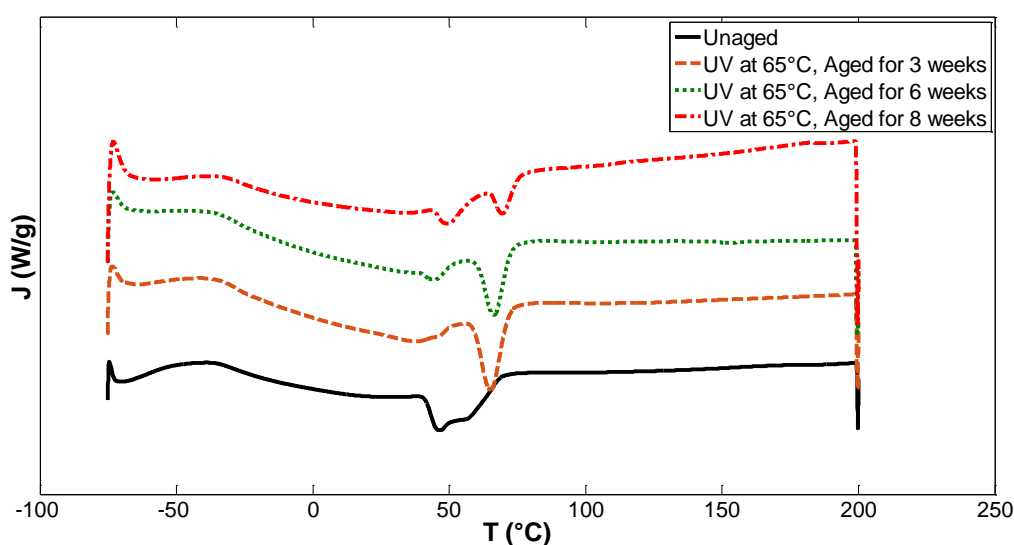


Figure 5.13: DSC first heating thermograms for the unaged and UV aged EVA-Exo Up.

The UV ageing process consists of photochemical degradation and physical variation in crystallisation (Jin et al. 2010b). The relative crystallinity, X_c , of the samples was calculated as a function of ageing duration through Eq. (3.1).

Figure (5.14) shows the changes in crystallinity versus ageing time. Analysis of the results of the first heating shows that crystallinity decreases due to degradation, which can influence the mechanical behaviour of EVA. It is also observed that there is no change seen during the second heating.

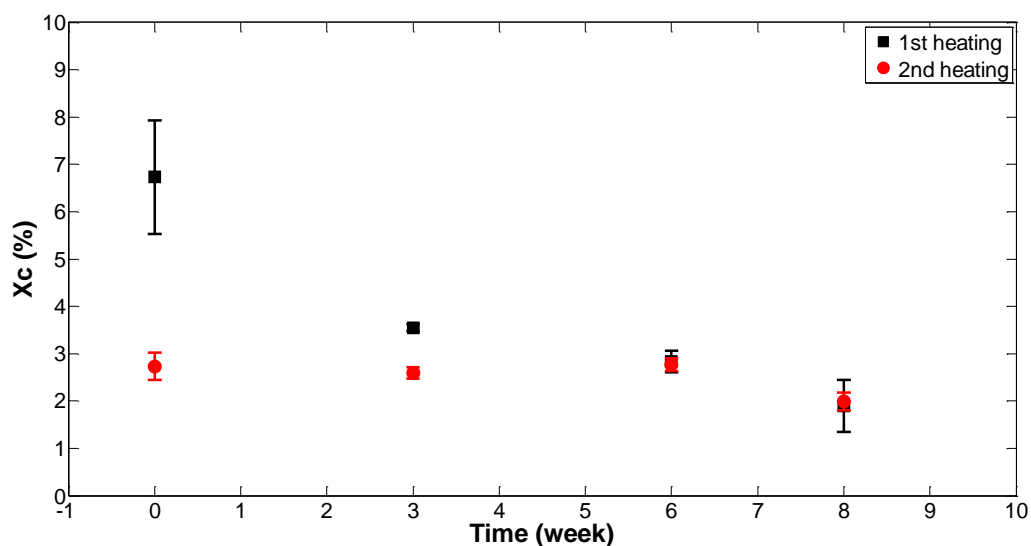


Figure 5.14: Crystallinity versus ageing time after first and second heating for unaged and UV aged EVA.

In order to understand the impact of chemical photodegradation on the structure of EVA crystallinity is plotted versus concentration of ester and carboxylic acid, respectively. Figures (5.15) and (5.16) show the relation between the concentration of ester and carboxylic acid with changes in crystallinity of the EVA respectively. The results show the crystallinity decreases by decreasing concentration of ester and increasing concentration of carboxylic acid. Therefore, continuing photodegradation can damage the material and affect the structure of it.

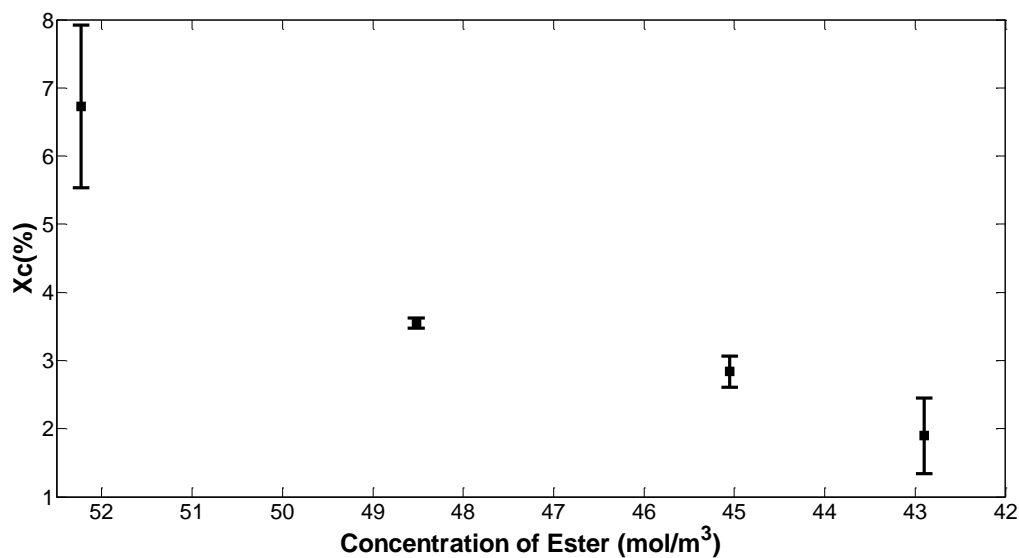


Figure 5.15: Variation of crystallinity versus changes in concentration of ester on the irradiated surface of UV aged EVA.

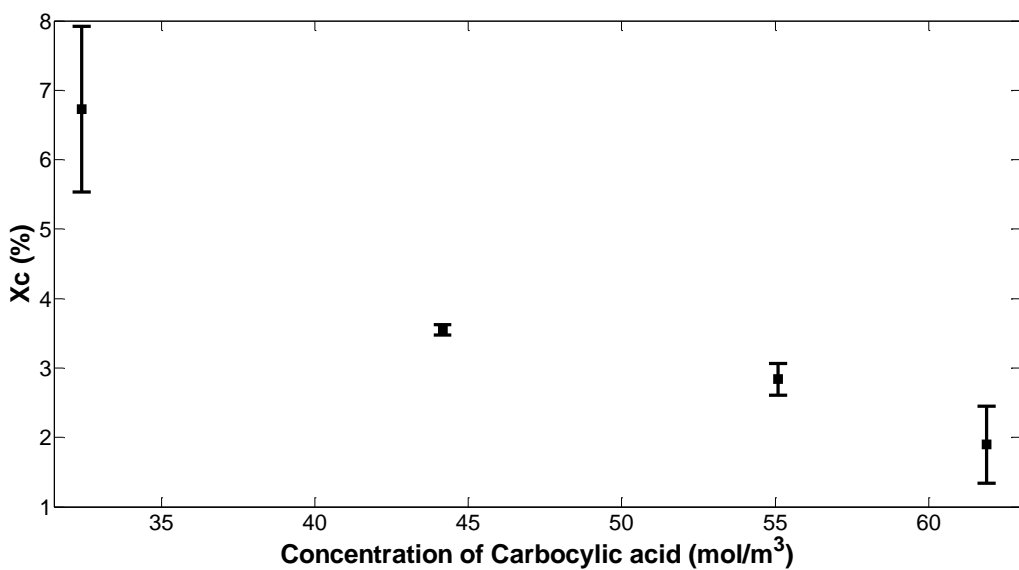


Figure 5.16: Variation of crystallinity versus changes in concentration of carboxylic acid on the irradiated surface of UV aged EVA.

The T_g determined by a step change in the heat flow, was found to be around -25°C for aged and unaged samples. Figure (5.17) shows T_g versus ageing time. The results show ageing has no significant impact on T_g .

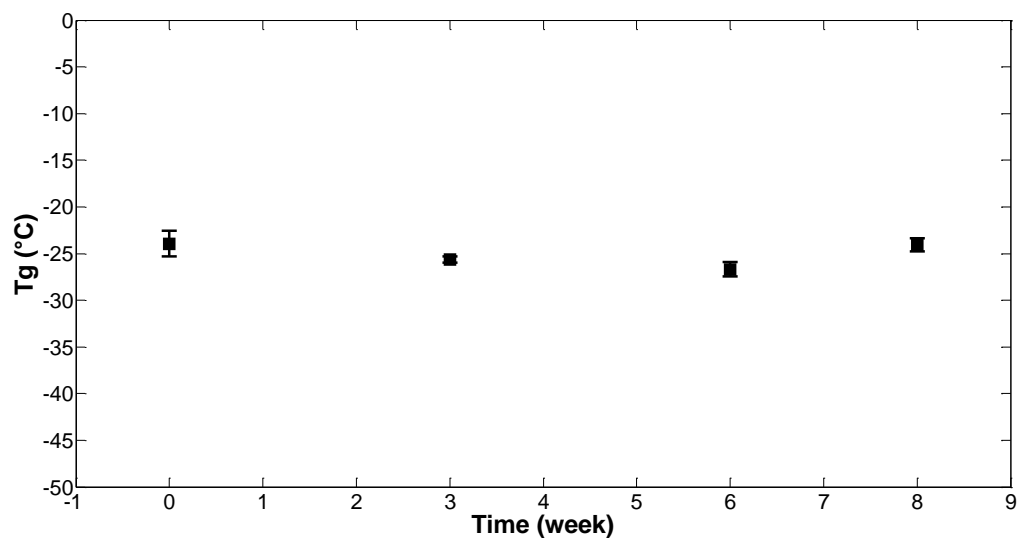


Figure 5.17: Glass transition temperature versus ageing for unaged and UV aged EVA.

5.3.4 Dynamic Mechanical Analysis (DMA)

The storage modulus (E') was determined as a function of temperature for the UV aged samples, as described in section (3.4.2). Figure (5.18) illustrates E' versus temperature. The curves show the different regions and transitions of a viscoelastic material as temperature increases (Dolores Fernández & Jesús Fernández 2007). There is a sharp decrease in modulus at around -30°C , which can be attributed to the glass transition and then another stepped decrease between 40°C and 70°C , which may be due to some crystal melting. These two stepped changes correlate well with the DSC identified T_g and melting point.

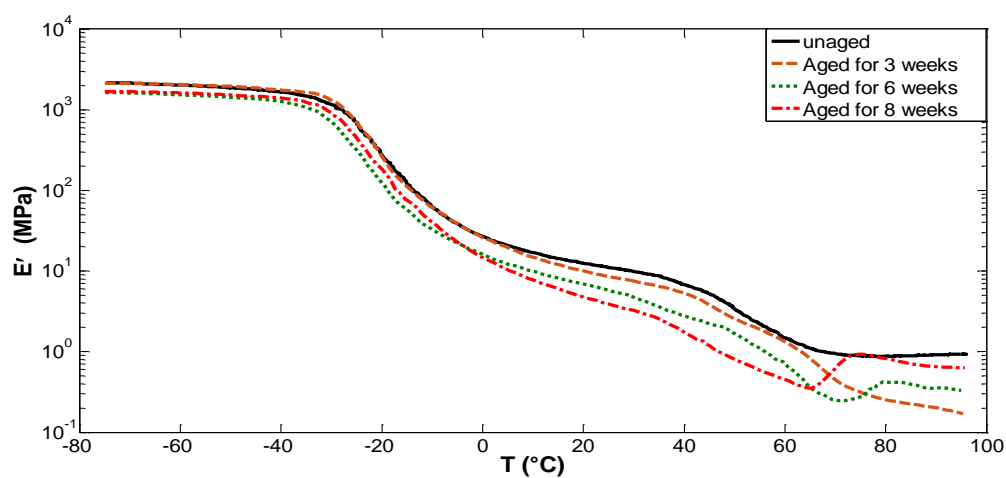


Figure 5.18: Storage modulus versus temperature for unaged and UV aged EVA.

Figure (5.19: a) shows $\tan(\delta)$ versus temperature for the UV aged samples. In the curves the peaks are attributed to the glass transition temperature of the samples (Varghese et al. 2002) which is shown in Figure (5.19: b). This also in correlation with DSC results (Figure (5.17)) and does not show a significant change in T_g .

The storage modulus at a given temperature was plotted against the ageing time to investigate the effect of ageing on the mechanical properties of the EVA. Figures (5.20: a-d) show this for four temperatures. These figures show E' reduces with increasing ageing time.

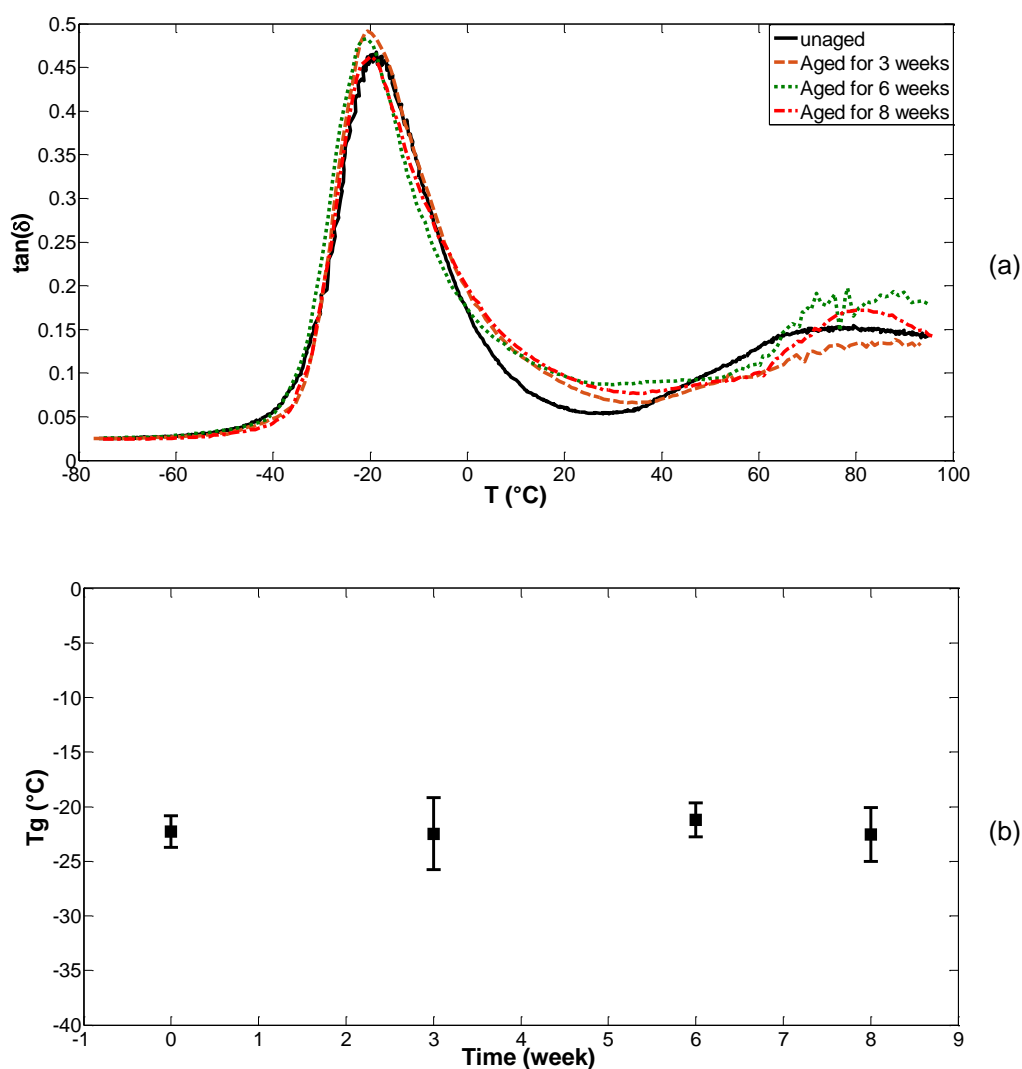


Figure 5.19: (a) $\tan(\delta)$ vs temperature for unaged and UV aged EVA, (b) T_g versus ageing duration based on Figure (5.19: a).

Examination of the Response of Ethylene-vinyl Acetate Film to UV Irradiation

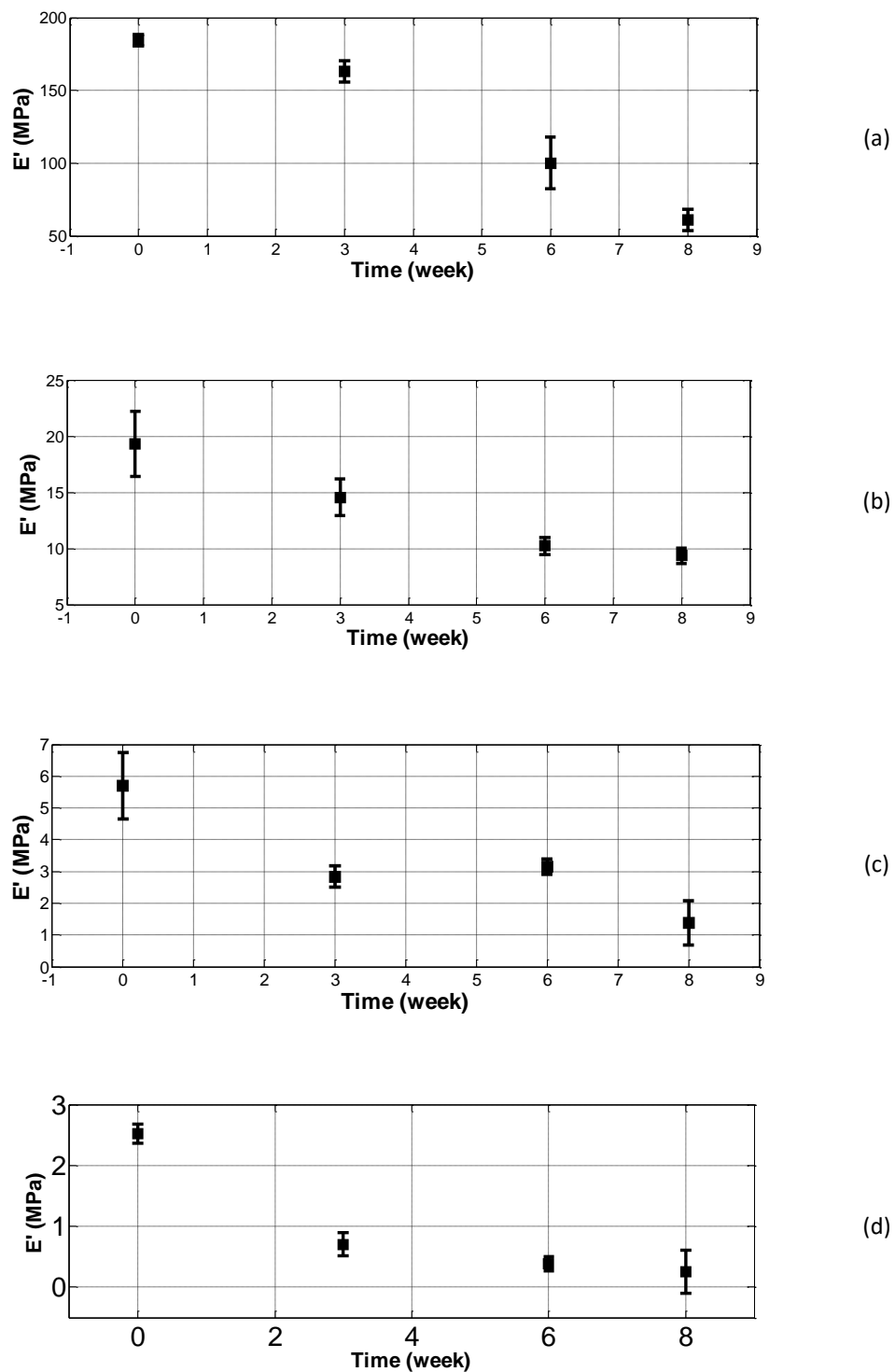


Figure 5.20: Storage modulus measured at (a) -20°C , (b) 0°C (c), 20°C (d) 40°C as a function of ageing time.

E' vs temperature for four temperature values was consolidated into one plot as a mean in order to approximate the general trend of E' . This can be seen in

Figure (5.21), which shows a decreasing storage modulus as the material ages. Further, the variation in modulus depends on temperature; as the measurement temperature increases, the dependence on the ageing duration weakens (Table (5.5)).

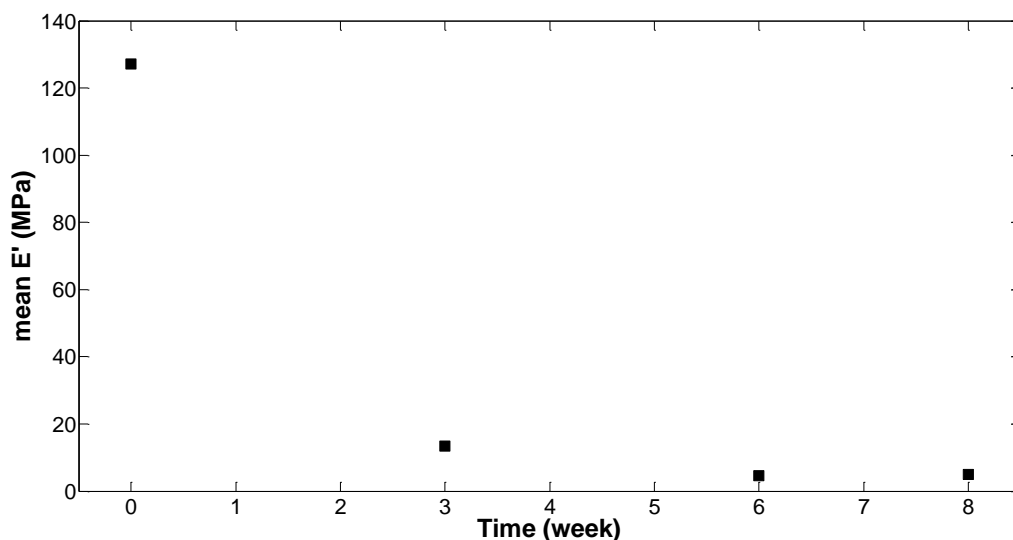


Figure 5.21: Mean storage modulus versus ageing time for EVA.

Table 5.5: The fitting parameters for storage modulus at different fixed temperatures based on Figures (5.20).

Temperature (°C)	Gradient	Intercept	R ²
-20	-15.9	194.7	0.96
0	-1.284	10.86	0.97
20	-0.4655	5.245	0.82
40	-0.2712	2.119	0.81

In order to understand the influence of photodegradation on the mechanical properties of EVA mean E' is plotted versus C_r and C_p . Figures (5.22) and (5.23) show the relation between the concentration of ester and carboxylic acid with changes in mean E' respectively. The results show the storage modulus decreases by decreasing concentration of ester and increasing concentration

Examination of the Response of Ethylene-vinyl Acetate Film to UV Irradiation

of carboxylic acid. Therefore, photodegradation damages the EVA's mechanical properties which are due to destructive influence of photochemical degradation.

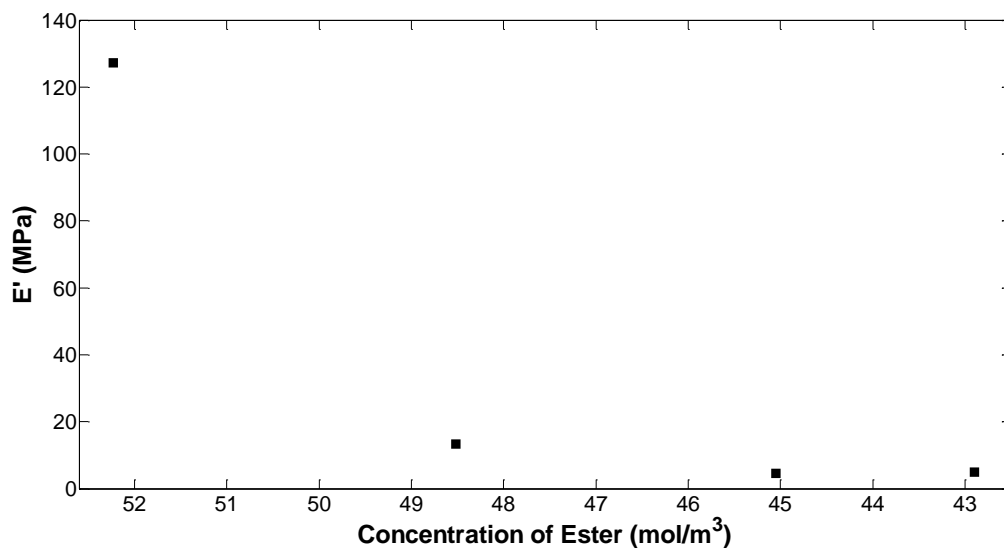


Figure 5.22: Average storage modulus versus concentration of ester on the irradiated surface of UV aged EVA.

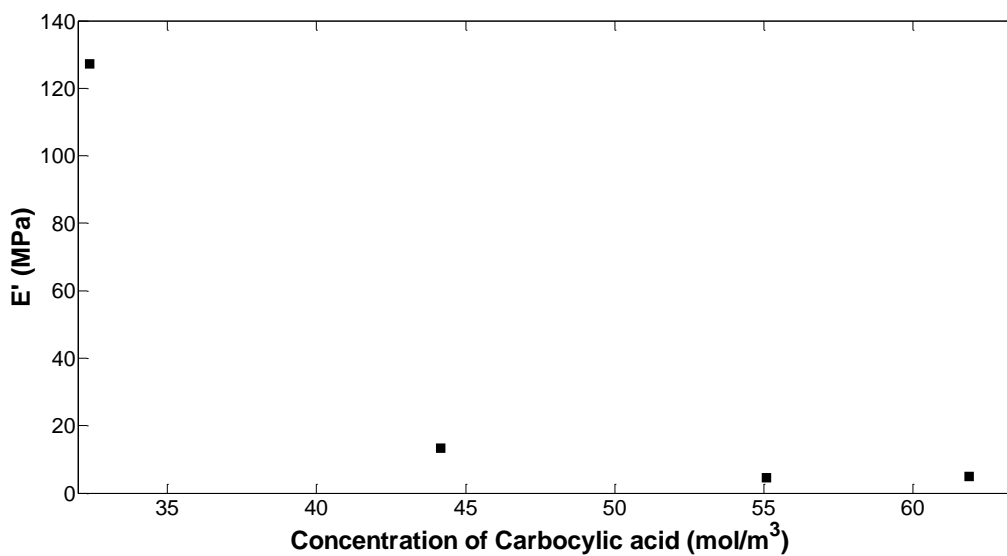


Figure 5.23: Average storage modulus versus concentration of carboxylic acid on the irradiated surface of UV aged EVA.

5.4 Conclusions

In this chapter the impact of UV irradiation on the photodegradation, structure and properties of EVA was investigated by exposing EVA to artificial UV ageing. For the sake of comparison some samples were kept in a desiccator away from the degradation factors as control samples and also some samples were aged in a dark laboratory oven at 65°C in order to isolate the UV from the thermal effects.

The FTIR-ATR spectra of unaged and UV aged EVA showed notable chemical changes occurred as a result of UV ageing. The absorbance peaks related to carboxylic acid, lactone and vinyl sharply increased after the UV irradiation. The changes on the irradiated side of the UV aged samples were more significant compared to other samples which show the dominant effect of UV in the chemical degradation of EVA. The differences in the FTIR-ATR spectra on the UV irradiated and non-irradiated side of the UV aged samples show that the intensity is depth dependant. The analytical results showed that the photochemical reaction is completed on the irradiated surface of EVA in around 5 year at 0.68 W/m^2 of continuous UV intensity. It should be considered that this time is much longer considering the real field condition and the glass top layer which absorbs a great portion of UV. DMA showed storage modulus at 1 Hz was significantly reduced with increases in temperature due to viscoelastic nature of the copolymer. Ageing had significant influence on the mechanical properties of the EVA and reduces the storage modules monotonically as a function of ageing degree. DSC results showed the crystallinity was massively affected by UV which suggested that property changes could be connected to structural modifications. Both DSC and DMA results showed that the photodegradation significantly affects the structure and mechanical properties of EVA.

In the next chapter moisture absorption of the EVA is studied and the influence of damp heat ageing on the properties of EVA in investigated.

Chapter 6

Investigation of Moisture Diffusion and the Response of Ethylene-vinyl Acetate Film to Damp- Heat

6.1 Introduction

The importance of moisture ingress and the impact of moisture on the durability and performance of PV modules have motivated many researchers to investigate moisture diffusion in the module and in particular, the encapsulant materials. However, the majority of these investigations have been carried out using Mocon[®] devices under ideal conditions and either in the presence of elemental gas, such as nitrogen, to degas the material and then with humidity applied to study the permeability. This method is an indirect method to calculate the moisture diffusion coefficient from direct measurements of the permeability and solubility.

Diffusion is the net movement of molecules from a region of high concentration to a region of low concentration. Water sorption in polymers is linked to the availability of free volume holes in the polymer chain networks and polymer-water affinity. The hole availability depends on factors such as polymer morphology, structure and crosslink density (Nogueira et al. 2001; Liu et al. 2003). The investigation and modelling of water/moisture absorption in polymers is of concern in many engineering applications and has been the subject of significant previous research (Ashcroft et al. 2012; Liu, Wildman, Ashcroft, et al. 2012b; a. Mubashar et al. 2009; A. Mubashar et al. 2009).

In this chapter the diffusion coefficient of EVA is determined as function of relative humidity. This was performed by applying the solution of the diffusion equation to moisture uptake experiments and extracting the diffusion coefficient (D) via curve fitting following with prediction of moisture concentration. Figure (6.1) illustrates the approach taken and techniques used in this chapter in order to investigate the impact of the damp heat ageing and moisture absorption on the structure and viscoelastic properties of EVA.

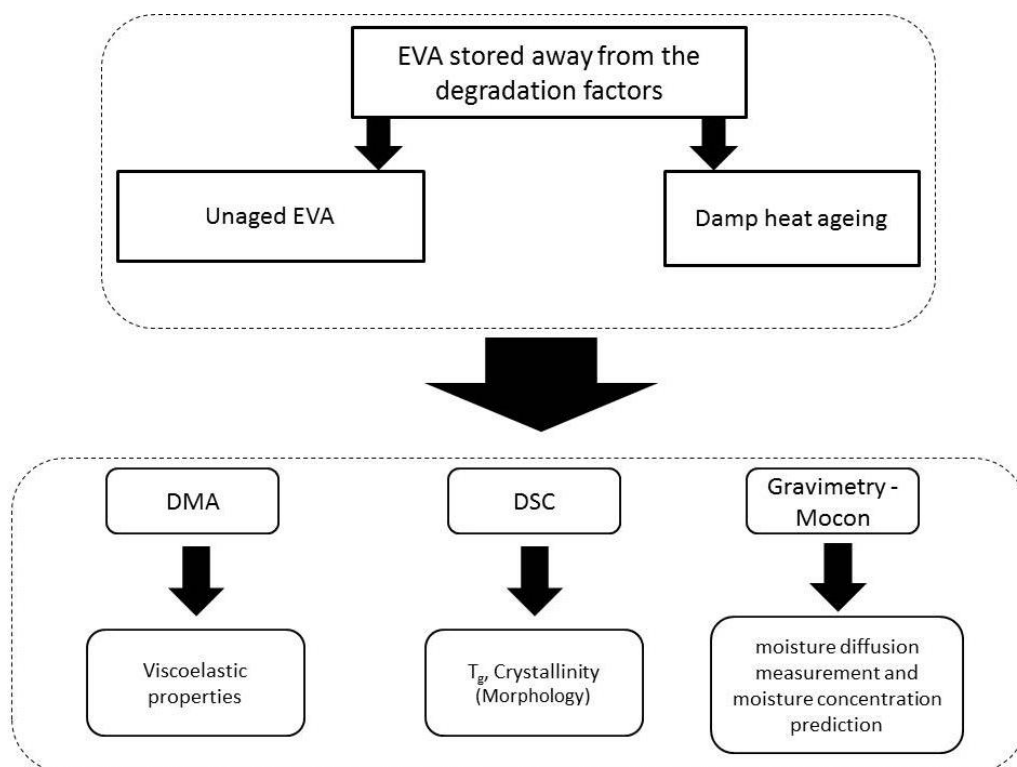


Figure 6.1: Flowchart of investigation of EVA's response to damp heat ageing.

6.2 Analytical Solution of the diffusion equation

6.2.1 Fickian Diffusion

Moisture absorption in a plane sheet can often be simplified to a one dimensional diffusion problem. The simplest moisture diffusion can be modelled through the solution of Fick's Second Law of diffusion (Siah 2010; Shirrell 1978; Crank 1975), which is represented mathematically by Eq. (6.1).

$$\frac{\partial c_{(x,t)}}{\partial t} = \frac{\partial}{\partial x} \left(D \frac{\partial^2 c_{(x,t)}}{\partial x} \right) \quad (6.1)$$

where $c_{(x,t)}$ is the moisture concentration and D is the diffusion coefficient, t and x are the time and spatial coordinate respectively. In the case where D is independent of the moisture concentration, Eq. (6.1) can be simplified to:

$$\frac{\partial c_{(x,t)}}{\partial t} = D \frac{\partial^2 c_{(x,t)}}{\partial x^2} \quad (6.2)$$

In the one dimensional case with uniform initial concentration of the penetrant throughout a plane sheet, the boundary conditions can be represented by

$$c_{(x,0)} = c_0 \text{ at } -l \leq x \leq l \text{ and } t = 0 \quad (6.3)$$

$$c_{(x,t)} = c_b \text{ at } x = -l, x = l \text{ and } t \geq 0 \quad (6.4)$$

where c_0 and c_b are the initial moisture concentration in the plate and the moisture concentration of the boundary/surface respectively and l is thickness of the sheet where in this case $l/2$ is used due to using free standing films in the gravimetric test.

The solution for Eq. (6.2) can be obtained by the method of separation of variables or by the Laplace transform (Crank 1975). The solution for 1-D Fickian diffusion in a plane sheet is

$$\frac{c(x,t)-c_0}{c_b-c_0} = 1 - \frac{4}{\pi} \sum_{n=0}^{\infty} \frac{(-1)^n}{(2n+1)} \exp\left[\frac{-(2n+1)^2\pi^2Dt}{4l^2}\right] \times \cos\left(\frac{(2n+1)\pi x}{2l}\right) \quad (6.5)$$

In our experiments it is assumed the material had no moisture content at $t = 0$ when the samples were placed in the environmental chamber, therefore, $c_0 = 0$ and $c_b = c_{sat}$. Eq. (6.5) can then be simplified to

$$\frac{c(x,t)}{c_{sat}} = 1 - \frac{4}{\pi} \sum_{n=0}^{\infty} \frac{(-1)^n}{(2n+1)} \exp\left[\frac{-(2n+1)^2\pi^2Dt}{4l^2}\right] \times \cos\left(\frac{(2n+1)\pi x}{2l}\right) \quad (6.6)$$

This gives the moisture content distribution, however to relate to gravimetric experiments the sum of moisture in the film is determined by integrating over the thickness $2l$, giving Eq. (6.7) (Crank 1975; Fan et al. 2009).

$$\frac{M_t}{M_{\infty}} = 1 - \frac{8}{\pi^2} \sum_{n=0}^{\infty} \frac{(-1)^n}{(2n+1)^2} \exp\left[\frac{-(2n+1)^2\pi^2Dt}{4l^2}\right] \quad (6.7)$$

where M_t and M_{∞} are the total mass of moisture at time t , saturated mass of moisture in the sheet. The relation between concentration and mass is presented as Eq. (6.8)-(6.9).

$$c_{sat} = \frac{M_{\infty}}{V} \quad (6.8)$$

$$c_0 = \frac{M_0}{V} \quad (6.9)$$

where V and M_0 are the volume and the initial mass of moisture respectively.

6.3 Results and discussion

The results of gravimetric, water vapour transmission, DSC and DMA are presented below based on the ageing conditions and experimental techniques described in sections (3.3) and (3.4) respectively.

6.3.1 Measurement of moisture diffusion coefficient and predicting moisture concentration

6.3.1.1 Gravimetric method

Figure (6.2) shows the absorption curve for EVA at 85°C-85% RH. As expected the moisture content increases with time. Under this condition, the samples were saturated after around 5 weeks, after which the sample weights were constant. Using the data shown in Figure (6.2), the value of the moisture diffusion coefficient were obtained by fitting Eq. (6.7) to the experimental gravimetric data, where the summation was taken to the first 50 terms. The resultant values for the moisture diffusion coefficient (D), the saturation moisture concentration (c_s) are presented in Table (6.1).

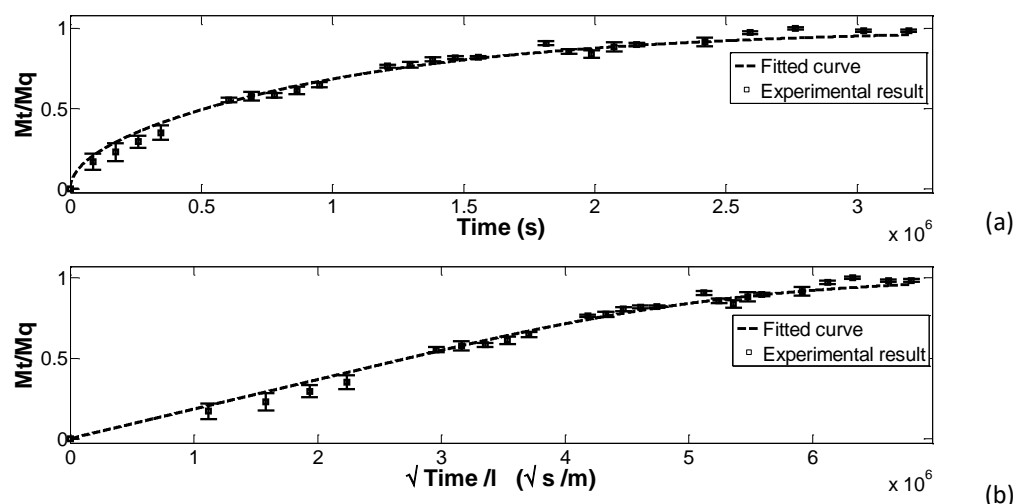


Figure 6.2: Moisture absorption curve for EVA film at 85°C-85% RH, (a) M_t/M_q vs time, (b) M_t/M_q vs $\sqrt{\text{time}/l}$.

Investigation of Moisture Diffusion and the Response of Ethylene-vinyl Acetate Film to Damp-Heat

Table 6.1: Gravimetry test results.

Sample	Condition	Thickness (mm)	WVTR (g/(m ² .day))	Permeability (gm.cm)/(cm ² .sec.Pa)	c _s (kg/m ³)	Diffusion (m ² /sec)	Solubility (gm/(cm ² .Pa))
EVA	85°C 85% RH	0.526	-	-	13.714	5.028 × 10 ⁻¹¹	-

6.3.1.2 Water Vapour Transmission Rate

As described in section (3.5.2) Water Vapour Transmission Rate (WVTR) is an indirect technique to measure the moisture diffusion coefficient. Table (6.2) presents the results of the WVTR test provided by RDM TEST Equipment® at the conditions detailed in Table (3.3).

Table 6.2: WVTR test results (the analyses were carried out on a MOCON® Permatran-W Water Vapour Permeability Instrument).

Sample	Condition	Thickness (mm)	WVTR (g/(m ² .day))	Permeability (gm.cm)/(cm ² .sec.Pa)	c _s (kg/m ³)	Diffusion (m ² /sec)	Solubility (gm/(cm ² .Pa))
EVA	40°C 100% RH	0.526	37.77	3.114 × 10 ⁻¹³	-	7.085 × 10 ⁻¹¹	4.395 × 10 ⁻⁷

The diffusion coefficient measured and calculated by both techniques are in agreement with the values from the literature (Table (2.3)), however, there is a difference of around 2×10^{-11} between the two values measured by Mocon® and gravimetric methods which can be due to the different test conditions, differences in the nature of tests where in the gravimetric method the EVA film was exposed to 85°C-85% RH for around 5 weeks but in the WVTR test the sample was exposed to 40°C and 100% RH for around 140 minutes in the presence of nitrogen to avoid any degradation and also experimental errors where in gravimetry the samples were not kept continuously at 85°C-85% RH and they were taken out for weight measurement.

In this study the diffusion coefficient measured by gravimetric test was used for predicting moisture concentration in depth.

6.3.1.3 Moisture concentration

Once moisture diffusion coefficient is determined, moisture concentration at any spot within the film at time t can be achieved via Eq. (6.6) (Karimi 2006). Figure (6.3) shows the moisture concentration inside the EVA film. The results show the moisture concentration increases by time until saturation point after around 5 weeks under constant condition of 85°C-85% RH.

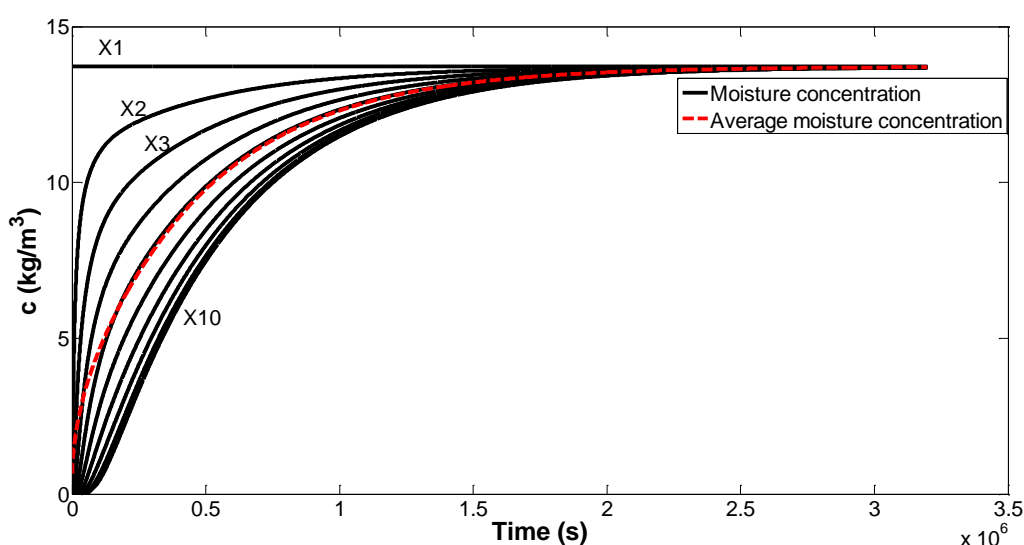


Figure 6.3: Simulated moisture concentration inside the EVA film at different depths (X1-X10) under the damp heat condition of 85°C-85% RH.

6.3.2 Differential Scanning Calorimetry (DSC)

The first heating thermograms of unaged and aged EVA at 85°C-85% RH and 22±3°C-85% RH are reproduced with offsets added for the sake of comparison which are presented in Figures (6.4: a-b). Unaged EVA shows a melting area between 40°C and 80°C with a single peak at 45°C and a shoulder at 55°C. The melting transition of the ethylene segment has been accepted as showing as a peak with a shoulder observed between 40°C to 80°C (Motta 1997; Li et al. 2013). As the ageing at 85°C-85% progresses the peak at 45°C disappears and the melting peak shows itself at 55°C. The secondary melting point is linked to the secondary crystallization which takes place between the primary

Investigation of Moisture Diffusion and the Response of Ethylene-vinyl
Acetate Film to Damp-Heat

crystallization and storage or exposure to elevated temperature (Oreski & Gernot M. Wallner 2010). It is reported that the ethylene copolymer has a two-stage crystallisation: primary and secondary. The secondary crystallisation is due to rearrangement of irregular polymer chains and the segments that are left in the amorphous phase, into the crystals (Akpalu et al. 1999; Feng & Kamal 2005; Alizadeh et al. 1999). The secondary melting point is assigned to the less organised crystal phase considering the fact that EVA containing 33% VAc is semi-crystalline and ageing may affect the less crystalline phase (Brogly et al. 1997a). In the case of $22\pm 3^{\circ}\text{C}$ -85% RH the thermograms do not change with ageing, which shows the significant effect of temperature on changes in the copolymer's structure.

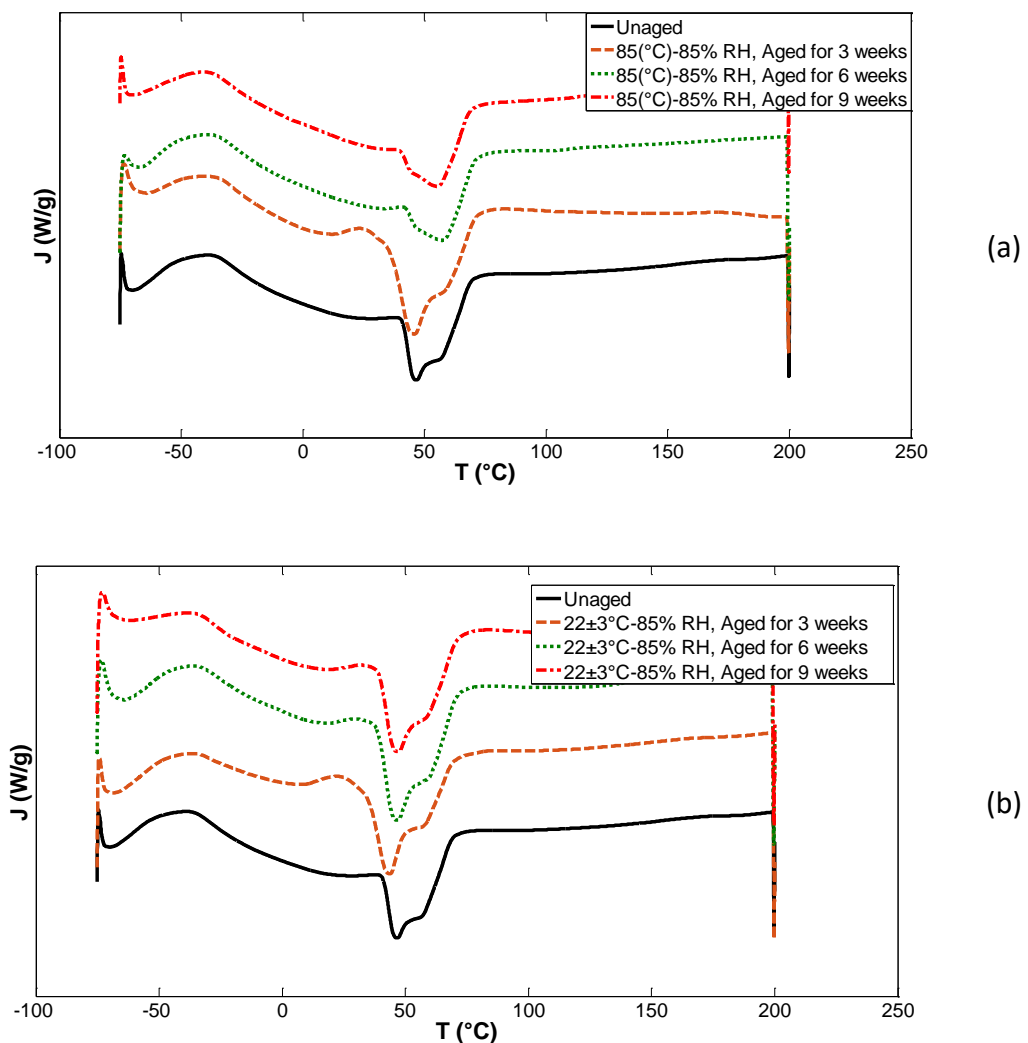


Figure 6.4: DSC first heating thermograms for the unaged and damp heat aged EVA at (a) 85°C -85% RH and (b) $22\pm 3^{\circ}\text{C}$ -85% RH-Exo Up.

Investigation of Moisture Diffusion and the Response of Ethylene-vinyl
Acetate Film to Damp-Heat

Figure (6.5: a-b) show T_g versus ageing time for the two different ageing conditions. T_g , typically identified by a step change in the heat flow was found to be around -25°C for aged and unaged samples, suggesting ageing has no significant effect on T_g .

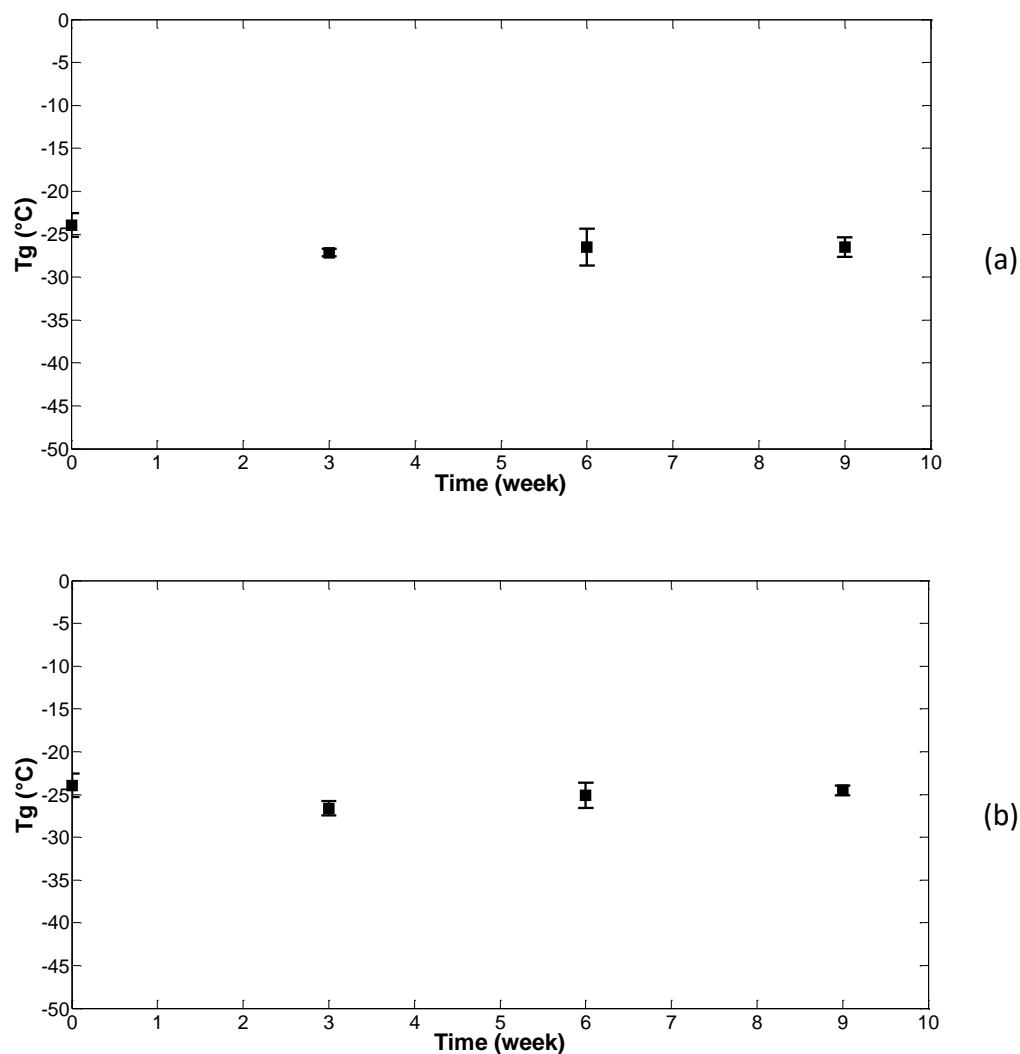


Figure 6.5: Glass transition temperature versus ageing time for EVA at (a) 85°C -85% RH and (b) $22\pm 3^\circ\text{C}$ -85% RH.

Figures (6.6: a-b) show X_c (calculated via Eq. (3.1)) versus ageing time for the two different ageing conditions. Analysis of the first heating results shows that in the case of ageing at 85°C -85% RH, crystallinity had increased after 3 weeks of ageing and then decreased to a value lower than the original crystallinity. The increase in the crystallinity is due to the secondary crystallization which

continues when EVA is aged above the glass transition temperature in the damp heat ageing and the crystals become larger (X. M. Shi et al. 2009) which has also been observed by other researchers using different techniques including DSC and WAXD (Oreski & Gernot M Wallner 2010; X.-M. Shi et al. 2009; Chen et al. 2009). The increasing crystallinity can also be due to the creation of double bonded water as presented in the study performed by (Iwamoto & Matsuda 2005; Iwamoto et al. 2003). The results of ageing at $22\pm 3^{\circ}\text{C}$ -85% show a similar trend but over a longer time scale, which would be expected as both moisture absorption and thermal degradation are thermally activated processes. It can also be seen that in both ageing environments there is no change in crystallinity during the second heating. It can be concluded, therefore, that moisture diffusion into the polymer structure causes an increase in crystallinity, however, elevated temperature has a greater influence on the structure of the EVA as the ageing time increases. It should also be mentioned again here that the first heating was to investigate the impact of ageing on EVA and the second heating was to erase the thermal history regarding the curing, storing conditions and the ageing in order to investigate the properties of EVA independent from these effects. In order to understand the relation between the moisture absorption and the structural changes in EVA, the changes of crystallinity were investigated as moisture concentration increases. Figure (6.7) shows crystallinity after first and second heating versus moisture concentration at the intervals of 0, 3, 6 and 9 weeks considering the EVA samples saturated in 5 weeks. The results of the first heating show crystallinity increases as the samples absorb moisture until the saturation point. After the saturation point the crystallinity decreases to a value lower than the initial value which shows the initial impact of moisture absorption which causes an increase in crystallinity however, with further ageing at damp heat condition after saturation point thermal degradation (described in chapter 4) plays a dominant role which causes a decrease in the crystallinity. The results of the second heating do not show any significant changes in the crystallinity due to the erased thermal history.

Investigation of Moisture Diffusion and the Response of Ethylene-vinyl Acetate Film to Damp-Heat

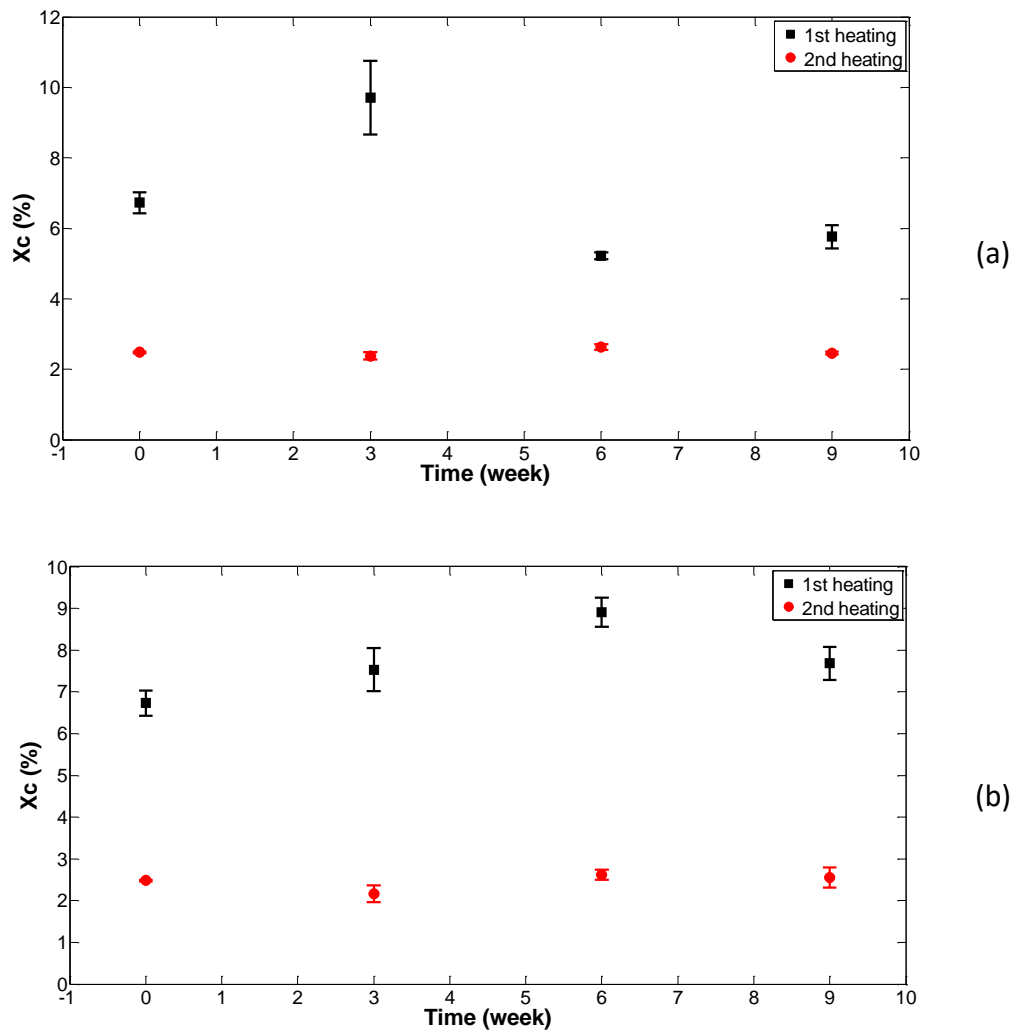


Figure 6.6: Crystallinity versus ageing time after first and second heating for unaged and aged EVA at (a) 85°C-85% RH and (b) 22±3°C-85% RH.

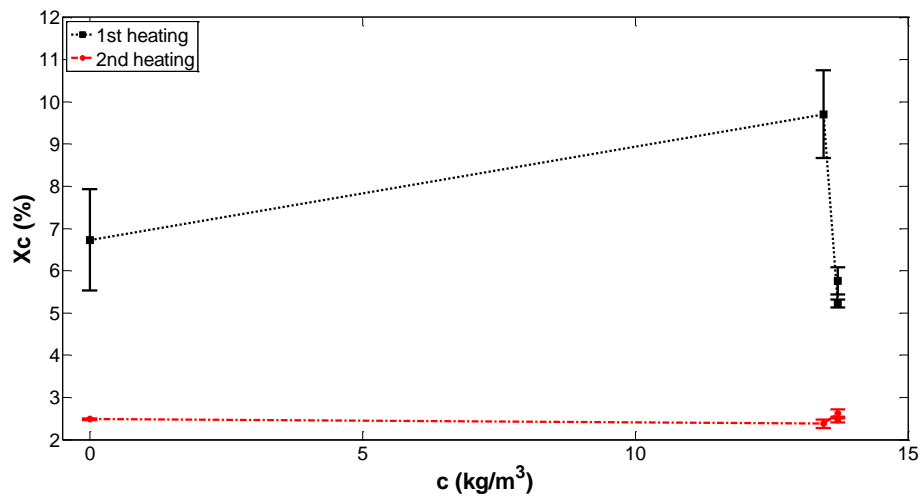


Figure 6.7: Crystallinity versus average concentration after first and second heating for unaged and aged EVA at 85°C-85% RH.

6.3.3 Dynamic Mechanical Analysis (DMA)

Figures (6.8: a-b) show the storage modulus (E') determined as a function of temperature at a frequency of 1 Hz for the two damp heat ageing conditions. As the temperature increases, E' decreases and the curves show the typical regions and transitions of a viscoelastic material, as described previously (Stark & Jaunich 2011). A four-decade difference is observed in E' between -75°C and 95°C with a sharp decrease at around -30°C, which can be attributed to the glass transition and then another stepped decrease between 40°C and 65°C which may be due to some crystal melting. Both transitions correlate well with the DSC identified T_g and melting points. The results show that the mechanical properties of EVA were affected more significantly under 85°C-85% RH condition due to the higher temperature and changes in the crystallinity, where E' has a significant increase after 3 weeks and then it drops to lower values than the original values as the ageing time increases.

Investigation of Moisture Diffusion and the Response of Ethylene-vinyl Acetate Film to Damp-Heat

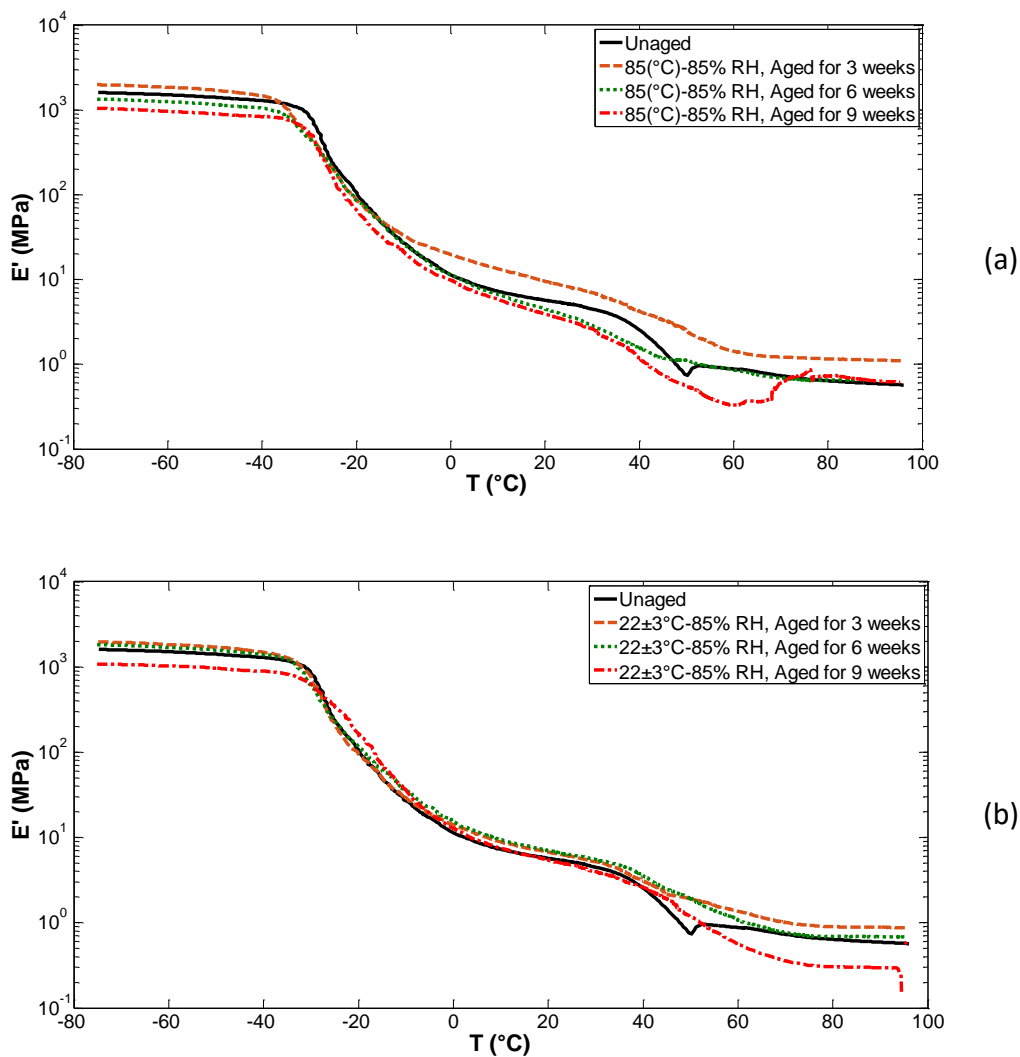


Figure 6.8: Storage modulus vs temperature for unaged and aged EVA at (a) 85°C-85% RH and (b) 22±3°C-85% RH.

Figures (6.9: a) and (6.10: a) show $\tan(\delta)$ versus temperature for two damp heat ageing conditions, in which the peak can be attributed to the glass transition temperature of the samples as shown in Figures (6.9: b) and (6.10: b) (Varghese et al. 2002). This also correlates well with the DSC results (Figure (6.5)). The plots do not show a significant change in T_g with ageing for either condition.

Investigation of Moisture Diffusion and the Response of Ethylene-vinyl
Acetate Film to Damp-Heat

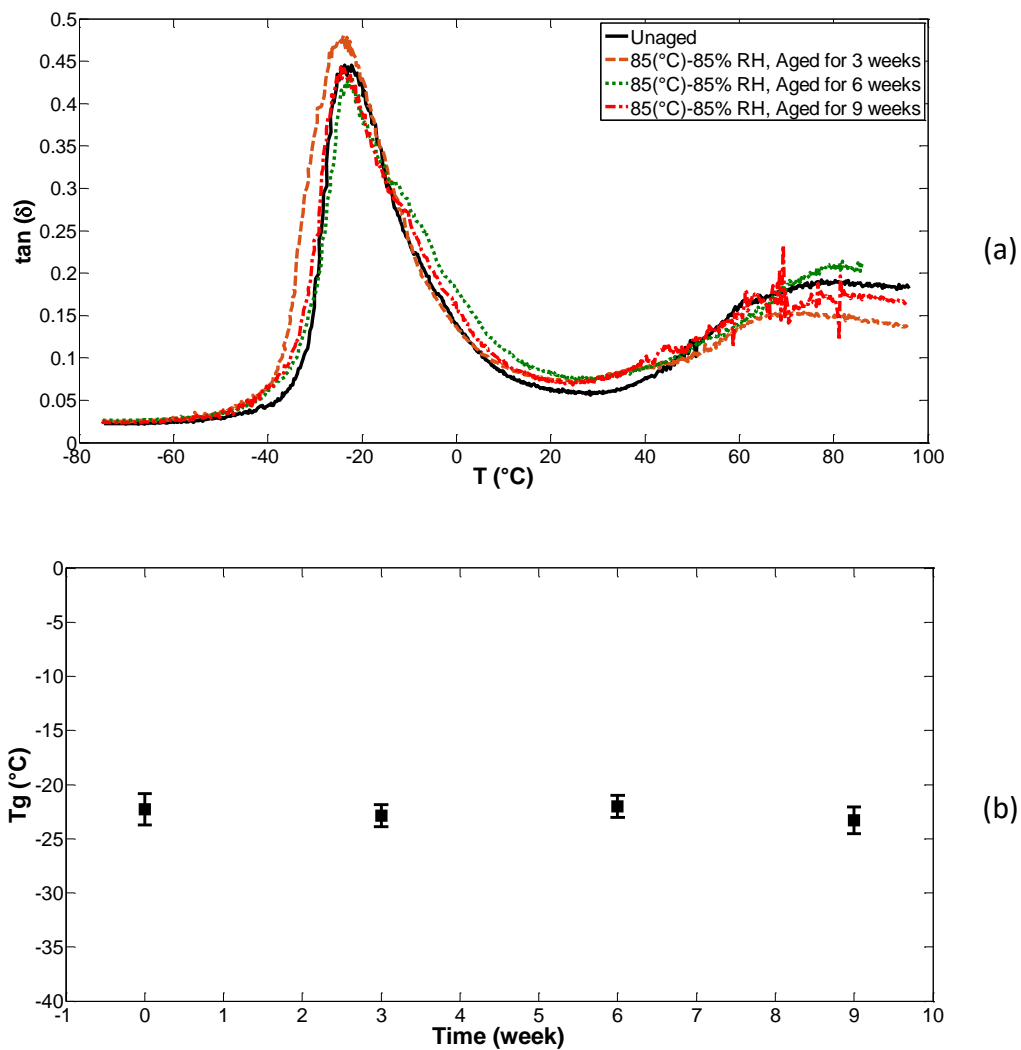


Figure 6.9: (a) $\tan(\delta)$ vs temperature for unaged and aged EVA at 85°C-85% RH, (b) T_g versus ageing duration based on Figure (6.9: a).

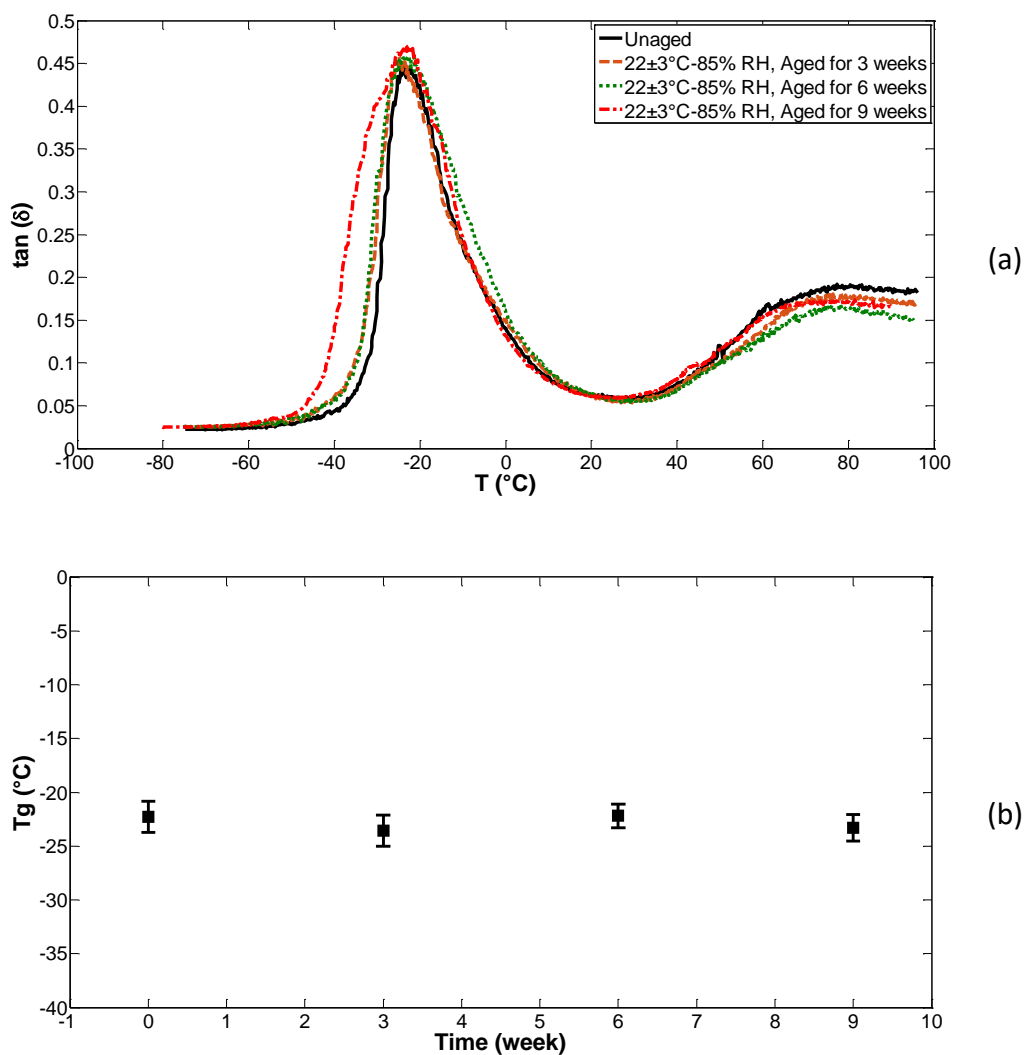


Figure 6.10: (a) $\tan(\delta)$ vs temperature for unaged and aged EVA at 22±3°C-85% RH, (b) T_g versus ageing duration based on Figure (6.10: a).

For further investigation of the effect of damp heat ageing on the mechanical properties of the EVA, the storage modulus at a given temperature was plotted against the ageing time for the aged and control samples. Figures (6.11: a-d) and (6.12: a-d) show plots of modulus as a function of ageing time measured at 0°C, 20°C, 40°C and 60°C. In the case of 85°C-85% RH after three weeks of damp heat ageing E' increased due to the increase in crystallinity (Figure (6.6)). However, one can see that E' reduces to lower than the initial value with increased time of ageing. At 22±3°C-85% RH E' shows a different behaviour. E' increases up to the sixth week of the ageing at damp environment and start to decrease after this point which is a similar trend to 85°C-85% RH but in a longer time scale and can be due to changes in structure

of EVA (presented in Figure (6.6)). Comparing the test results of both damp heat conditioning conditions, shows the significant impact of moisture diffusion into the copolymers structure at the early stage of the exposure which increases the crystallinity but on the other hand the impact of heat on the polymer ageing and mechanical degradation is noticeable and causes a decrease in E' as pointed out in chapter 4 where the storage modules reduced by thermal ageing as a function of ageing degree. In other words moisture diffusion and thermal degradation competes in damp heat ageing in particular in the early stage of ageing. However, the analysis of the results of the damp heat test at 85°C-85% RH indicate that the effect of heat is more dominant as the ageing time increases.

Investigation of Moisture Diffusion and the Response of Ethylene-vinyl
Acetate Film to Damp-Heat

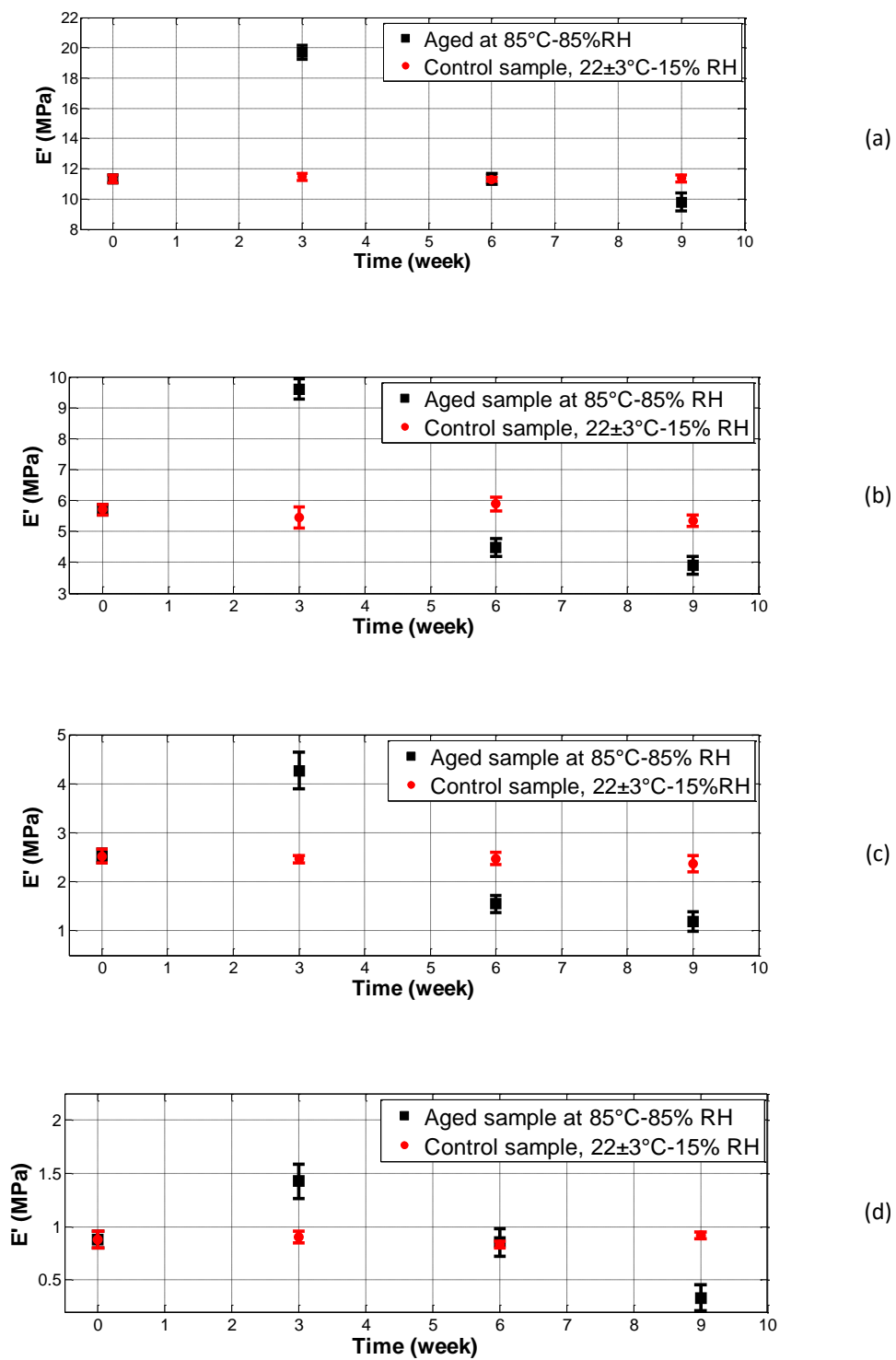


Figure 6.11: Storage modulus measured at (a) 0°C, (b) 20°C (c), 40°C (d) 60°C as a function of ageing time at 85°C-85% RH.

Investigation of Moisture Diffusion and the Response of Ethylene-vinyl
Acetate Film to Damp-Heat

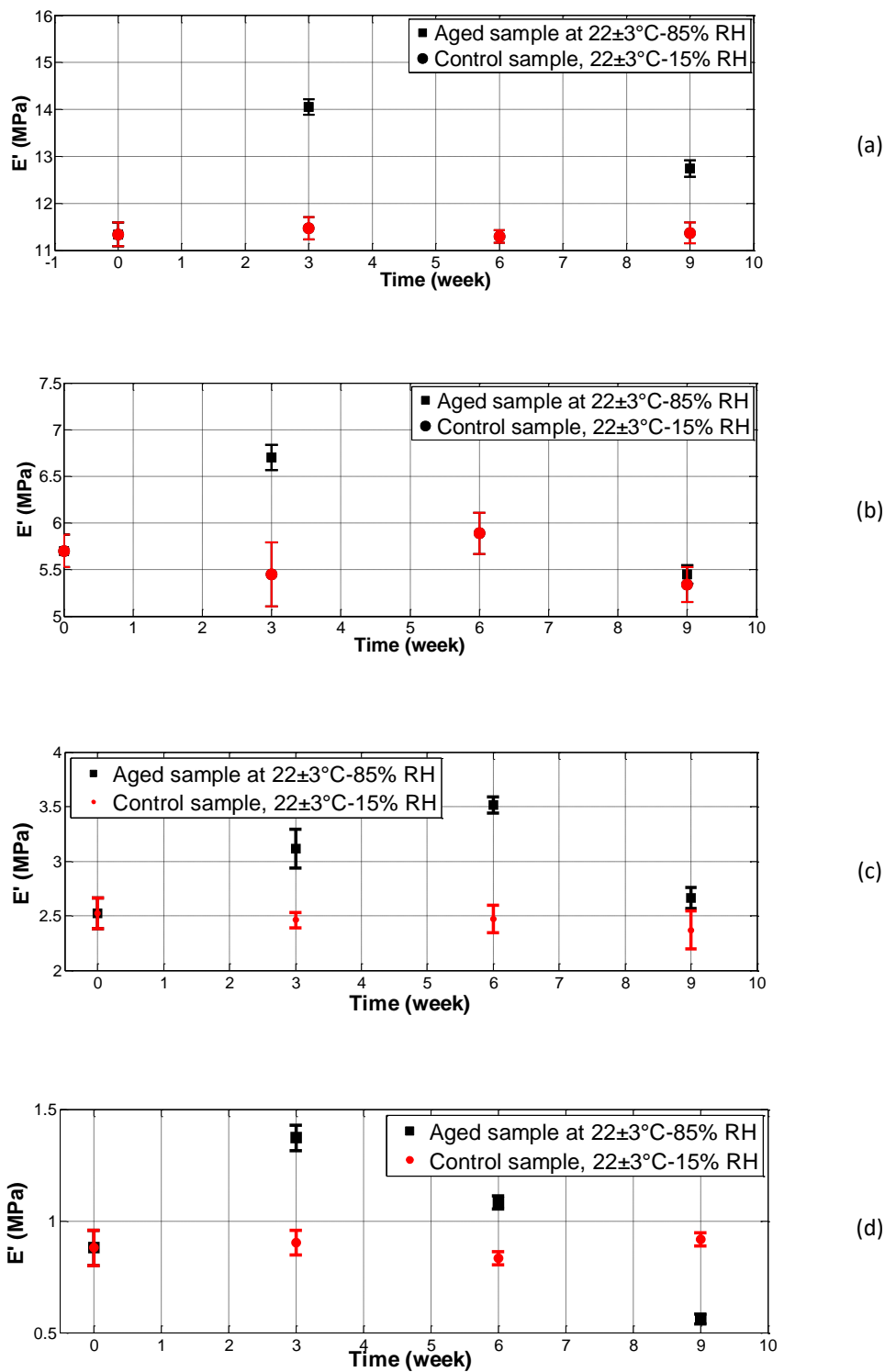


Figure 6.12: Storage modulus measured at (a) 0°C , (b) 20°C (c), 40°C (d) 60°C as a function of ageing time at $22\pm 3^\circ\text{C}$ -85% RH.

In order to have a clear view of the general trend, E' versus ageing time for four fixed temperature values (Figures (6.11: a-d) and (6.12: a-d)) were

Investigation of Moisture Diffusion and the Response of Ethylene-vinyl Acetate Film to Damp-Heat

combined into one plot as a mean storage modulus versus ageing time. The consolidated results are shown in Figure (6.13), which shows a decrease in storage modulus after the third week of ageing at 85°C-85% RH as the material ages. In the case of 22±3°C-85% RH the storage modulus was increasing up to week six of ageing and then started to decrease. The impact of damp heat ageing can be divided into the effect of moisture which increases the modulus at the early exposure time and ageing effect of heat which has an opposite and dominant influence as the ageing time increases. In the case of 85°C-85% RH the samples absorb and lose moisture faster due to the higher test temperature which results in a sharp decrease in crystallinity and E' as its consequence. But when the test temperature is 22°C the samples moisture desorption is slower which results in a gradual decrease in crystallinity and E' , therefore, moisture affects the properties of EVA at the early stage of the test and up to the saturation point where temperature plays a significant role after this point. Both increasing and decreasing storage modulus can cause serious problems such as delamination and problems in mismatches in thermal expansion and cracking of the cell and wiring (Oreski & Gernot M. Wallner 2010). Thus, the damp heat ageing can result in significant problems during service lifetime of a PV module.

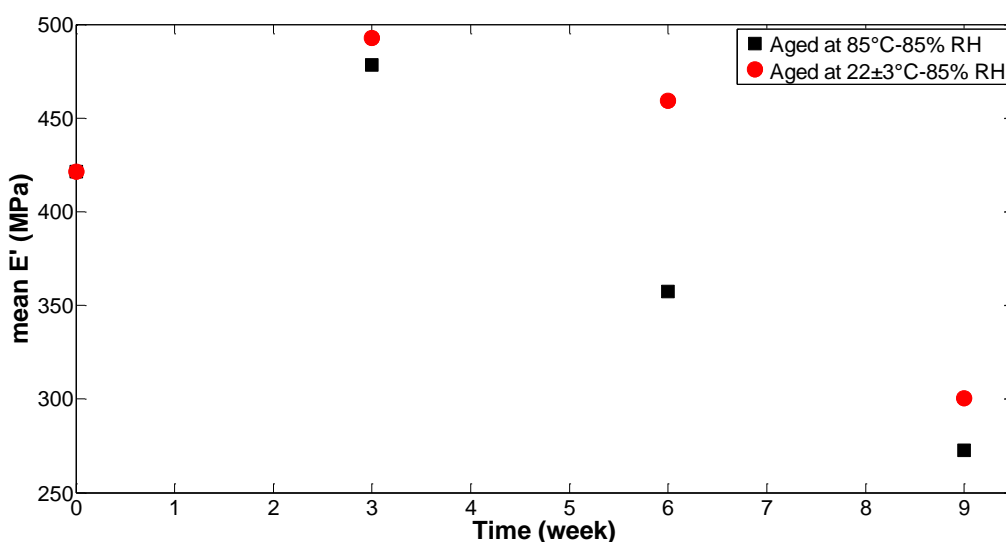


Figure 6.13: Average storage modulus versus ageing time for EVA aged at 85°C-85% RH and 22±3°C-85% RH.

Since the moisture diffusion and concentration play an important role in the first stage of the damp heat ageing it is needed to investigate the relation between the moisture absorption in EVA and the changes in the mechanical properties the changes of the storage modulus is plotted versus the moisture concentration. Figure (6.14) shows the variation of storage modulus at different moisture concentrations. It can be seen that the storage modulus increase by increasing absorbed moisture in EVA up to the saturation point but after this point the storage modulus decreases which can be correlated to the changes in the crystallinity and the influence of thermal degradation after the saturation point. Therefore, it can be concluded that after saturation point, the thermal degradation affects the mechanical properties of the EVA more significantly.

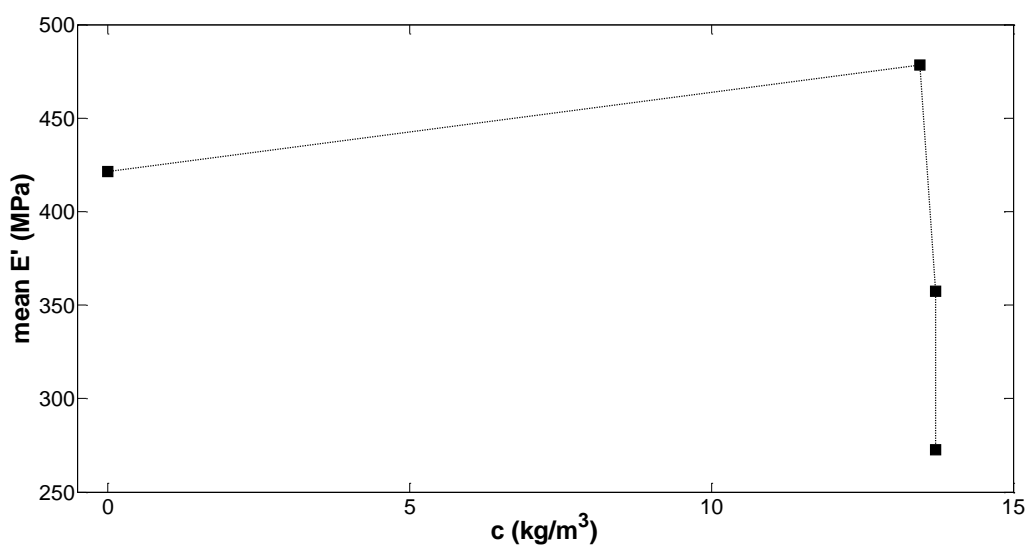


Figure 6.14: Average storage modulus versus average moisture concentration for EVA aged at 85°C-85% RH.

6.4 Conclusions

The response of the EVA copolymer to damp heat ageing was investigated at two conditions, with the same RH level and different temperatures ($22\pm 3^\circ\text{C}$ -85% RH and 85°C -85% RH). Various techniques were applied in order to

measure the moisture absorption coefficient, viscoelastic properties and investigate the morphological changes in response to damp heat ageing.

The results of the calorimetry indicated that the glass transition temperature was unaffected by the ageing, however, the crystallinity increased after three weeks of ageing, but then decreased on further ageing at 85°C-85% RH. At 22±3°C-85% RH the crystallinity increased up to the sixth weeks and then decreased with further ageing. The DSC results show significant influence of temperature on the structure of EVA. These results also suggested that property changes could be connected to the structural modifications. The storage modulus was shown to be strongly dependent on the crystallinity and correlated well with the structural changes in the EVA seen in the DSC. The results showed the long term damp heat has noticeable influence on the mechanical properties of EVA and cause decrease in E' . Comparing the DSC and DMA results against the variation of moisture concentration indicated the crystallinity and the storage modulus increased by increasing moisture concentration up to the saturation point and started to decrease after the samples reached the saturation. This can be due to the thermal degradation (described in chapter 4) which plays a dominant role after the saturation point.

As mentioned in chapter 4 PV modules will be subjected to different degradation factors in service. This chapter investigated the combination of humidity and heat which showed different results than the heat only and UV only ageing. The next chapter reviews and discusses the results with a comparative view in order to achieve a better understanding of the impact of the different ageing factors on the mechanical properties of EVA.

Chapter 7

Comparative study of ageing impact on the structure and mechanical properties EVA under different ageing conditions

7.1 Introduction

PV modules need to have a lifetime of 20-25 years to be economically reasonable. In this regard the encapsulation material should be stable at high UV exposure, elevated temperatures and humid environments. However, EVA undergoes chemical and physical degradation on exposure to harsh environmental conditions.

EVA undergoes complex degradation mechanisms owing to the interaction between the degradation factors. To tackle and simplify this interaction the logical approach was first to establish the properties and response of EVA in isolation before considering the complex interaction between the environmental degradation factors in the field. In this chapter, the response of Ethylene-vinyl Acetate (EVA) film particularly the changes in crystallinity, storage modulus and the dependence of the material properties on different ageing conditions were compared. In the next sections the ageing impact of degradation factors is compared in order to identify the dominant ageing factor.

7.2 Comparative study of UV, thermal and damp heat ageing impact on the properties of EVA

For further investigation of the effect of ageing on the structure and mechanical properties of EVA it is worth studying the impact of ageing factors comparatively. Figure (7.1) shows the changes in crystallinity versus ageing duration for different ageing conditions (see section (3.3)). The results show that the impact of UV on reduction in crystallinity is greater than other ageing factors considering that UV ageing was performed at 50°C while thermal ageing was at 85°C. This is because the product of thermochemical degradation at the in-service temperature of PV modules is acetic acid (as shown in Figure (2.4)) which is not significant where EVA undergoes a complex degradation process via Norrish reactions which yield to formation of acetic acid, carboxylic acid, ketone, lactone, vinyl and etc. However, it was also noticed that thermal only ageing has more deteriorating impact than damp heat ageing. The results showed that the initial effect of damp heat was moisture absorption and significant increase in crystallinity and storage modulus up to the saturation point which can cause some severe problems during service lifetime of a PV module and can lead to cracking of the solar cells and their wiring connections (Oreski & Gernot M Wallner 2010) and should be considered by PV module manufacturers.

Comparative study of ageing impact on the structure and mechanical properties EVA under different ageing conditions

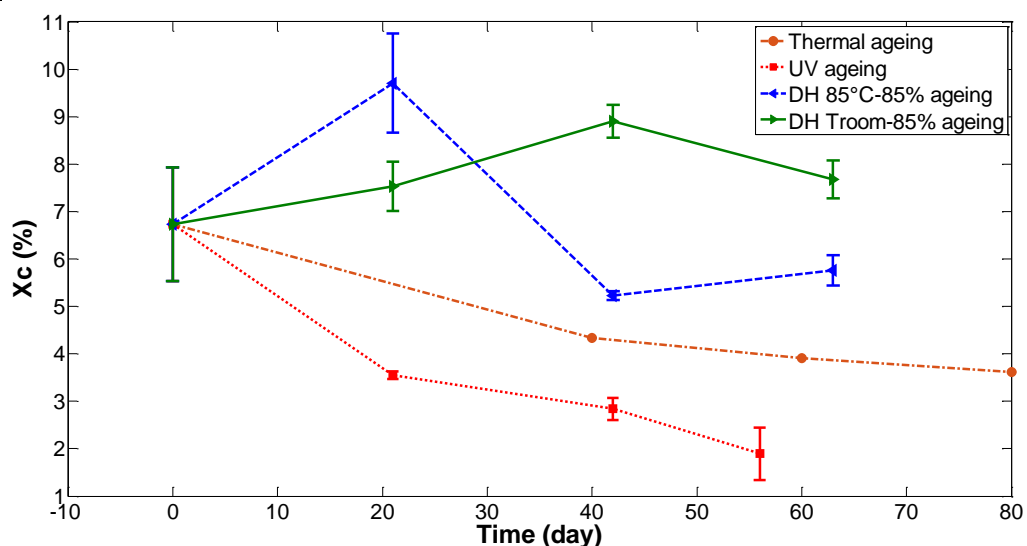


Figure 7.1: Crystallinity versus ageing duration for different ageing conditions.

Figures (7.2: a-c) show storage modulus (E') at three fixed temperatures. These results show a decreasing storage modulus as the material ages for UV and thermal ageing but in the case of damp heat ageing there is an initial increase due to the moisture diffusion into the copolymer's structure and increase in crystallinity of EVA as a result of creation of double bonded water (Iwamoto & Matsuda 2005; Iwamoto et al. 2003) which is followed by a decrease in E' as ageing time increases. As shown in Figures (7.2) the reduction in E' is at a greater rate in the case of UV ageing which is due to the influence of UV in crystallinity reduction (Figure (7.1)), chemical degradation of EVA (Figures (5.7)-(5.9)) and also presence of antioxidants (S Isarankura Na Ayutthaya & Wootthikanokkhan 2008) therefore it can be concluded that UV is the dominant ageing factor among all degradation factors. These findings are important in terms of the influence of degradation factors on the mechanical properties of EVA and the criteria in selection of suitable modules for different climatic conditions (Oreski & Gernot M Wallner 2010).

In the next section the results regarding the chemical changes in EVA after ageing and the influence of ageing on the chemical structure of EVA will be discussed for the sake comparison.

Comparative study of ageing impact on the structure and mechanical properties EVA under different ageing conditions

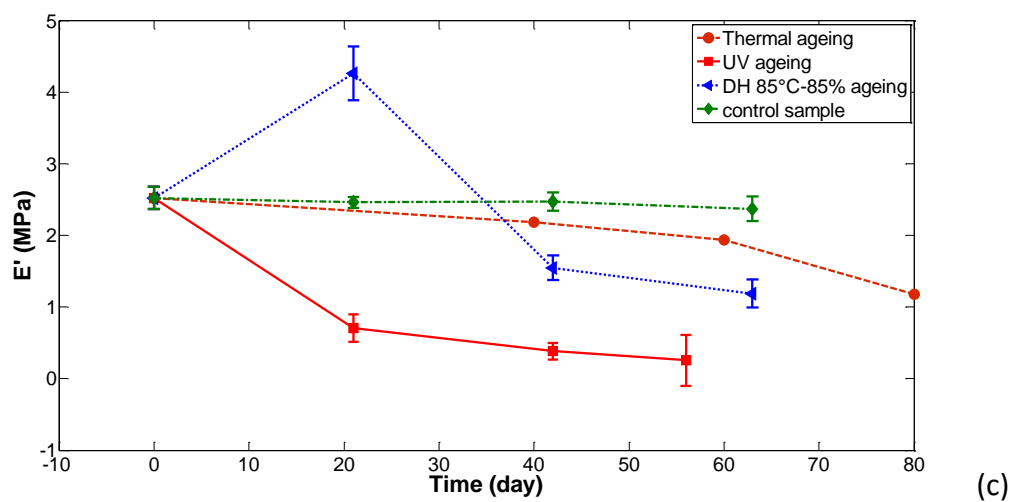
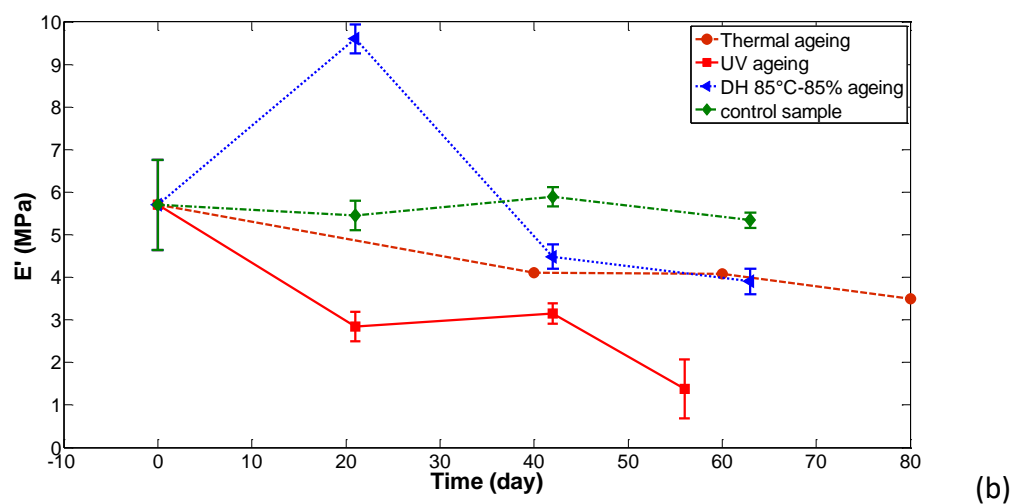
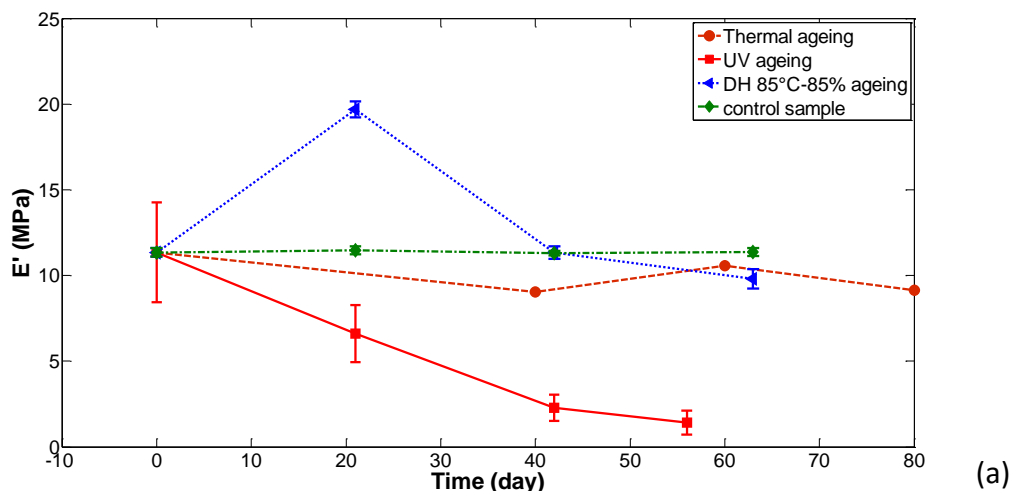


Figure 7.2: Comparative effect of degradation factors on the storage modulus of EVA at (a) 0°C, (b) 20°C, (c) 40°C versus ageing duration for control sample and aged EVA at different conditions.

7.3 Comparative study of influence of the UV thermal and damp-heat ageing factors on chemical changes in EVA

In order to understand the influence of different ageing factors the produced results are reviewed with a comparative view. The TGA and FTIR-ATR results showed that acetic acid is the common degradation product in both thermal degradation and photodegradation of EVA however, in the case thermal degradation acetic acid is formed through the so-called deacetylation process in the early stage of the decomposition and is the main degradation product (Figure (4.3)) where quantities of other products (CO, CO₂ and CH₄) are negligible (Marcilla & Sempere 2004). There is also a second stage of degradation which occurs above 400°C which is not considered in this study. The degradation behaviour of EVA is significantly dependant on vinyl acetate concentration (VAc) and in this study EVA with 33% VAc is studied to focus on the PV industry grade EVA. On the other hand photodegradation of EVA is a more complex process and occurs by different processes than thermal degradation where Norrish reactions are the dominant photodegradation processes despite the effect of elevated temperature presented in chapter 4. In photodegradation of EVA acetic acid is formed via ester elimination (Copuroglu & Sen 2005) and through decomposition of vinyl acetate segment represented by Norrish I and Norrish II as shown in Figure (5.3). Apart from acetic acid formation photodegradation of EVA has other products which have significant influence in the durability and performance of EVA. These products include carboxylic acid, vinylene and vinyl which cause yellowing and affect the optical transmission and deteriorate the performance of EVA as the encapsulant (Morlat-Therias et al. 2007). The absorbance peaks related to other products including carboxylic acid, lactone and vinyl sharply increased on the irradiated surface after the UV irradiation where no significant changes

Comparative study of ageing impact on the structure and mechanical properties EVA under different ageing conditions

were observed in other samples which show the dominant effect of UV in the chemical degradation of EVA. The differences in the FTIR-ATR spectra on the UV irradiated and non-irradiated side of the UV aged samples show that the intensity is depth dependant. In this study photodegradation on the UV exposed surface of EVA is predicted by a numerically developed model which shows in case of unprotected UV exposure the degradation process completes in around 0.5 year where It is reported in the literature that laboratory environmental chamber conditions may be different from in-service conditions and for instance the reduction in optical transmission after 6 month in an environmental chamber is much less than desired PV lifetime (M D Kempe 2008) and also it is reported that discolouration of EVA can develop in around 5 years (Czanderna & Pern 1996). The differences in results come from different sample types where in the previous studies laminated samples with low iron top glass have been used where most of the harmful UV is absorbed by glass but in this study free film is used and the exposure was not protected. The developed method is validated with FTIR-ATR results and can be used in wide range of application including polymer degradation and solar energy capture.

Damp heat had a different effect than UV and elevated temperature where the main difference in IR spectra before and after damp heat ageing was observed at between 3400 and 3700 cm^{-1} . The observed changes were related to moisture diffusion into the EVA's structure and bonded water formation which also caused an increase in the crystallinity of EVA in the early stage of damp heat ageing and up to the saturation point however, the increase in crystallinity has not been observed in EVA with VAc lower than 30% (X.-M. Shi et al. 2009) which shows the significant impact of VAc on the ageing behaviour of EVA. It should be mentioned that the PV degree EVA has VAc of 33% which is also used in this study.

7.4 Conclusion

In this chapter the influence of different ageing factors on the crystallinity, mechanical properties and chemical ageing behaviour of EVA was discussed with a comparative view. The results showed all degradation factors cause a reduction in crystallinity and mechanical properties of EVA in a long term exposure. However, damp heat causes an initial increase in crystallinity and storage modulus which was followed by a decrease in them as ageing time increases. ATR-FTIR, DSC and DMA results indicated that UV has a greater degrading influence comparing to other degradation factors which is due to the photodegradation process EVA undergoes which yields to formation of different chemical components where the thermochemical degradation of EVA results in formation of mainly acetic acid under working temperature of PV modules. It should also be mentioned that the damage caused by the environmental factors and changes in mechanical properties can cause mismatches in thermal expansion, delamination and damage to solar cells which eventually results in failure of a PV modules in the field.

The next chapter presents achievements and conclusions of the research. The recommendation for future works will be also included in the next chapter.

Chapter 8

Conclusion and Recommendations for Future Work

8.1 Conclusions

This work aimed to fully understand and predict the degradation of the encapsulant material, EVA, under different environmental conditions using artificial laboratory ageing and associate changes in mechanical properties by examining the link between the chemistry, the structure and the mechanical behaviour. This led to better understanding of module degradation and lead to production of more durable PV modules. Based on the experimental results and corresponding numerical analysis the following conclusions can be made:

- The thermal degradation of EVA was investigated using techniques that enabled the viscoelastic properties and thermal stability to be measured. The findings showed
 - The activation energy of deacetylation was unaffected by the ageing process.
 - The chemical changes due to thermal activation did not significantly influence the lifetime of the EVA.
 - Ageing reduced the crystallinity and storage modulus as a function of ageing degree.
 - DSC results suggested that property changes could be connected to structural modifications.
- The photodegradation of EVA and its influence on the structure and mechanical properties were investigated using ATR-FTIR, DSC and DMA.

- The IR spectra showed notable increases in the absorbance peaks related to carboxylic acid, ketone and vinyl on UV ageing.
- The most significant changes were observed on the UV exposed side of the sample, where the UV non-exposed side of the samples were not affected.
- The differences in the ATR-FTIR spectra on the UV affected and back side of the UV aged samples shows that the intensity is depth dependant.
- DSC and DMA analysis showed that the structure and the storage modulus of the samples were extremely influenced by UV exposure respectively and a sharp decrease was observed in the crystallinity and accordingly in storage modulus.
- A numerical model was developed to enable the prediction of the photodegradation in EVA. The model showed a good agreement on the UV exposed surface but there were significant discrepancies on the non-irradiated surface which could be due to the presence of UV absorber in the EVA which explains why no effect of UV was observed on the non-irradiated side.
- The response of EVA to damp heat environment was investigated at two conditions with same RH level and different temperatures.
 - The measurement of moisture absorption coefficient was carried out by gravimetry and WVTR technique (Mocon device). The measured values were in a same range and in agreement with the literature. However, there was a slight difference in the measured values which could be because of the different test conditions and different nature of the tests.
 - The distribution of the moisture concentration in depth was modelled and the impact of moisture concentration on the crystallinity and storage modulus of EVA were investigated.

- The calorimetry results indicated that the crystallinity increases in the initial stage of damp heat ageing due to incorporation of moisture into the polymer's structure however it decreases as ageing time increases.
- The rate of the decrease in crystallinity was shown to have dependency on the temperature as the higher temperature resulted in greater rate of decrease in crystallinity after the initial increase.
- DMA results showed that the storage modulus has strong dependency on the crystallinity and follows the structural changes of EVA.
- A comparative analysis to include the effect of all ageing factors was applied to give a better understanding of the degradation factors.
 - All degradation factors cause a reduction in crystallinity and mechanical properties of EVA in a long term ageing.
 - ATR-FTIR, DSC and DMA results indicated that UV has a greater degrading influence comparing to other degradation factors which can be summarised as $UV > T > DH$.

8.2 Recommendations for future work

This work focused on investigating the chemical degradation of encapsulant to understand the degradation mechanisms to be able to develop a predictive model for lifetime behaviour prediction and link the chemical degradation to the changes in the structure and mechanical properties of the EVA. Although extensive work has been conducted, more work is still required to enhance the modelling part and use other techniques to be able to improve the understanding of the degradation of EVA to include other aspects of degradation such as delamination and extend the knowledge by incorporating field conditions. This should include:

- Considering the combining effect of environmental factors and the interaction between them on the degradation of EVA: In this work the impact of degradation factors on chemical degradation, structure and mechanical properties of EVA was investigated in isolation. In the field PV Modules are subjected to the combination of elevated temperatures, light

and humidity. It is important that the interaction between the effects of these environmental factors and effect of daily cycling including moisture absorption and desorption to be investigated in order to enhance the understanding regarding the field conditions.

- Investigating the impact of the discolouration on optical properties of EVA: UV exposure causes discolouration in EVA which affects its optical properties and the efficiency of the modules. It is essential to find out the relation between the degree of discolouration, light transmission through EVA and electrical efficiency in order investigate the rate of loss in modules' efficiency versus degree of discolouration.
- Enhance the photodegradation model by including the effect of UV absorbers to be able predict the photodegradation in depth: UV exposure causes serious damages to EVA which starts from the surface and develops in depth. In order to be able to predict the photodegradation in depth it is essential to use different experimental techniques to have access to data in depth of EVA and develop a predictive model which includes the effect of additives such as UV absorber to achieve a valid accurate model. In this regards the experimental results and the initial model developed in this research can pave the way to improve the model.
- Investigating the influence of UV ageing on moisture diffusion coefficient: Moisture diffusion coefficient was measured and moisture concentration was modelled accordingly in this research at single condition however, in the field modules are exposed to cyclic conditions and the moisture diffusion coefficient might be affected by degradation factors due to the structural changes caused by these factors. Therefore, it is important to investigate the impact of degradation factors on the moisture diffusion in EVA.

References

- A. L. Rosenthal, M. G. Thomas, and S.J.D., 1994. A ten year review of performance of photovoltaic systems. In *NREL Photovoltaic Performance and Reliability Workshop, NREL/CP-411-7414*. pp. 279–285. Available at: <http://ieeexplore.ieee.org/stamp/stamp.jsp?arnumber=346934>.
- A.K. Plessing, E. von S., 2003. No Title. In R. W. L. G.M. Wallner, ed. *Proceedings of Polymeric Solar Materials*. Leoben, pp. XII1–XII8.
- Abdelkader, A.F. & White, J.R., 2005. Water absorption in epoxy resins: The effects of the crosslinking agent and curing temperature. *Journal of Applied Polymer Science*, 98, pp.2544–2549.
- Abrusci, C. et al., 2012. Photodegradation and biodegradation by bacteria of mulching films based on ethylene-vinyl acetate copolymer: Effect of pro-oxidant additives. *Journal of Applied Polymer Science*, 126(5), pp.1664–1675. Available at: <http://doi.wiley.com/10.1002/app.36989> [Accessed December 1, 2014].
- Agroui, K. et al., 2007. Quality control of EVA encapsulant in photovoltaic module process and outdoor exposure. *Desalination*, 209(1-3), pp.1–9. Available at: <http://linkinghub.elsevier.com/retrieve/pii/S0011916407000926> [Accessed October 28, 2014].
- Akpalu, Y.A. et al., 1999. Structure Development during Crystallization of Homogeneous Copolymers of Ethene and 1-Octene: Time-Resolved Synchrotron X-ray and SALS Measurements. *Macromolecules*, 32, pp.765–770. Available at: <http://pubs.acs.org/doi/abs/10.1021/ma9810114>.
- Alizadeh, a. et al., 1999. Influence of Structural and Topological Constraints on the Crystallization and Melting Behavior of Polymers. 1. Ethylene/1-Octene Copolymers †. *Macromolecules*, 32(19), pp.6221–6235. Available at: <http://pubs.acs.org/doi/abs/10.1021/ma990669u>.
- Allen, N.S. et al., 2001. Aspects of the thermal oxidation, yellowing and stabilisation of ethylene vinyl acetate copolymer. , 71, pp.1–14.
- Allen, N.S. et al., 1994. Physicochemical aspects of the environmental degradation of poly(ethylene terephthalate). *Polymer Degradation and Stability*, 43(2), pp.229–237. Available at: <http://linkinghub.elsevier.com/retrieve/pii/0141391094900744> [Accessed December 1, 2014].
- Allen, R.D. et al., 2005. Design of experiments for the qualification of EVA expansion characteristics. *Robotics and Computer-Integrated Manufacturing*, 21(4-5), pp.412–420. Available at: <http://linkinghub.elsevier.com/retrieve/pii/S0736584504001231>

[Accessed December 1, 2014].

- Androsch, R., 1999. Melting and crystallization of poly(ethylene-co-octene) measured by modulated d.s.c. and temperature-resolved X-ray diffraction. *Polymer*, 40(10), pp.2805–2812. Available at: <http://linkinghub.elsevier.com/retrieve/pii/S0032386198004704> [Accessed December 10, 2014].
- Anon, 2014. Renewable Energy Association. *REA Publications*. Available at: <http://www.r-e-a.net/resources/rea-publications>.
- Anon, 2013. *UK Solar PV Strategy Part 1: Roadmap to a Brighter Future*, London. Available at: https://www.gov.uk/government/uploads/system/uploads/attachment_data/file/249277/UK_Solar_PV_Strategy_Part_1_Roadmap_to_a_Brighter_Future_08.10.pdf.
- Ashcroft, I.A. et al., 2012. Environmental Ageing of Epoxy-Based Stereolithography Parts Part 2: Effect of absorbed moisture on Mechanical Properties. *Plastic, Rubber and Composites*, 41(3), pp.129–136. Available at: <https://dspace.lboro.ac.uk/2134/8687>.
- Ashcroft, I.A. et al., 2001. The effect of environment on the fatigue of bonded composite joints. Part 1: testing and fractography. *Composites Part A: Applied Science and Manufacturing*, 32(1), pp.45–58. Available at: <http://linkinghub.elsevier.com/retrieve/pii/S1359835X00001317>.
- Ayutthaya, S.I.N. & Wootthikanokkhan, J., 2008. Investigation of the photodegradation behaviors of an ethylene/vinyl acetate copolymer solar cell encapsulant and effects of antioxidants on the photostability of the material. *Journal of Applied Polymer Science*, 107(6), pp.3853–3863. Available at: <http://doi.wiley.com/10.1002/app.27428> [Accessed December 1, 2014].
- Ayutthaya, S.I.N. & Wootthikanokkhan, J., 2008. Investigation of the photodegradation behaviors of an ethylene/vinyl acetate copolymer solar cell encapsulant and effects of antioxidants on the photostability of the material. *Journal of Applied Polymer Science*, 107(6), pp.3853–3863. Available at: <http://doi.wiley.com/10.1002/app.27428> [Accessed November 3, 2014].
- Badiee, A., Wildman, R. & Ashcroft, I., 2014. Effect of UV aging on degradation of ethylene-vinyl acetate (EVA) as encapsulant in photovoltaic (PV) modules N. G. Dhere, ed. , 9179, p.917900. Available at: <http://proceedings.spiedigitallibrary.org/proceeding.aspx?doi=10.1117/1.2.2062007> [Accessed October 22, 2014].
- Bauer, F. et al., 1999. TG-FTIR and isotopic studies on coke formation during the MTG process. *Microporous and Mesoporous Materials*, 29(1-2), pp.109–115. Available at: <http://linkinghub.elsevier.com/retrieve/pii/S1387181198003242>.
- Berman, D., Biryukov, S. & Faiman, D., 1995. EVA laminate browning after 5

- years in a grid-connected, mirror-assisted, photovoltaic system in the Negev desert: effect on module efficiency. *Solar Energy Materials and Solar Cells*, 36(4), pp.421–432. Available at: <http://linkinghub.elsevier.com/retrieve/pii/0927024894001987> [Accessed December 2, 2014].
- Berman, D. & Faiman, D., 1997. EVA browning and the time-dependence of I–V curve parameters on PV modules with and without mirror-enhancement in a desert environment. *Solar Energy Materials and Solar Cells*, 45(4), pp.401–412. Available at: <http://linkinghub.elsevier.com/retrieve/pii/S0927024896000876> [Accessed December 2, 2014].
- Bianchi, O. et al., 2011. Changes in activation energy and kinetic mechanism during EVA crosslinking. *Polymer Testing*, 30(6), pp.616–624. Available at: <http://linkinghub.elsevier.com/retrieve/pii/S0142941811000742> [Accessed August 7, 2014].
- Brogly, M., Nardin, M. & Schultz, J., 1997a. Effect of vinylacetate content on crystallinity and second-order transitions in ethylene vinyl acetate copolymers. *Journal of Applied Polymer Science*, 64(10), pp.1903–1912. Available at: [http://doi.wiley.com/10.1002/\(SICI\)1097-4628\(19970606\)64:10<1903::AID-APP4>3.0.CO;2-M](http://doi.wiley.com/10.1002/(SICI)1097-4628(19970606)64:10<1903::AID-APP4>3.0.CO;2-M) [Accessed December 1, 2014].
- Brogly, M., Nardin, M. & Schultz, J., 1997b. Effect of vinylacetate content on crystallinity and second-order transitions in ethylene?vinylacetate copolymers. *Journal of Applied Polymer Science*, 64(10), pp.1903–1912. Available at: <http://doi.wiley.com/10.1002/%28SICI%291097-4628%2819970606%2964%3A10%3C1903%3A%3AAID-APP4%3E3.0.CO%3B2-M>.
- Bruker Optics, 2011. *Application Note AN # 79 Attenuated Total Reflection (ATR) – a versatile tool for FT-IR spectroscopy Refractive index*, Available at: https://www.bruker.com/fileadmin/user_upload/8-PDF-Docs/OpticalSpectroscopy/FT-IR/ALPHA/AN/AN79_ATR-Basics_EN.pdf.
- Camino, G. et al., 2000. Investigation of flame retardancy in EVA. *Fire and Materials*, 24(2), pp.85–90. Available at: <http://doi.wiley.com/10.1002/1099-1018%28200003/04%2924%3A2%3C85%3A%3AAID-FAM724%3E3.0.CO%3B2-T> [Accessed November 27, 2014].
- Carlsson, T. et al., 2006. Absorption and desorption of water in glass/ethylene-vinyl-acetate/glass laminates. *Polymer Testing*, 25(5), pp.615–622. Available at: <http://linkinghub.elsevier.com/retrieve/pii/S0142941806000821> [Accessed October 23, 2014].
- Chen, S., Zhang, J. & Su, J., 2009a. Effect of Damp-Heat Aging on the Properties of Ethylene-Vinyl Acetate Copolymer and Ethylene- Acrylic Acid Copolymer Blends.

- Chen, S., Zhang, J. & Su, J., 2009b. Effect of Hot Air Aging on the Properties of Ethylene- Vinyl Acetate Copolymer and Ethylene-Acrylic Acid Copolymer Blends. , 112, pp.1166–1174.
- Chiu, M.-C. & Wang, M.-J.J., 2007. Professional footwear evaluation for clinical nurses. *Applied ergonomics*, 38(2), pp.133–41. Available at: <http://www.ncbi.nlm.nih.gov/pubmed/16765904> [Accessed December 1, 2014].
- Claassen, R. S.; Butler, B.L., 1980. Introduction to solar materials science. *Solar materials science*, pp.3–51. Available at: <http://adsabs.harvard.edu/abs/1980sms..book....3C>.
- Copuroglu, M. & Sen, M., 2005. A comparative study of UV aging characteristics of poly(ethylene-co-vinyl acetate) and poly(ethylene-co-vinyl acetate)/carbon black mixture. *Polymers for Advanced Technologies*, 16(1), pp.61–66. Available at: <http://doi.wiley.com/10.1002/pat.538> [Accessed December 1, 2014].
- Çopuroğlu, M. & Şen, M., 2004. A comparative study of thermal ageing characteristics of poly(ethylene-co-vinyl acetate) and poly(ethylene-co-vinyl acetate)/carbon black mixture. *Polymers for Advanced Technologies*, 15(7), pp.393–399. Available at: <http://doi.wiley.com/10.1002/pat.485> [Accessed October 21, 2014].
- Costache, M.C., Jiang, D.D. & Wilkie, C.A., 2005. Thermal degradation of ethylene–vinyl acetate copolymer nanocomposites. *Polymer*, 46(18), pp.6947–6958. Available at: <http://linkinghub.elsevier.com/retrieve/pii/S0032386105007329> [Accessed November 27, 2014].
- Crank, J., 1968. *Diffusion in Polymers* G. S. P. John Crank, ed.,
- Crank, J., 1975. *Mathematics of Diffusion*, Oxford: Oxford University Press.
- Czanderna, a. W. & Jorgensen, G.J., 1997. Service lifetime prediction for encapsulated photovoltaic cells/minimodules. *AIP Conference Proceedings*, 394, pp.295–312. Available at: <http://scitation.aip.org/content/aip/proceeding/aipcp/10.1063/1.52899>.
- Czanderna, A.W. & Pern, F.J., 1996. Encapsulation of PV modules using ethylene vinyl acetate copolymer as a pottant: A critical review. *Solar Energy Materials and Solar Cells*, 43(2), pp.101–181. Available at: <http://linkinghub.elsevier.com/retrieve/pii/0927024895001506>.
- Department of Energy & Climate Change, 2013. *UK renewable energy roadmap: 2013 update*, London. Available at: https://www.gov.uk/government/uploads/system/uploads/attachment_data/file/255182/UK_Renewable_Energy_Roadmap_-_5_November_-_FINAL_DOCUMENT_FOR_PUBLICATION_.pdf.
- Dhere, Neelkanth G. and Pandit, Mandar, B., 2001. Study of Delamination in Acceleration Tested PV Modules Authors. In *17th European Photovoltaic Solar Energy Conference*. Munich.

- Dhere, N.G., 2000. PV module Durability in Hot and Dry Climate. In *16th European Photovoltaic Solar Energy Conference*.
- Dolores Fernández, M. & Jesús Fernández, M., 2007. Thermal decomposition of copolymers from ethylene with some vinyl derivatives. *Journal of Thermal Analysis and Calorimetry*, 91(2), pp.447–454. Available at: <http://link.springer.com/10.1007/s10973-007-8552-3>.
- E. U. Reisner, G. Stollwerck, H. Peerlings, F.S., 2006. Humidity in a solar module - Horror vision or negligible? In *European Photovoltaic Solar Energy*. Dresden.
- Elmahdy, A.E. et al., 2010. Stress measurement in East Asian lacquer thin films owing to changes in relative humidity using phase-shifting interferometry. *Proceedings of the Royal Society A: Mathematical, Physical and Engineering Sciences*, 467(2129), pp.1329–1347. Available at: <http://rspa.royalsocietypublishing.org/cgi/doi/10.1098/rspa.2010.0414> [Accessed October 30, 2014].
- Fan, X.J., Lee, S.W.R. & Han, Q., 2009. Experimental investigations and model study of moisture behaviors in polymeric materials. *Microelectronics Reliability*, 49, pp.861–871.
- Feng, L. & Kamal, M.R., 2005. Crystallization and melting behavior of homogeneous and heterogeneous linear low-density polyethylene resins. *Polymer Engineering & Science*, 45(8), pp.1140–1151. Available at: <http://doi.wiley.com/10.1002/pen.20389>.
- Flynn, J.H., 1995. A critique of lifetime prediction of polymers by thermal analysis. *Journal of Thermal Analysis and Calorimetry*, 44(2), pp.499–512. Available at: <http://link.springer.com/10.1007/BF02636139>.
- Gilbert, J. et al., 1962. Carbonization of polymers I—Thermogravimetric analysis. *Polymer*, 3, pp.1–10. Available at: <http://linkinghub.elsevier.com/retrieve/pii/0032386162900605> [Accessed November 27, 2014].
- Glikman, J.-F. et al., 1986. Photolysis and photo-oxidation of ethylene-ethyl acrylate copolymers. *Polymer Degradation and Stability*, 16(4), pp.325–335.
- Globus, A. et al., 2004. Teleoperated modular robots for lunar operations. In *American Institute of Aeronautics and Astronautics Inc*. Chicago, pp. 788–807.
- Gu, H. et al., 2012. Thermal degradation kinetics of semi-aromatic polyamide containing benzoxazole unit. *Journal of Thermal Analysis and Calorimetry*, 107, pp.1251–1257.
- Gulmine, J. et al., 2002. Polyethylene characterization by FTIR. *Polymer Testing*, 21(5), pp.557–563. Available at: <http://linkinghub.elsevier.com/retrieve/pii/S0142941801001246>.
- Hamed Gholami, Gholam Reza Razavi, M.S., 2011. Examination Synthesis of

- Fluorapatite with Using Free Model (TG) and Kissinger Method. In *International Conference on Advanced Materials Engineering*. Singapore: IACSIT Press, pp. 41–44.
- Harris, K. & Annut, A., 2013. *Digest of United Kingdom Energy Statistics Production team : Iain MacLeay*,
- Häußler, L. , Pompe, G., Albrecht, V., Voigt, D., 1998. Bestimmung des Vinylacetat-Gehaltes in eva copolymeren. Möglichkeiten und Grenzen der Anwendung MS-gekoppelter Analysenmethoden. *Thermal Analysis and Calorimetry*, 52(1), pp.131–143.
- Heng-Yu Li, Laura-Emmanuelle Perret-Aebi, Ricardo Theron, Christophe Ballif, Yun Luo, R.F., 2010. Towards in-line determination of EVA Gel Content during PV modules Lamination Processes. In *Proceedings of the 25th PVSC Conference*.
- Herrick, C.E., 1966. Solution of the Partial Differential Equations Describing Photodecomposition in a Light-absorbing Matrix having Light-absorbing Photoproducts. *IBM Journal of Research and Development*, 10(1), pp.2–5. Available at: <http://ieeexplore.ieee.org/lpdocs/epic03/wrapper.htm?arnumber=5392099>.
- Hülsmann, P. et al., 2010. Measuring and simulation of water vapour permeation into PV modules under different climatic conditions. In N. G. Dhere, J. H. Wohlgemuth, & K. Lynn, eds. *SPIE*. pp. 777307–777307–6. Available at: <http://proceedings.spiedigitallibrary.org/proceeding.aspx?articleid=753890> [Accessed December 5, 2014].
- Hülsmann, P., Heck, M. & Köhl, M., 2013. Simulation of Water Vapor Ingress into PV-Modules under Different Climatic Conditions. *Journal of Materials*, 2013, pp.1–7. Available at: <http://www.hindawi.com/journals/jma/2013/102691/>.
- Hülsmann, P., Philipp, D. & Köhl, M., 2009. Measuring temperature-dependent water vapor and gas permeation through high barrier films. *The Review of scientific instruments*, 80(11), p.113901. Available at: <http://www.ncbi.nlm.nih.gov/pubmed/19947736> [Accessed September 12, 2014].
- Iwamoto, R. et al., 2003. Basic Interactions of Water with Organic Compounds. *The Journal of Physical Chemistry B*, 107(31), pp.7976–7980. Available at: <http://dx.doi.org/10.1021/jp030561n> \n <http://pubs.acs.org/doi/pdf/10.1021/jp030561n>.
- Iwamoto, R. & Matsuda, T., 2005. Interaction of water in polymers: Poly(ethylene-co-vinyl acetate) and poly(vinyl acetate). *Journal of Polymer Science Part B-Polymer Physics*, 43(7), pp.777–785. Available at: [file:///U:/Documents/Literature/Water IR/iwamoto.water_interact_poly.jpolymersci.05.pdf](file:///U:/Documents/Literature/Water%20IR/iwamoto.water_interact_poly.jpolymersci.05.pdf).

- J. Brandrup, E.H.I., 1999. *Polymer handbook* 4th ed. E. A. Grulke, ed., New York: Wiley-Interscience.
- J. C. McVeigh, 1983. *Sun Power: An Introduction to the Applications of Solar Energy* 2nd (2013) ed., Oxford: Pergamon Press.
- Jin, J., Chen, S. & Zhang, J., 2009. Investigation of UV aging influences on the crystallization of ethylene-vinyl acetate copolymer via successive self-nucleation and annealing treatment. *Journal of Polymer Research*, 17(6), pp.827–836. Available at: <http://link.springer.com/10.1007/s10965-009-9374-8> [Accessed October 23, 2014].
- Jin, J., Chen, S. & Zhang, J., 2010a. UV aging behaviour of ethylene-vinyl acetate copolymers (EVA) with different vinyl acetate contents. *Polymer Degradation and Stability*, 95(5), pp.725–732. Available at: <http://linkinghub.elsevier.com/retrieve/pii/S0141391010000911> [Accessed October 23, 2014].
- Jin, J., Chen, S. & Zhang, J., 2010b. UV aging behaviour of ethylene-vinyl acetate copolymers (EVA) with different vinyl acetate contents. *Polymer Degradation and Stability*, 95(5), pp.725–732. Available at: <http://linkinghub.elsevier.com/retrieve/pii/S0141391010000911> [Accessed August 7, 2014].
- Jorgensen, G.J. & McMahon, T.J., 2008. Accelerated and outdoor aging effects on photovoltaic module interfacial adhesion properties. *Progress in Photovoltaics: Research and Applications*, 16(6), pp.519–527. Available at: <http://doi.wiley.com/10.1002/pip.826> [Accessed November 20, 2014].
- Kaczaj, J. & Trickey, R., 1969. Multiple isothermal degradation method for determination of combined vinyl acetate in vinyl acetate-ethylene copolymers. *Analytical Chemistry*, 41(11), pp.1511–1512. Available at: <http://pubs.acs.org/doi/abs/10.1021/ac60280a017> [Accessed November 27, 2014].
- Kamath, P.M. & Wakefield, R.W., 1965. Crystallinity of ethylene–vinyl acetate copolymers. *Journal of Applied Polymer Science*, 9(9), pp.3153–3160. Available at: <http://doi.wiley.com/10.1002/app.1965.070090919> [Accessed December 9, 2014].
- Kapur, J., Proost, K. & Smith, C.A., 2009. Determination of moisture ingress through various encapsulants in glass/glass laminates. In *2009 34th IEEE Photovoltaic Specialists Conference (PVSC)*. IEEE, pp. 001210–001214. Available at: <http://ieeexplore.ieee.org/lpdocs/epic03/wrapper.htm?arnumber=5411235>.
- Karimi, M., 2006. *Diffusion in Polymer Solids and Solutions*.
- Kempe, M., 2006. Modeling of rates of moisture ingress into photovoltaic modules. *Solar Energy Materials and Solar Cells*, 90(16), pp.2720–2738. Available at:

<http://linkinghub.elsevier.com/retrieve/pii/S0927024806001632>
[Accessed November 3, 2014].

- Kempe, M.D., 2008. Accelerated UV test methods and selection criteria for encapsulants of photovoltaic modules. In *2008 33rd IEEE Photovoltaic Specialists Conference*. IEEE, pp. 1–6. Available at: <http://ieeexplore.ieee.org/lpdocs/epic03/wrapper.htm?arnumber=4922771> [Accessed November 21, 2014].
- Kempe, M.D., 2005. Control of moisture ingress into photovoltaic modules. *Conference Record of the Thirty-first IEEE Photovoltaic Specialists Conference, 2005.*, pp.503–506. Available at: <http://ieeexplore.ieee.org/lpdocs/epic03/wrapper.htm?arnumber=1488180>.
- Kempe, M.D., 2008. Replacement for the Back-Sheet and Encapsulant Layers Preprint.
- Kempe, M.D., 2005. Rheological and Mechanical Considerations for Photovoltaic Encapsulants. In *DOE Solar Energy Technologies Program Review Meeting*. Denver.
- Kempe, M.D., 2010. Ultraviolet light test and evaluation methods for encapsulants of photovoltaic modules. *Solar Energy Materials and Solar Cells*, 94, pp.246–253.
- Kempe, M.D., Moricone, T.J. & Kilkenny, M., 2011. Accelerated Stress Testing of Encapsulants for Medium- Concentration CPV Applications. In *Photovoltaic Specialists Conference (PVSC), 2009 34th IEEE*. Pennsylvania: NREL/CP-5200-46085. Available at: <http://www.nrel.gov/docs/fy11osti/46085.pdf>.
- Ken, Z., 1990. *Harnessing Solar Power the Phphotovoltaics Challenge*, New York: Plenum Press.
- Kim, N. & Han, C., 2013. Experimental characterization and simulation of water vapor diffusion through various encapsulants used in PV modules. *Solar Energy Materials and Solar Cells*, 116, pp.68–75. Available at: <http://linkinghub.elsevier.com/retrieve/pii/S0927024813001724> [Accessed July 15, 2014].
- King, D.L. et al., 2000. Photovoltaic module performance and durability following long-term field exposure. *Progress in Photovoltaics: Research and Applications*, 8(2), pp.241–256. Available at: <http://doi.wiley.com/10.1002/%28SICI%291099-159X%28200003/04%298%3A2%3C241%3A%3AAID-PIP290%3E3.0.CO%3B2-D> [Accessed November 20, 2014].
- Klemchuk, P. et al., 1997. Investigation of the degradation and stabilization of EVA-based encapsulant in field-aged solar energy modules. *Polymer Degradation and Stability*, 55(3), pp.347–365. Available at: <http://linkinghub.elsevier.com/retrieve/pii/S0141391096001620> [Accessed November 3, 2014].

- Kojima, T., 2004. Ultraviolet-ray irradiation and degradation evaluation of the sealing agent EVA film for solar cells under high temperature and humidity. *Solar Energy Materials and Solar Cells*, 85, pp.63–72. Available at: <http://linkinghub.elsevier.com/retrieve/pii/S0927024804002041> [Accessed November 3, 2014].
- Kojima, T. & Yanagisawa, T., 2004. The evaluation of accelerated test for degradation a stacked a-Si solar cell and EVA films. *Solar Energy Materials and Solar Cells*, 81(1), pp.119–123. Available at: <http://linkinghub.elsevier.com/retrieve/pii/S0927024803002356> [Accessed December 1, 2014].
- Krauter, S. et al., 2011. PV MODULE LAMINATION DURABILITY. In *ISES Solar Word Congress*. Kassel. Available at: http://www.pib-berlin.com/images/pdf/publication/ISES-2011-Krauter_et_al-Module_Lamination_Durability.pdf.
- Křížanovský, L. & Mentlík, V., 1978. The use of thermal analysis to predict the thermal life of organic electrical insulating materials. *Journal of Thermal Analysis*, 13(3), pp.571–580. Available at: <http://link.springer.com/10.1007/BF01912396>.
- Lacoste, J. et al., 1991. Polyethylene hydroperoxide decomposition products. *Polymer Degradation and Stability*, 34(1-3), pp.309–323.
- Lange, R.F.M. et al., 2011. The lamination of (multi)crystalline and thin film based photovoltaic modules. *Progress in Photovoltaics: Research and Applications*, 19(2), pp.127–133. Available at: <http://doi.wiley.com/10.1002/pip.993> [Accessed November 3, 2014].
- Lee, K.-Y. & Kim, K.-Y., 2008. 60Co γ -ray irradiation effect and degradation behaviors of a carbon nanotube and poly(ethylene-co-vinyl acetate) nanocomposites. *Polymer Degradation and Stability*, 93(7), pp.1290–1299. Available at: <http://linkinghub.elsevier.com/retrieve/pii/S0141391008001213> [Accessed December 1, 2014].
- Li, C. et al., 2004. Crystallization of partially miscible linear low-density polyethylene/poly(ethylene-co-vinylacetate) blends. *Materials Letters*, 58(27-28), pp.3613–3617. Available at: <http://linkinghub.elsevier.com/retrieve/pii/S0167577X04005129> [Accessed December 1, 2014].
- Li, H. et al., 2013. Optical transmission as a fast and non-destructive tool for determination of ethylene-co-vinyl acetate curing state in photovoltaic modules. , (October 2011), pp.187–194.
- Liu, M. et al., 2003. Study on diffusion behavior of water in epoxy resins cured by active ester. *Physical Chemistry Chemical Physics*, 5, pp.1848–1852.
- Liu, X., Wildman, R.D., Ashcroft, I. a., et al., 2012a. Modelling the mechanical response of urushi lacquer subject to a change in relative humidity. *Proceedings of the Royal Society A: Mathematical, Physical and*

- Engineering Sciences*, 468(2147), pp.3533–3551. Available at: <http://rspa.royalsocietypublishing.org/cgi/doi/10.1098/rspa.2012.0008> [Accessed August 7, 2014].
- Liu, X., Wildman, R.D., Ashcroft, I. a., et al., 2012b. Modelling the mechanical response of urushi lacquer subject to a change in relative humidity. *Proceedings of the Royal Society A: Mathematical, Physical and Engineering Sciences*, 468(2147), pp.3533–3551. Available at: <http://rspa.royalsocietypublishing.org/cgi/doi/10.1098/rspa.2012.0008> [Accessed October 23, 2014].
- Liu, X., Wildman, R.D. & Ashcroft, I.A., 2012. Experimental investigation and numerical modelling of the effect of the environment on the mechanical properties of polyurethane lacquer films. *Journal of Materials Science*, 47(13), pp.5222–5231. Available at: <http://link.springer.com/10.1007/s10853-012-6406-2> [Accessed October 30, 2014].
- Loo, Y.-L. et al., 2005. Thin crystal melting produces the low-temperature endotherm in ethylene/methacrylic acid ionomers. *Polymer*, 46(14), pp.5118–5124. Available at: <http://linkinghub.elsevier.com/retrieve/pii/S0032386105004805> [Accessed December 10, 2014].
- Malmström, J., Wennerberg, J. & Stolt, L., 2003. A study of the influence of the Ga content on the long-term stability of Cu(In,Ga)Se₂ thin film solar cells. *Thin Solid Films*, 431–432, pp.436–442. Available at: <http://linkinghub.elsevier.com/retrieve/pii/S0040609003001858> [Accessed December 5, 2014].
- Marcilla, a., Gómez, a. & Menargues, S., 2005. TG/FTIR study of the thermal pyrolysis of EVA copolymers. *Journal of Analytical and Applied Pyrolysis*, 74(1-2), pp.224–230. Available at: <http://linkinghub.elsevier.com/retrieve/pii/S0165237005000331> [Accessed October 31, 2014].
- Marcilla, A. & Sempere, F.J., 2004. Differential scanning calorimetry of mixtures of EVA and PE . Kinetic modeling. , 45, pp.4977–4985.
- Marín, M.L. et al., 1996. Thermal degradation of ethylene (vinyl acetate). *Journal of Thermal Analysis*, 47(1), pp.247–258. Available at: <http://link.springer.com/10.1007/BF01982703> [Accessed November 28, 2014].
- Markus Bregulla, Michael Köhl, Benjamin Lampe, Gernot Oreski, Daniel Philipp, Gernot Wallner, K.-A.W., 2007. DEGRADATION MECHANISMS OF ETHYLENE-VINYL-ACETATE COPOLYMER – NEW STUDIES INCLUDING ULTRA FAST CURE FOILS. In *The compiled state-of-the-art of PV solar technology and deployment. 22nd European Photovoltaic Solar Energy Conference*. Milan, pp. 5–8.
- McGrattan, B.J., 1994. Examining the Decomposition of Ethylene-Vinyl Acetate Copolymers Using TG/GC/IR. *Applied Spectroscopy*, 48, pp.1472–

1476.

- Mcintosh, K.R. et al., 2009. THE EFFECT OF ACCELERATED AGING TESTS ON THE OPTICAL PROPERTIES OF SILICONE AND EVA ENCAPSULANTS. In *Proceedings of the 24th European PVSEC (2009)*. Michigan. Available at: <http://www.dowcorning.com/content/publishedlit/06-1042.pdf>.
- McMahon, T.J., 2004. Accelerated testing and failure of thin-film PV modules. *Progress in Photovoltaics: Research and Applications*, 12(23), pp.235–248. Available at: <http://doi.wiley.com/10.1002/pip.526> [Accessed November 20, 2014].
- McNeill, I.C. et al., 1976. The thermal degradation of copolymers of vinyl acetate with methyl methacrylate and other monomers. *European Polymer Journal*, 12(5), pp.305–312. Available at: <http://linkinghub.elsevier.com/retrieve/pii/0014305776901567> [Accessed November 27, 2014].
- Moly, K.A. et al., 2005. Nonisothermal crystallisation, melting behavior and wide angle X-ray scattering investigations on linear low density polyethylene (LLDPE)/ethylene vinyl acetate (EVA) blends: effects of compatibilisation and dynamic crosslinking. *European Polymer Journal*, 41(6), pp.1410–1419. Available at: <http://linkinghub.elsevier.com/retrieve/pii/S001430570400374X> [Accessed December 1, 2014].
- Moly, K.A. et al., 2005. Nonisothermal crystallisation, melting behavior and wide angle X-ray scattering investigations on linear low density polyethylene (LLDPE)/ethylene vinyl acetate (EVA) blends: Effects of compatibilisation and dynamic crosslinking. *European Polymer Journal*, 41(6), pp.1410–1419.
- Morlat-Therias, S. et al., 2007. Polymer/carbon nanotube nanocomposites: Influence of carbon nanotubes on EVA photodegradation. *Polymer Degradation and Stability*, 92(10), pp.1873–1882. Available at: <http://linkinghub.elsevier.com/retrieve/pii/S0141391007002054> [Accessed August 7, 2014].
- Morshedian, J., 2009. The Accuracy of Approximation Equations in the Study of Thermal Decomposition Behaviour of Some Synthesized Optically Active Polyamides. , 18(11), pp.103–128.
- Motta, C., 1997. The effect of copolymerization on transition temperatures of polymeric materials. *Journal of thermal analysis*, 49(1), pp.461–464. Available at: <http://link.springer.com/10.1007/BF01987471> [Accessed October 30, 2014].
- Mubashar, a. et al., 2009. Moisture absorption–desorption effects in adhesive joints. *International Journal of Adhesion and Adhesives*, 29(8), pp.751–760. Available at: <http://linkinghub.elsevier.com/retrieve/pii/S0143749609000499> [Accessed October 23, 2014].

- Mubashar, A. et al., 2009. Modelling Cyclic Moisture Uptake in an Epoxy Adhesive. *The Journal of Adhesion*, 85, pp.711–735.
- Muralidhara, K.S. & Sreenivasan, S., 2010. Thermal Degradation Kinetic Data of Polyester , Cotton and Polyester-Cotton Blended Textile Material. , 11(2), pp.184–189.
- Myer Ezrin, Gary Lavigne, Petet Klemchuk, W. Holley, S. Agro, J. Galica, L. Thomas, R.Y., 1995. Discolouration of EVA Encapsulant in Photovoltaic Cells. *ANTEC*, pp.3957 – 3960. Available at: <http://syringeless.com/ANTEC1995.pdf>.
- Nogueira, P. et al., 2001. Effect of water sorption on the structure and mechanical properties of an epoxy resin system. *Journal of Applied Polymer Science*, 80, pp.71–80.
- Oreski, G. & Wallner, G., 2005. Delamination behaviour of multi-layer films for PV encapsulation. *Solar Energy Materials and Solar Cells*, 89(2-3), pp.139–151. Available at: <http://linkinghub.elsevier.com/retrieve/pii/S0927024805000668> [Accessed November 3, 2014].
- Oreski, G. & Wallner, G.M., 2010. Damp heat induced physical aging of PV encapsulation materials. *2010 12th IEEE Intersociety Conference on Thermal and Thermomechanical Phenomena in Electronic Systems*, pp.1–6. Available at: <http://ieeexplore.ieee.org/lpdocs/epic03/wrapper.htm?arnumber=5501297>.
- Oreski, G. & Wallner, G.M., 2010. DAMP HEAT INDUCED PHYSICAL AGING OF PV ENCAPSULATION MATERIALS.
- Órfão, J.J.M. & Martins, F.G., 2002. Kinetic analysis of thermogravimetric data obtained under linear temperature programming - A method based on calculations of the temperature integral by interpolation. *Thermochimica Acta*, 390, pp.195–211.
- Osterwald, C.R. et al., 2002. Degradation Analysis of Weathered Crystalline-Silicon PV Modules Preprint. In *IEEE PV Specialists Conference*. Louisiana. Available at: <http://www.nrel.gov/docs/fy02osti/31455.pdf>.
- Osterwald, C.R. & McMahon, T.J., 2009. History of accelerated and qualification testing of terrestrial photovoltaic modules: A literature review. *Progress in Photovoltaics: Research and Applications*, 17(1), pp.11–33. Available at: <http://doi.wiley.com/10.1002/pip.861> [Accessed November 21, 2014].
- Osterwald, C.R., McMahon, T.J. & del Cueto, J.A., 2003. Electrochemical corrosion of SnO₂:F transparent conducting layers in thin-film photovoltaic modules. *Solar Energy Materials and Solar Cells*, 79(1), pp.21–33. Available at: <http://linkinghub.elsevier.com/retrieve/pii/S092702480200363X> [Accessed November 20, 2014].

- Palacios, J. et al., 2012. Thermal degradation kinetics of PP/OMMT nanocomposites with mPE and EVA. *Polymer Degradation and Stability*, 97(5), pp.729–737. Available at: <http://linkinghub.elsevier.com/retrieve/pii/S0141391012000663> [Accessed October 23, 2014].
- Peike, C. et al., 2012. Impact of Permeation Properties and Backsheet-Encapsulant Interactions on the Reliability of PV Modules. *ISRN Renewable Energy*, 2012, pp.1–5. Available at: <http://www.hindawi.com/journals/isrn.renewable.energy/2012/459731/> [Accessed August 7, 2014].
- Pern, F., 1996. Factors that affect the EVA encapsulant discoloration rate upon accelerated exposure. *Solar Energy Materials and Solar Cells*, 41-42, pp.587–615. Available at: <http://linkinghub.elsevier.com/retrieve/pii/092702489500128X>.
- Pern, F., Glick, S., & Czanderna, A., 1996. EVA encapsulants for pv modules: Reliability issues and current R&D status at NREL. *Renewable Energy*, 8(1-4), pp.367–370. Available at: <http://linkinghub.elsevier.com/retrieve/pii/0960148196888793> [Accessed December 3, 2014].
- Pern, F.J., 1997. Ethylene-Vinyl Acetate (EVA) encapsulants for photovoltaic modules: degradation and discoloration mechanisms and formulation modifications for improved photostability. *Angewandte Makromolekulare Chemie*, 252, pp.192–216.
- Pern, F.J., 1993. Luminescence and absorption characterization of ethylene-vinyl acetate encapsulant for PV modules before and after weathering degradation. *Polymer Degradation and Stability*, 41(2), pp.125–139. Available at: <http://linkinghub.elsevier.com/retrieve/pii/014139109390035H> [Accessed November 3, 2014].
- Pern, F.J. et al., 2000. Photothermal Stability of Various Module Encapsulants and The Effects of Superstrate and Substrate Materials Studied for PVMat Sources. In Denver, pp. 67–68.
- Pern, F.J. & Glick, S.H., 2003. *Adhesion Strength Study of EVA Encapsulants on Glass Substrates*, Denver.
- Pern, F.J. & Glick, S.H., 1997. Improved Photostability of NREL- Developed EVA Pottant Formulations for PV Module Encapsulation. , (September).
- Pielichowski, K. & Njuguna, J., 2005. *Thermal Degradation of Polymeric Materials*, Smithers Rapra Technology. Available at: http://app.knovel.com/web/toc.v/cid:kpTDPM000C/viewerType:toc/root_slug:thermal-degradation-polymeric/b-off-set:0/b-cat-name:Plastics%26%20Rubber/b-cat-slug:plastics-rubber/b-cat-id:214/b-sub-cat-id:8/b-topic-name:Properties%26amp%3B%20Testing/b-topic-slug:properties-amp-testing/b-off-set:0/b-order-by:copyright_year/b-sort-by:descending/b-filter-by:all-content [Accessed February 4, 2015].

- Post, E. et al., 1995. Study of recyclable polymer automobile undercoatings containing PVC using TG / FTIR. , 263.
- Price, D.M. & Church, S.P., 1997. FTIR evolved gas analysis of the decomposition products of cellulose diacetate. *Thermochimica Acta*, 294(1), pp.107–112. Available at: <http://linkinghub.elsevier.com/retrieve/pii/S0040603196031504>.
- Quintana, M.A. et al., 2002. Commonly observed degradation in field-aged photovoltaic modules. In *Conference Record of the Twenty-Ninth IEEE Photovoltaic Specialists Conference, 2002*. IEEE, pp. 1436–1439. Available at: <http://ieeexplore.ieee.org/lpdocs/epic03/wrapper.htm?arnumber=1190879> [Accessed November 3, 2014].
- Rashtchi, S. et al., 2012. Measurement of moisture content in photovoltaic panel encapsulants using spectroscopic optical coherence tomography: a feasibility study N. G. Dhere & J. H. Wohlgemuth, eds. , p.847200. Available at: <http://proceedings.spiedigitallibrary.org/proceeding.aspx?doi=10.1117/12.928959>.
- Rimez, B., Rahier, H., Van Assche, G., Artoos, T., Biesemans, M., et al., 2008. The thermal degradation of poly(vinyl acetate) and poly(ethylene-co-vinyl acetate), Part I: Experimental study of the degradation mechanism. *Polymer Degradation and Stability*, 93(4), pp.800–810. Available at: <http://linkinghub.elsevier.com/retrieve/pii/S0141391008000207> [Accessed November 20, 2014].
- Rimez, B., Rahier, H., Van Assche, G., Artoos, T. & Van Mele, B., 2008. The thermal degradation of poly(vinyl acetate) and poly(ethylene-co-vinyl acetate), Part II: Modelling the degradation kinetics. *Polymer Degradation and Stability*, 93(6), pp.1222–1230. Available at: <http://linkinghub.elsevier.com/retrieve/pii/S0141391008000190> [Accessed November 20, 2014].
- Riva, a. et al., 2003. Fire retardant mechanism in intumescent ethylene vinyl acetate compositions. *Polymer Degradation and Stability*, 82(2), pp.341–346. Available at: <http://linkinghub.elsevier.com/retrieve/pii/S0141391003001915> [Accessed November 27, 2014].
- Rodríguez-Vázquez, M. et al., 2006. Degradation and stabilisation of poly(ethylene-stat-vinyl acetate): 1 – Spectroscopic and rheological examination of thermal and thermo-oxidative degradation mechanisms. *Polymer Degradation and Stability*, 91(1), pp.154–164. Available at: <http://linkinghub.elsevier.com/retrieve/pii/S0141391005002065> [Accessed December 9, 2014].
- S. Dietrich, M. Sander, M. Ebert, J.B., 2008. Mechanical Assessment of Large Photovoltaic Modules by Test and Finite Element Analysis. In *23rd European Photovoltaic Solar Energy Conference*. Valencia, Spain, pp.

- 2889 – 2892. Available at: <http://www.eupvsec-proceedings.com/proceedings?paper=3604>.
- S.-H. Schulze, S. Dietrich, M. Ebert, J.B., 2008. Development of Test Methods for Polymer Material Characterization in View of Long-Term Durability of PV-Modules. In *23rd European Photovoltaic Solar Energy Conference*. Valencia, Spain, pp. 2903 – 2907. Available at: <http://www.eupvsec-proceedings.com/proceedings?paper=3650>.
- Salin, I.M. & Seferis, J.C., 1993. Kinetic analysis of high-resolution TGA variable heating rate data. *Journal of Applied Polymer Science*, 47, pp.847–856.
- Sánchez-Jiménez, P.E., Criado, J.M. & Pérez-Maqueda, L. a., 2008. Kissinger kinetic analysis of data obtained under different heating schedules. *Journal of Thermal Analysis and Calorimetry*, 94(2), pp.427–432. Available at: <http://link.springer.com/10.1007/s10973-008-9200-2>.
- Sascha Dietrich, Matthias Pander, M.E., 2009. Mechanical challenges of PV-modules and its embedded cells experiments and finite element analysis. In *24th European Photovoltaic Solar Energy Conference*. Hamburg, pp. 3427–3431.
- Schulze, S.-H. et al., 2009. Influence of Vacuum Lamination Process on Laminate Properties – Simulation and Test Results. In *24th European Photovoltaic Solar Energy Conference*. Hamburg, pp. 3367–3372.
- Sheats, J.R. & Diamond, J.J., 1988. Photochemistry In Strongly Absorbing Media. , pp.4922–4938.
- Shi, X. et al., 2009. Effect of Damp-Heat Aging on the Structures and Properties of Ethylene-vinyl Acetate Copolymers with Different Vinyl Acetate Contents.
- Shi, X.M. et al., 2009. Effect of damp-heat aging on the structures and properties of ethylene-vinyl acetate copolymers with different vinyl acetate contents. *Journal of Applied Polymer Science*, 112(4), pp.2358–2365.
- Shi, X.M., 2008. Non-isothermal crystallization and melting of ethylene-vinyl acetate copolymers with different vinyl acetate contents. *EXPRESS Polymer Letters*, 2(9), pp.623–629. Available at: http://www.expresspolymlett.com/articles/EPL-0000692_article.pdf [Accessed October 31, 2014].
- Shi, X.-M. et al., 2009. Effect of damp-heat aging on the structures and properties of ethylene-vinyl acetate copolymers with different vinyl acetate contents. *Journal of Applied Polymer Science*, 112(4), pp.2358–2365. Available at: <http://doi.wiley.com/10.1002/app.29659>.
- Shirrell, C.D., 1978. *Diffusion of Water Vapor in Graphite/Epoxy Composites, Advanced Composite Materials-Environmental Effects*, ASTM STP 658 J. R. Vinson, ed., American Society for Testing and Materials.
- Siah, L.F., 2010. Moisture Sensitivity of Plastic Packages of IC Devices. , pp.503–522. Available at:

<http://www.springerlink.com/index/10.1007/978-1-4419-5719-1>.

- Skowronski, T., Rabek, J.F. & Y, B.N.B., 1984. Photodegradation of Some Poly(Vinyl Chloride) (PVC) Blends: PVC/Ethylene-Vinyl Acetate (EVA) Copolymers and PVC/Butadiene-Acrylonitrile (NBR) Copolymers. , 24(4).
- Smil, V., 2006. *Energy: A Beginner's Guide.*, Oxford: Oneworld.
- Starink, M., 2003a. The determination of activation energy from linear heating rate experiments: a comparison of the accuracy of isoconversion methods. *Thermochimica Acta*, 404(1-2), pp.163–176. Available at: http://eprints.soton.ac.uk/18822/1/The_Determination_of_Activation_.._by_MJ_Starink.pdf.
- Starink, M., 2003b. The determination of activation energy from linear heating rate experiments: a comparison of the accuracy of isoconversion methods. *Thermochimica Acta*, 404(1-2), pp.163–176. Available at: <http://linkinghub.elsevier.com/retrieve/pii/S0040603103001448> [Accessed August 7, 2014].
- Stark, W. & Jaunich, M., 2011. Investigation of Ethylene/Vinyl Acetate Copolymer (EVA) by thermal analysis DSC and DMA. *Polymer Testing*, 30(2), pp.236–242. Available at: <http://linkinghub.elsevier.com/retrieve/pii/S0142941810002126> [Accessed October 23, 2014].
- Stone, J.L., 1993a. Photovoltaics: Unlimited Electrical Energy from the Sun. *Physics Today*, 46(9), p.22. Available at: <http://scitation.aip.org/content/aip/magazine/physicstoday/article/46/9/10.1063/1.881362> [Accessed December 28, 2014].
- Stone, J.L., 1993b. Photovoltaics: Unlimited Electrical Energy from the Sun. *Physics Today*, 46(9), p.22. Available at: <http://scitation.aip.org/content/aip/magazine/physicstoday/article/46/9/10.1063/1.881362> [Accessed November 21, 2014].
- Sultan, B.-Å. & Sörvik, E., 1991a. Thermal degradation of EVA and EBA—A comparison. I. Volatile decomposition products. *Journal of Applied Polymer Science*, 43(9), pp.1737–1745. Available at: <http://doi.wiley.com/10.1002/app.1991.070430917> [Accessed November 27, 2014].
- Sultan, B.-Å. & Sörvik, E., 1991b. Thermal degradation of EVA and EBA—A comparison. II. Changes in unsaturation and side group structure. *Journal of Applied Polymer Science*, 43(9), pp.1747–1759. Available at: <http://doi.wiley.com/10.1002/app.1991.070430918> [Accessed November 27, 2014].
- Sultan, B.-Å. & Sörvik, E., 1991c. Thermal degradation of EVA and EBA—A comparison. III. Molecular weight changes. *Journal of Applied Polymer Science*, 43(9), pp.1761–1771. Available at: <http://doi.wiley.com/10.1002/app.1991.070430919> [Accessed November 27, 2014].

- Tambe, S.P. et al., 2008. Ethylene vinyl acetate and ethylene vinyl alcohol copolymer for thermal spray coating application. *Progress in Organic Coatings*, 62(4), pp.382–386. Available at: <http://linkinghub.elsevier.com/retrieve/pii/S0300944008000489> [Accessed December 1, 2014].
- Trombetta, M. et al., 2000. An FT-IR study of the internal and external surfaces of HZSM5 zeolite. *Applied Catalysis A: General*, 192(1), pp.125–136. Available at: <http://linkinghub.elsevier.com/retrieve/pii/S0926860X99003385>.
- Varghese, H. et al., 2002. Dynamic mechanical behavior of acrylonitrile butadiene rubber/poly(ethylene-co-vinyl acetate) blends. *Journal of Polymer Science Part B: Polymer Physics*, 40(15), pp.1556–1570. Available at: <http://doi.wiley.com/10.1002/polb.10204>.
- Vázquez, M. & Rey-Stolle, I., 2008. Photovoltaic module reliability model based on field degradation studies. *Progress in Photovoltaics: Research and Applications*, 16(5), pp.419–433. Available at: <http://doi.wiley.com/10.1002/pip.825> [Accessed November 21, 2014].
- Vieth, W.R., 1991. *Diffusion in and Through Polymers: Principles and Applications*, Oxford University Press,.
- Visoly-Fisher, I. et al., 2003. Factors Affecting the Stability of CdTe/CdS Solar Cells Deduced from Stress Tests at Elevated Temperature. *Advanced Functional Materials*, 13(4), pp.289–299. Available at: <http://doi.wiley.com/10.1002/adfm.200304259> [Accessed December 5, 2014].
- Vyazovkin, S., 2006. MODEL-FREE KINETICS Staying free of multiplying entities without necessity *. , 83, pp.45–51.
- W. Herrmann, N. Bogdanski, F.R. et al., 2010. PV module degradation caused by thermomechanical stress: real impacts of outdoor weathering versus accelerated testing in the laboratory. In *The Special Patrol Insertion/Extraction Optics and Photonics (SPIE'10)*.
- W.H. Holley, S.C. Agro, J.P.G. and R.S. & Yorgensen, 1996. UV Stability and module testing of non-browning experimental PV encapsulants. In *25th IEEE PVSC*. Washington, pp. 1259–1262.
- Wang, H., Tao, X. & Newton, E., 2004. Thermal degradation kinetics and lifetime prediction of a luminescent conducting polymer. *Polymer International*, 53, pp.20–26.
- Wenger, H.J. et al., 1991. Decline of the Carrisa Plains PV power plant: the impact of concentrating sunlight on flat plates. In *The Conference Record of the Twenty-Second IEEE Photovoltaic Specialists Conference - 1991*. IEEE, pp. 586–592. Available at: <http://ieeexplore.ieee.org/lpdocs/epic03/wrapper.htm?arnumber=169280> [Accessed December 2, 2014].
- Wohlgemuth, J.H. & Petersen, R.C., 1991. Solarex experience with ethylene

vinyl acetate encapsulation. *Solar Cells*, 30(1-4), pp.383–387. Available at: <http://linkinghub.elsevier.com/retrieve/pii/037967879190071V> [Accessed November 3, 2014].

- X. E. Cai, H.S., 1999. Apparent activation energies of the non-isothermal degradation of EVA copolymer. *Thermal analysis and calorimetry*, 55, pp.67–76.
- Zanetti, M. et al., 2001. Synthesis and thermal behaviour of layered silicate ± EVA nanocomposites. , 42, pp.4501–4507.

Appendix A

Water Vapour Transmission Rate Results



Job Number: 21101

RDM Test Equipment Co. Ltd
 Unit 39 Golds Business Park
 Elsenham, Herts CM22 6JX
 Tel: +44 (0) 1279 817171
 Fax: +44 (0) 1279 81574
 e-mail: sales@rdmtest.com
 Web site: www.rdmtest.com

**TESTING
 SERVICE**

Attn: Amir Badiee
 University of Nottingham
 University Park
 Nottingham
 NG7 2RD

mocon®

Water Vapor Transmission Rate Results
 We are pleased to submit the results of our
 transmission rate measurements of your material
 submitted under:

PO #: Amir Badiee

Dated: 05/06/2014

Test Conditions:

Test Gas	Water Vapor	Test Temperature	40 (°C)	(°F)
Test Gas Concentration	NA	Carrier Gas	Nitrogen	
Test Gas Humidity	100 % RH	Carrier Gas Humidity	0 % RH	

Test Results:

Sample	Thickness (mils)	WVTR g/(m ² .d)	Permeability (gm*cm)/(cm ² *sec.Pa)	Diffusion cm ² /sec	Solubility gm/(cm ³ .Pa)
Sample A	20.70	37.77	3.114×10^{-13}	7.085×10^{-07}	4.395×10^{-07}

Note: Above samples were analyzed on a MOCON Permatran-W Water Vapor Permeability Instrument.

Remarks:

Test Operator: Michael James

Date: 05/06/2014

Test Operator: MB

Date: 5/6/14

Reviewed By: MB

Date: 5/6/14

Mike James
 Laboratory QA Officer

This information represents our best judgement based on work done, but the company (RDM Test Equipment Ltd) assumes no liability whatsoever in connection with the use of information or findings contained herein.



RDM 039/1

Appendix B

Original DSC curves

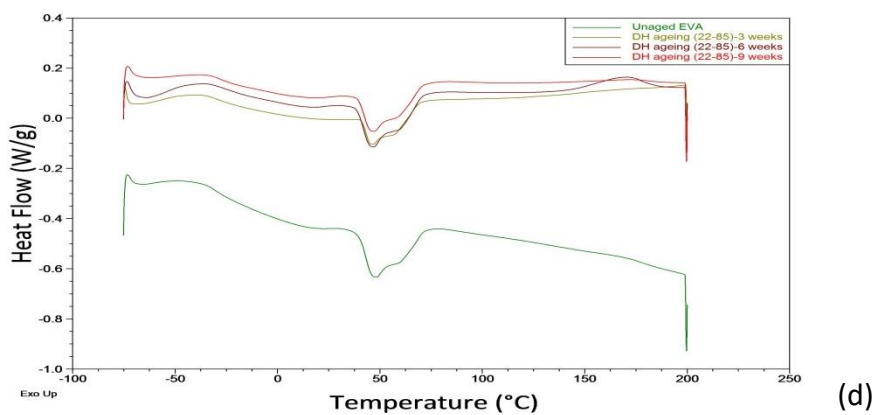
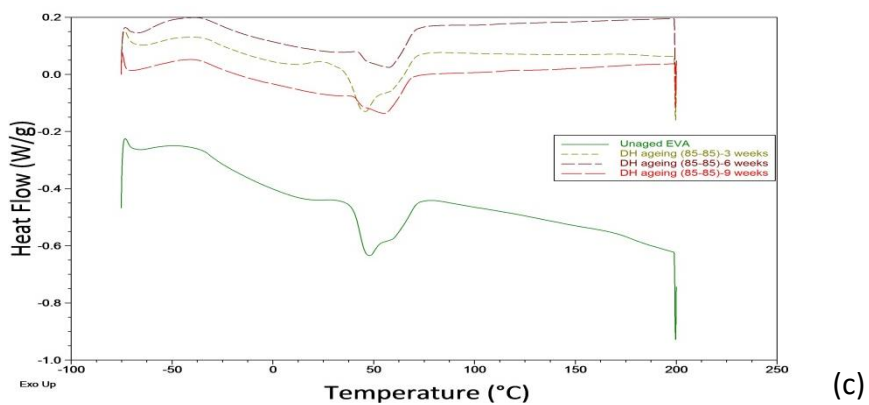
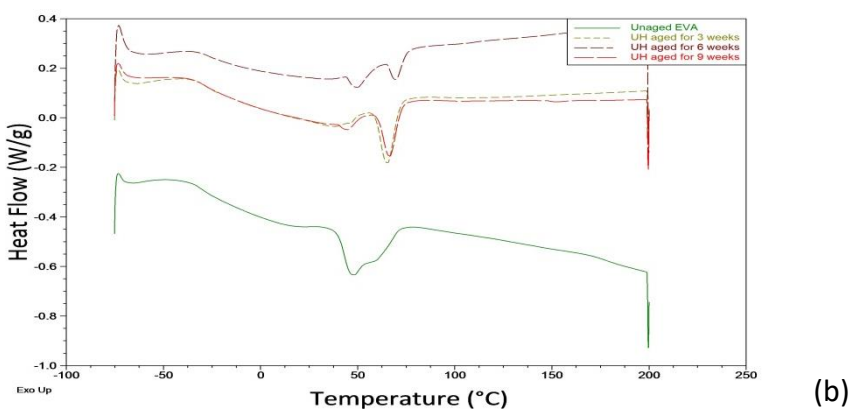
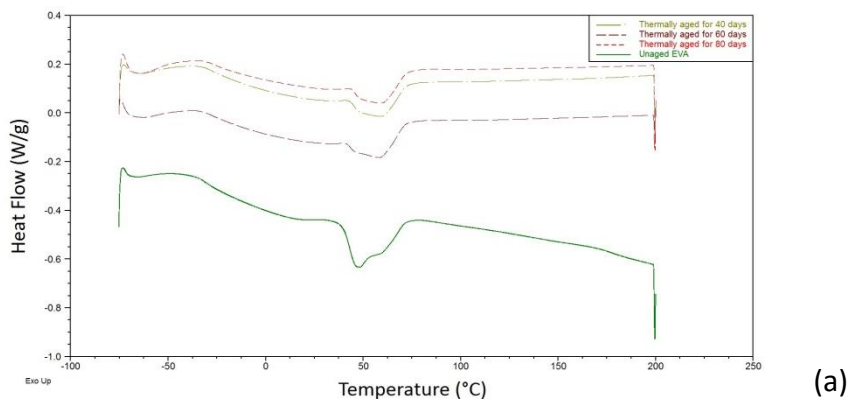


Figure App.1: Original DSC curves related to (a) Figure (4.15), (b) Figure (5.13), (c) Figure (6.4: a), (d) Figure (6.4: b).

Appendix C

Publications

Technical papers in peer-reviewed journals

- Status: Available online
Title: "The thermo-mechanical degradation of ethylene vinyl acetate used as a solar panel adhesive and encapsulant"
doi:10.1016/j.ijadhadh.2016.03.008

Conferences

- PVSAT-10, Loughborough, UK-Poster presentation 2014
Title: "Measurement of Moisture Diffusion Coefficient and Effect of Damp-Heat Aging on the Structure and Properties of Ethylene-vinyl Acetate (EVA) Copolymer as Encapsulant in Photovoltaic (PV) Modules"
- SPIE, San Diego, USA-Oral presentation 2014
Title: "Effect of UV Aging on Degradation of Ethylene-vinyl Acetate (EVA) as Encapsulant in Photovoltaic (PV) Modules"
Proc. SPIE 9179; doi: 10.1117/12.2062007